Strategies for Improving Methane Production from CO_2 and Electricity in Bioelectrochemical Systems

Dandan Liu

Thesis committee

Promotor

Prof. Dr C.J.N. Buisman
Professor of Biological Recovery and Re-use Technology
Wageningen University & Research

Co-promotor

Dr A. ter Heijne
Assistant professor, Sub-department of Environmental Technology
Wageningen University & Research

Other members

Prof. Dr A.J.M. Stams, Wageningen University & Research

Prof. Dr Aijie Wang, Chinese Academy of Sciences, Beijing, China

Prof. Dr L. T. Angenent, University of Tübingen, Germany

Dr A.W. Jeremiasse, MAGNETO Special Anodes B.V., Schiedam, The Netherlands

This research was conducted under the auspices of the Graduate School for Socio-Economic and Natural Sciences of the Environment (SENSE)

Strategies for Improving Methane Production from CO_2 and Electricity in Bioelectrochemical Systems

Dandan Liu

Thesis

submitted in fulfilment of the requirements for the degree of doctor
at Wageningen University
by the authority of the Rector Magnificus,
Prof. Dr A.P.J. Mol,
in the presence of the
Thesis Committee appointed by the Academic Board
to be defended in public
on Friday 13 April 2018
at 4 p.m. in the Aula.

Dandan Liu
Strategies for improving methane production from CO_2 and electricity in bioelectrochemical systems
188 pages.

PhD thesis, Wageningen University, Wageningen, the Netherlands (2018)
With references, with summary in English

ISBN : 978-94-6343-759-2
DOI : https://doi.org/10.18174/443010

谨以此书

献给我的父母

Contents

Chapter 1. General introduction

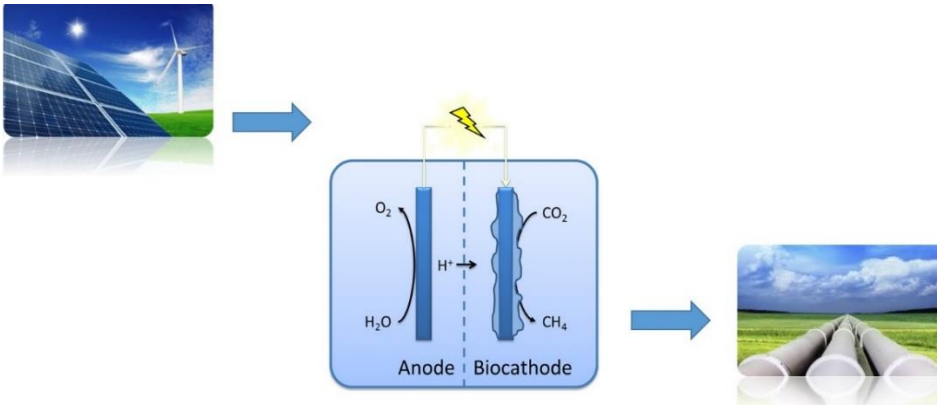

1.1 Renewable energy sources and production potential

Several decades of economic growth have driven an increase in energy demand, which leads to an increase in greenhouse gas emissions from human activities. The development of renewable energy, which is continuously replenished by nature, is of vital importance to meet the dual goals of addressing energy crisis and reducing environmental impact (Lozano et al. 2018). Renewable energy can be derived from solar, wind, water, biomass and geothermal energy. In total, renewable energy can provide more than 3000 times of the global energy consumption (Zervos et al. 2010) (Figure 1). The growth of capacity, environmental and social impact of renewable energy stimulates the global energy transition. According to European Renewable Energy Council, the share of total renewable energy compared to the global energy demand will rise from 16.6 % in 2010 to 47.7 % in 2040 (Demirbas 2009).

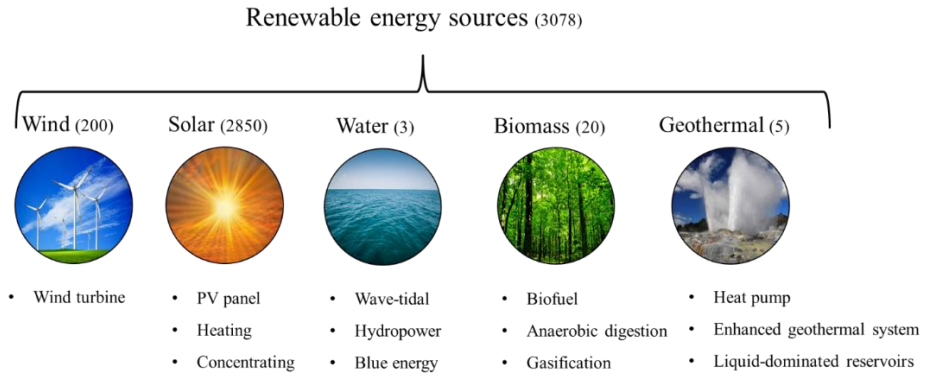

Figure 1. Overview of the renewable energy sources and belonging technologies as examples according to (Ellabban et al. 2014). The potential of each renewable energy source is elucidated as the times of the current global energy needs shown between brackets (Zervos et al. 2010)

This abundant renewable energy is withdrawn using various technologies and converted into usable forms of energy such as electricity, heat, and biofuels (Figure 2). In the renewable energy markets of 2015, electricity had the largest energy capacity of 1849 GW, which is around 4.3 times higher than the heat production (435 GW) and 19.3 times higher than the biofuel production (96 GW). Renewable electricity is mainly generated from water (hydropower), accounting for 60%, followed by the wind with 20% and the solar with 15%, biomass with 4%, and geothermal with 1%. As the production of renewable electricity is huge compared with renewable biofuels, technology which can convert electrical energy into biofuels is desired to enlarge the renewable biofuel market in the future. Moreover, biofuels are generally more easily stored and transported than electrical energy (Chen et al. 2009).

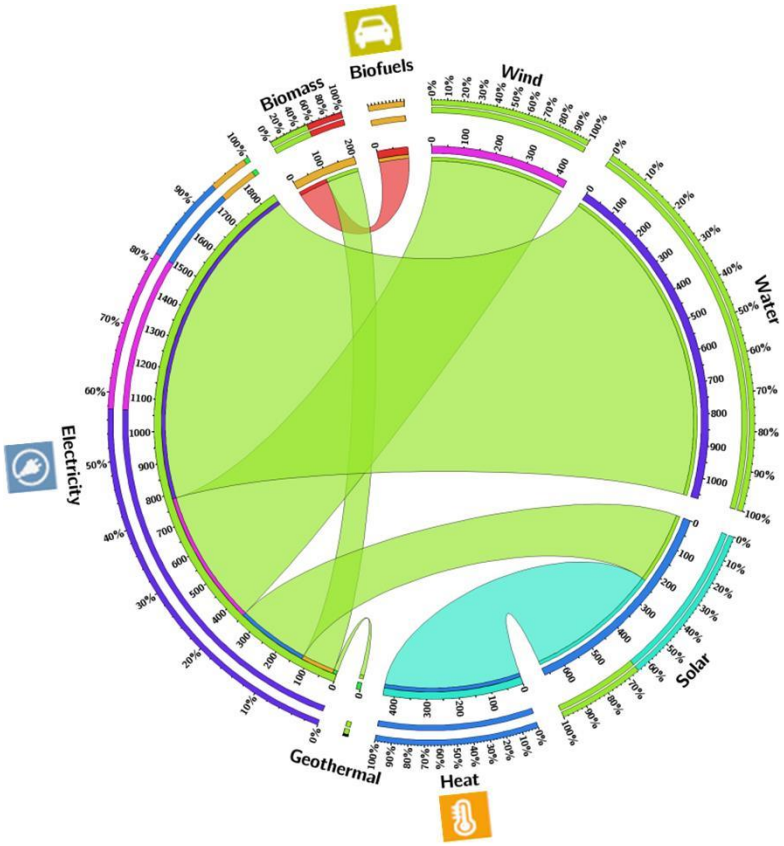

Figure 2. Renewable electricity, heat, and biofuels were summarized circularly by different renewable energy sources (wind, solar, water, biomass and geothermal) according to the renewable energy indicators of 2015 (Galán et al. 2016). The numbers inside the circle

indicate the energy capacity in gigawatt, i.e. GW (Huskinson et al.). The numbers outside the circle represent the proportions of different energy sources. Electricity, heat, and biofuel are shown in green, blue, red band, respectively. Wind and water were used to generate renewable electricity, which accounted for approximately 80% of the electricity. The leftover 20% of the electricity was derived from sun (35%), biomass (50%), and geothermal (100%). The other 50% of biomass was used for biofuel production. Solar energy was the sole source for renewable heat production (65% of solar energy).

1.2 Electricity storage technologies are important for renewable energy development

Renewable energy is intermittent and site-specific, because the availability and intensity of renewable energy sources are normally climate and weather dependent, e.g. dependent on the solar radiation or wind speed (Chauhan and Saini 2014). Except for the fluctuating renewable energy supply, the energy demand is also varying, especially the electricity demand. For example, a peak of household electrical demand appears from 15:00 to 24:00, whereas renewable electricity production by PV panels occurs from 10:00 to 15:00 (Fares and Webber 2017). The mismatch between renewable electrical supply and demand affects the stability of the power grid. The fluctuations in the networks of the power grid can deteriorate the power systems (Lund et al. 2015). Therefore, to make the best use of renewable electricity, developing flexible electricity storage systems is essential (Twidell and Weir 2015, Azari et al. 2014). In addition, the interest in renewable electricity storage is increasing because renewable electricity dominates the renewable energy market and will continue expanding in the future (Decourt and Debarre 2013).

In general, electricity storage has three important characteristics: duration, volumetric capacity, and efficiency. It is worth to notify that long-term storage and high storage capacity are both crucial requirements for electricity storage technologies aiming to increase the network stability. A comparison of different electricity storage technologies is shown in Figure 3. Chemical energy carriers, such as hydrogen and substitute natural gas (namely methane), seems to be the only way to store energy in long-term on large-scale (Figure 3a). Besides, substitute natural gas can be easily integrated into the existing infrastructure (e.g. gas grid). However, the chemical-based energy storage is still at an early development stage with lower energy efficiencies (< 50%) and requires high upfront capital

costs, compared with the much more mature mechanical-based energy storage with high energy efficiencies (> 85%; e.g. Flywheel, CAES and PHS) (Figure 3b). Nevertheless, mechanical energy storage technologies (like pumped hydro storage) are normally constrained by the site availability, which prevents its worldwide implementation (Decourt and Debarre 2013).

(a)

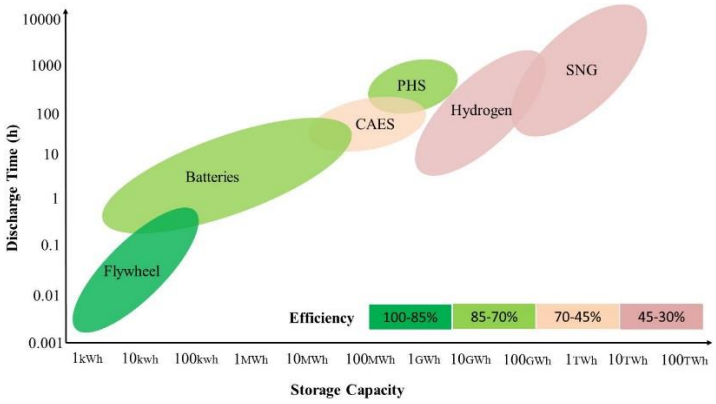

(b)

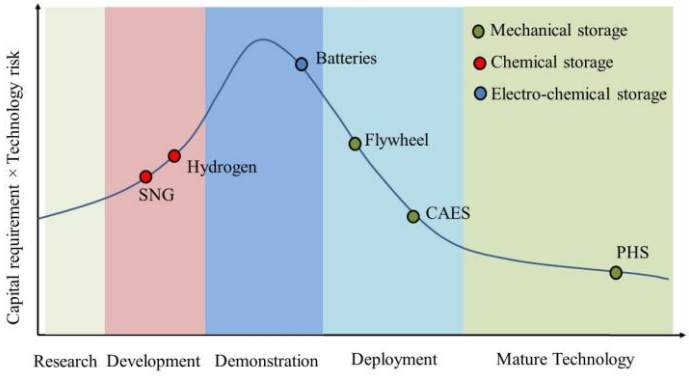

Figure 3. Overview of different electricity storage technologies including flywheels, batteries or capacitors, compressed air energy storage(CAES), pumped hydro storage(PHS), hydrogen and substitute natural gas(SNG). (a) Comparison of energy efficiency according to (Decourt and Debarre 2013), storage capacity and storage duration based on (Schaaf et al. 2014); Herein the energy efficiency is the ratio between the released energy and the initial electrical energy input (Ibrahim et al. 2008). (b) Evolution curve of different storage

technologies, that are categorised into three different storage principles: mechanical, chemical and electrochemical-based on (Decourt and Debarre 2013).

1.3 Power-to-Gas technologies provide sustainable renewable electricity storage

Storage of renewable electricity in the form of CH_4 is a promising technology. On the one hand, CH_4, as a chemical energy carrier, provides high storage flexibility by taking the advantage of existing nature gas pipeline infrastructure. On the other hand, CO_2 can be recycled during the entire storage and usage chain process, in combination with the conversion of CO_2 and combustion of CH_4, which helps mitigate the global warming effect (Bailera et al. 2017). Since the first "Power-to-Gas" concept was proposed in Japan (Hashimoto 1994), a large number of "Power-to-Gas" projects has already been conducted worldwide. The total number of these projects is around 45, among which 40% of the projects have been taken place in Germany (Bailera et al. 2017). The overview of "Power-to-Gas" technologies are shown in Figure 4. These projects can be categorized into 1-step or 2-step process for the conversion of renewable energy into CH_4.

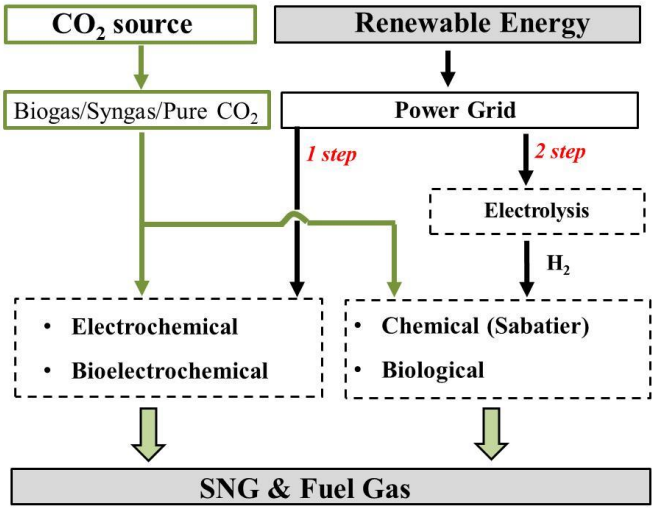

Figure 4. Renewable electricity storage in the form of methane by Power-to-Gas technologies. The CO_2 sources can be from biogas, syngas or pure CO_2 (Sterner 2009). Depending on the stages involved during the conversion of renewable electric energy into

the final product (CH_4), the Power-to-Gas technologies are divided into two groups: 1-step process and 2-step process.

The 2-step process consists of the water electrolysis process and the methanation process. H_2 is initially produced from renewable electricity (i.e. water electrolysis), then it is consumed to produce CH_4 from CO_2 (i.e. methanation). In the methanation process, CH_4 can be produced by either the Sabatier reaction or anaerobically biological conversion. The Sabatier reaction is a thermochemical methanation catalyzed by metals (e.g. nickel or ruthenium-based aluminum carrier) and operated at a temperature of 300-400 ℃ and pressure of 50-200 bar (Müller et al. 2013, Leonzio 2016). The anaerobic biological reaction is biological methanation using hydrogenotrophic methanogenesis operated at a temperature of 50-70 ℃. The biological methanation has the advantage over the thermochemical methanation as the impurities in the CO_2 source (biogas) (e.g. H_2S, siloxanes) have little effect on biological methanation, whereas these impurities will poison metal catalysts and thus need to be eliminated prior to the catalytic thermochemical methanation.

In the 1-step process, electrical energy is supplied directly to the (bio)electrochemical cell for CO_2 reduction to CH_4. Compared with the electrochemical reduction requiring specific electrode structure and precious metal catalysts (Kim et al. 2017), the bioelectrochemical reduction can occur at room temperature (20-30℃) and atmospheric pressure with inexpensive renewable catalysts generated by microorganisms. Thermodynamically, the 1-step process requires less energy than the 2-step process due to that producing H_2 needs a higher cell voltage than CH_4 formation(Geppert et al. 2016a). Collectively, the bioelectrochemical CO_2 reduction shows promise for application as a sustainable renewable energy storage technology.

The first methane-producing BES was reported in 1999, in which H_2-consuming microorganisms utilized electrically reduced neutral red as a sole electron donor to drive their metabolisms and produce methane from CO_2 (Park et al. 1999). Since then methane-producing BESs have been a spurt of interest attracting many researchers from a variety of disciplines, for instance, bioprocess engineering, material science, electrochemistry and microbiology. However, this technology is still in its infancy with lots of scientific and technical issues to be further addressed.

1.4 Methane production in BESs

A methane-producing BES consists of several components including (Figure 5): (1) anode where oxidation reaction (e.g. water oxidation) takes places to provide electrons for CO_2 reduction in the biocathode ; (2) biocathode where CH_4 is produced by microorganism, together with electrons supplied from oxidation reaction in the anode via the external circuit; (3) generally a separator, for instance, a cation exchange membrane where positive charged ions (e.g. Na^+, K^+, H^+) migrate through from anodic chamber to the cathodic chamber to keep the solution electroneutral; (4) external electrical energy that is required to drive the reaction ($CO_2 + 2H_2O \rightarrow CH_4 + 2O_2$; $\Delta G = 817.98$ kJ/mol), which is thermodynamically needed.

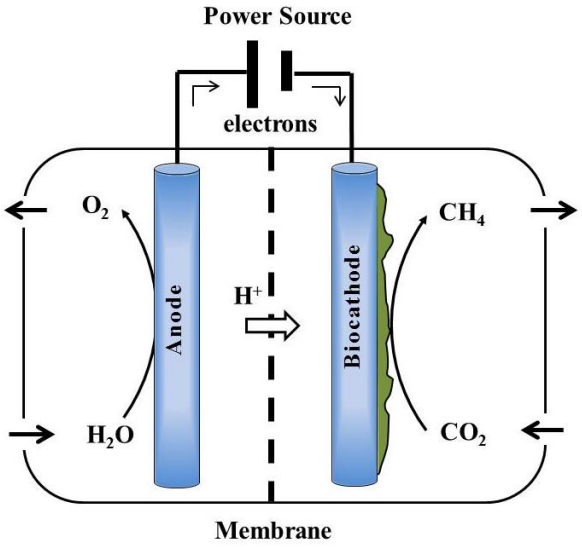

Figure 5. Schematic diagram of a dual-chamber methane-producing BES, with water as electron donor. These electrons from water oxidation flow from anode to the cathode driven by the applied power. To maintain electroneutrality, positive ions (e.g. protons) pass through a cation exchange membrane. Electrons are finally used by microorganisms to convert CO_2 to CH_4 in the biocathode.

To facilitate the methane production in the biocathode, the microorganisms present in the cathode must actively develop. Among the microorganisms, hydrogenotrophic methanogens (e.g. *Methanobacterium*) are prevalent and have been found to play an important role in the performance of methane-producing BESs (Siegert et al. 2015, Cai et

al. 2016a, Cheng et al. 2009). Therefore, the inoculum is mostly from an anaerobic environment which is rich in hydrogenotrophic methanogens, e.g. a mixture of microbiomes from anaerobic digesters (Siegert et al. 2015, Villano et al. 2010), sediments (Siegert et al. 2015), existing microbial electrolysis cell's anolyte effluents (Cheng et al. 2009), the petroleum reservoir's formation water (Kuramochi et al. 2013) and pure cultures of *Mehanobacterium*-like *archaeon* stain IM1(Beese-Vasbender et al. 2015a), as well as *Methanothermobacter thermautotrophicus* strain ΔH (Sato et al. 2013a).

Nowadays, it is generally accepted that water and wastewater (acetate) are the two applicable electron donors used for methane-producing BESs (Geppert et al. 2016a). Table 1 summarizes the aspects of these two kinds of electron donors. When wastewater (acetate) is used as electron donor, the main advantage is that wastewater can be treated simultaneously due to anodic microbial metabolism. Because these anodic microorganisms normally grow on carbon-based electrode materials (e.g. graphite felt/rod/plate), the cost of the anode electrode material is relatively inexpensive compared with anode electrode materials for water oxidation (e.g. platinum iridium plate). However, acetate cannot provide enough electrons for conversion of the total CO_2 within the system according to the stoichiometry of the whole reaction ($CH_3COOH \rightarrow CH_4 + CO_2$), the only way to obtain pure CH_4 in the off-gas of the whole system is to use other electron donors, like externally supplied H_2 from electrolysis of water. In addition, the methane production rate in the biocathode is limited by the anodic microbial metabolic rate, which is not a problem for the abiotic water oxidation. Overall, it is hard to judge which electron donor is better than the other. The suitable electron donor for methane-producing BESs depends on the goal of application and the available operational conditions.

Table 1. A comparison of two different electron donors: water and organic wastewater (acetate).

Water	Organic wastewater (acetate)
++ Adequate availability with natural supply (e.g. seawater).	+ Moderate availability depend on the location and discharge size.
+ O_2 produced as a valuable economic compound used on site (e.g. hospital).	- Overall a mixture of CO_2 and CH_4 produced without enough electrons to reduce all CO_2. .
- Performance deterioration due to O_2 diffusion from the anode to the cathode.	+ No risk of O_2 deterioration.
+ No nutrient addition for the abiotic anode.	- Nutrient addition for bioanode growth.
+ Unlimited reaction rate up to 10000 A/m^2.	- Limited reaction rate by bioanode activity lower than 100 A/m^2.
- Higher energy input	+ Low energy input
- High risk of anodic corrosion, only precious metal electrode is resistant to corrosion (e.g. iridium, platinum).	+ Less risk of anodic corrosion and inexpensive carbon-based electrode can be used (e.g. graphite felt/rod, activated carbon granules.
- Two-steps, upgrading the biogas outside anaerobic digester	+ One-step, placing the electrode inside anaerobic digester

1.5 Key parameters to assess performance of methane-producing BESs

Understanding the factors that influence the performance of methane-producing BESs has become the focus of the research field during the past decade. The pre-acclimation of inoculum with hydrogenotrophic methanogens has been shown to stimulate biocathode start-up and performance (Siegert et al. 2015, LaBarge et al. 2017). Different cathode materials affect the growth and adhesion of cathodic biofilm (Cheng et al. 2009, Zeppilli et al. 2016a, Van Eerten-Jansen et al. 2012, Siegert et al. 2014a). Anion exchange membrane showed lower energy demand per unit of removed CO_2 compared to cation exchange membranes (Zeppilli et al. 2016). Different electron donors also affect the system energy efficiency (Van Eerten-Jansen et al. 2012). In this thesis, we use the methane production rate and the system efficiencies (including current-to-methane, voltage and energy efficiencies) to assess the performance of methane-producing BESs. For bioelectrochemical systems, the energy input in the form of either cathode potential (potentiostatic operation) or cathodic current (galvanostatic operation) plays an important role in operating systems to obtain certain reation rates (Molenaar et al. 2016, Rabaey and Rozendal 2010). The cathode potential defines the thermodynamic driving force of the reaction and therefore affects the reaction rate, whereas the set cathode current defines the reaction rate directly and thus the potential has to be adjusted to ensure a certain reaction rate. In general, the results of these two electrical energy supply strategies are equal. However, cathode potential, rather than cathodic current, is typically controlled in most studies of methane-producing BESs (Geppert et al. 2016a). Therefore, we only elucidate the cathode potential in more detail in this thesis.

1.5.1 Cathode potential

Cathode potential is a key factor that determines the mechanisms of methane production from CO_2 reduction because the electrode potential is determined by the half-reaction taking place at the electrode. Figure 6 summarizes the different (bio)electrochemical reactions that occur at different cathode potentials on the biocathode of methane-producing BESs. The mechanisms of methane production on the biocathode are categorized into the direct electron transfer (Cheng et al. 2009) and the mediated electron transfer via hydrogen (Villano et al. 2010), formate and acetate (van Eerten-Jansen et al. 2015). The formation of these intermediates can be catalyzed by cell-derived enzymes on the cathodic electrode

surface (Deutzmann et al. 2015). Normally, these intermediates are rapidly consumed resulting in undetectable concentrations (Deutzmann et al. 2015). Therefore, many studies point out that the absence of detectable intermediates (hydrogen, formate and/or acetate) cannot serve as a solid proof for the direct electron transfer. Revealing the maze of mechanisms for the methane-producing biocathode have gained massive interest in the past years, although it is still unclear how these different mechanisms cope with each other at different operational parameters, such as cathode potential.

According to Figure 6, the more negative the cathode potential is poised, the more likely the mediated electron transfer occurs. So far, most of the methane-producing biocathodes are operated at cathode potentials more negative than -0.7 V vs. Ag/AgCl, as more negative cathode potential provides a larger driving force compared to the thermodynamic equilibrium, which will increase the current and thus result in higher methane production rates(Geppert et al. 2016a).

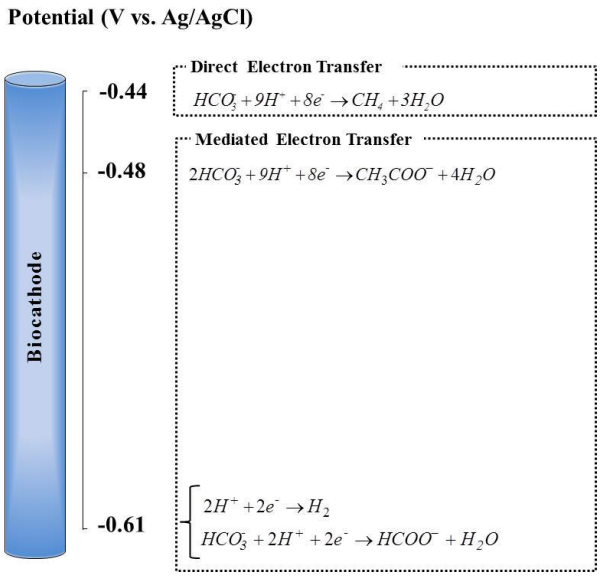

Figure 6. Overview of cathodic reactions in methane-producing BESs adapted from (Geppert et al. 2016a). The standard electrode potential was calculated based on Gibb's free energy of each half reaction at standard biological conditions (1 M or 1 bar for all the chemicals involved in each reaction, pH 7 and 298 K).

The equilibrium cathode potential at which the reaction takes place can be calculated according to the following procedures. Examples are shown for both direct conversion of CO_2 to CH_4 (1) and mediator production in the form of H_2 (2).

(1) For the direct electron transfer process, the reaction of CH_4 formation (Reaction 1.) is firstly written according to the International Union of Pure and Applied Chemistry (IUPAC) convention (Bard et al. 1985). Secondly, the cathode potential at actual conditions is then calculated based on the Nernst equation (Equation 1.)

$$HCO_3^- + 9H^+ + 8e^- \rightarrow CH_4 + 3H_2O$$ Reaction 1.

$$E_{cat} = E_{cat}^0 - \frac{RT}{8F}\ln\left(\frac{p_{CH_4}}{[H^+]^9[HCO_3^-]}\right) = -\frac{-175.46\times1000}{8\times96485} - \frac{8.314\times298}{8\times96485}\times\ln\left[\frac{1}{(10^{-7})^9\times1}\right] = -0.24\ V$$

Equation 1.

where $E_{cat}^0 = -\frac{\Delta G_r^0}{8F}$ is the standard cathode potential (0.23V); R is the ideal gas law constant (8.314 J/Kmol); T is the absolute temperature (298 K); F is Faraday's constant (96485 C/mol); P_{CH4} is the CH_4 partial pressure (1 bar); $[H^+]$ is the concentration of the protons at pH 7 (10^{-7} M); $[HCO_3^-]$ is the concentration of bicarbonate (1 M).

(2) For the mediated electron transfer via H_2 process, the reaction of H_2 evolution (Reaction 2.) is also written according to the IUPAC convention. Secondly, the cathode potential at biological conditions is then calculated based on the Nernst equation (Equation 2.).

$$2H^+ + 2e^- \rightarrow H_2$$ Reaction 2.

$$E_{cat} = E_{cat}^0 - \frac{RT}{8F}\ln\left(\frac{p_{H2}}{[H^+]^2}\right) = -\frac{-0\times1000}{8\times96485} - \frac{8.314\times298}{8\times96485}\times\ln\left[\frac{1}{(10^{-7})^2}\right] = -0.41\ V$$

Equation 2.

Where $E_{cat}^0 = -\frac{\Delta G_r^0}{8F}$ is the standard cathode potential (0 V); R is the ideal gas law constant (8.314 J/Kmol); T is the absolute temperature (298 K); F is Faraday's

constant (96485 C/mol); P_{H2} is the H_2 partial pressure (1 bar); $[H^+]$ is the concentration of the protons at pH 7 (10^{-7} M).

1.5.2 Methane production rate

To compare the performance of different methane-producing BESs, the methane production rate reported in the literature is normalized by the projected surface area or the geometric volume of the cathode electrode. Normalizing the performance to the project surface area of the cathode electrode is quite common in BES studies because the shapes of the electrode materials are mostly flat (Wei et al. 2011), e.g. graphite felt, carbon cloth/paper. However, it probably overestimates the performance when a three-dimensional (3D) porous conductive material is used as a cathode electrode. As shown in Figure 7, higher methane production rates were achieved by 3D cathode electrodes when the methane production rate is reported in terms of the project surface area of the cathode electrode. Therefore, normalizing performance to the geometric volume of the cathode electrode is reasonable for 3D natural electrode materials from an engineering perspective (Jourdin et al. 2015), e.g. activated granules, stainless steel foam. Collectively, both the electrode type and system configuration determine in which form the methane production rate are reported.

Herein we summarised methane production rates reported in methane-producing BES studies so far in terms of cathode project surface and cathode volume as shown in Figure 7. The methane production rate has not increased since 2009 and has reached the maximum value around 30 L CH_4/m^2 cat_{proj}/d in 2009 and 1.6 m^3 CH_4/m^3 cat/d in 2015. This maximum value is, however, negligible compared with methane production rates of 10000-33000 L CH_4/m^2 cat_{proj}/d in the technology coupling electrolyser (H_2 production) with biological methanation (discussed in the previous section) . These data are calculated based on current densities of 6000-20000 A/m^2 cat_{proj} achieved in the electrolysis process. We assume that current-to-hydrogen efficiency is 70% in the electrolysis process, and the hydrogen produced is used to generate CH_4 in biological methanation process (a stoichiometry of H_2/CH_4= 4) with only 5% of energy loss ends up in the microorganisms' metabolism and growth (Geppert et al. 2016a). Therefore, the key for practical application of methane-producing BES is to focus on obtaining high-rate methane production, to improve its competitiveness with other "Power-to-Gas" technologies.

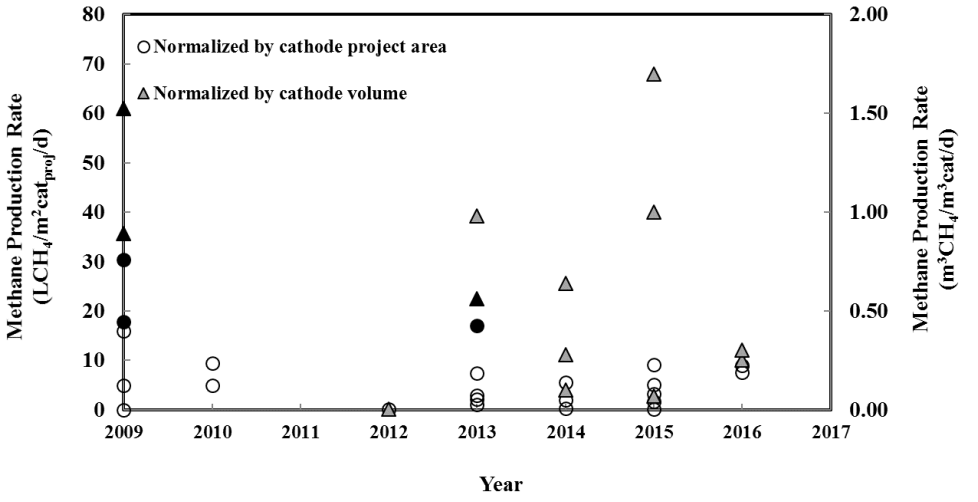

Figure 7. Development of methane production rate in methane-producing BESs (Geppert et al. 2016a). Methane production rates are expressed in the unites of L CH_4/m^2 cat_{proj}/d (circles) and m^3 CH_4/m^3 cat/d (triangles). The open circles and grey triangles represent the flat cathode electrodes, whereas the filled black circles and triangles indicate the 3D cathode electrodes. Since 2009, the maximum methane production rate has been quite stable. The methane production rates vary considerably among different studies because of different goals of each study and the methane-producing BESs performed under a variety of operational conditions and system set-ups.

1.5.3 Current-to-methane, voltage, and energy efficiencies

The current-to-methane efficiency is described (Van Eerten-Jansen et al. 2013a) as the efficiency of capturing electrons from the electric current in the form of CH_4, which is calculated as shown in Equation 3. In methane-producing BESs, the current-to-methane efficiency is normally lower than 100% as a result of competing electron consumption processes including biomass growth, generating side products like H_2 and/or volatile fatty acids (VFAs), and reducing oxygen which crossovers through an ion exchange membrane. In turn, the crossover of methane from cathode to anode through the ion exchange membrane can also occur, lowering the current-to-methane efficiency.

$$\eta_{\text{current-to-methane}} = \frac{N_{CH4\times}8\times F}{\int_{t=0}^{t} I\,dt} \qquad \text{Equation 3.}$$

Where N_{CH4} is the mole of methane produced during a certain amount of time (t); 8 is the moles of electrons demanding to produce per mole of CH_4; F is the Faraday constant (96485 C/mol e^-); I is the current (A).

The voltage efficiency is described as the part of the applied cell voltage which ends up as CH_4 in the form of Gibb's free energy of oxidation of CH_4 by oxygen into water (Van Eerten-Jansen et al. 2012), which is calculated as shown in Equation 4.

$$\eta_{voltage} = \frac{-\Delta G_{CH_4}}{E_{cell} \times 8 \times F} \qquad \text{Equation 4.}$$

Where ΔG_{CH_4} is the Gibb's free energy of oxidation of CH_4 (890 kJ/mol CH_4) (Rader and Logan 2010); E_{cell} is the applied cell voltage (V); 8 is the moles of electrons demanding to produce per mole of CH_4; F is the Faraday constant (96485 C/mol e^-).

Similar to the current-to-methane efficiency, the voltage efficiency normally cannot achieve 100%. The loss of the voltage efficiency is irreversible, involving the different processes in the methane-producing BES system (Figure 8.). The ionic voltage loss is attributed to the electrolyte resistance of the anolyte and catholyte, and electrode resistance (ter Heijne et al. 2006). The electrode overpotential is related to charge transfer process and mass diffusion process (He and Mansfeld 2009). For example, the biofilm on the biocathode catalyzes hydrogen evolution which significantly increases the charge transfer from the biocathode to the protons for hydrogen gas and/or atomic hydrogen production (Jeremiasse et al. 2010). The pH gradient voltage loss, especially over the membrane in a dual-chamber methane-producing BES, gradually develops during the operating time for two reasons: (1) two opposite half reactions taking place at these two chambers: protons are produced in the anode and in turn consumed in the biocathode (Zeppilli et al. 2016a); (2) the primary cations in the anolyte (e.g. Na^+, K^+), which are typically 10^5 higher concentrations than protons, transfer through cation exchange membrane instead of protons (Kim et al. 2007). The transport voltage loss is caused mainly by the membrane, which prevents the diffusion of certain kinds of ions between the anolyte and the catholyte (ter Heijne et al. 2006). Detailed calculations of these irreversible losses can be found in (Sleutels 2010).

The energy efficiency is described as the external electrical energy that ends up in CH_4 (Van Eerten-Jansen et al. 2012). The energy efficiency is calculated as Equation 5.

$$\eta_{energy} = \eta_{current-to-methane} \times \eta_{voltage} \quad \text{Equation 5.}$$

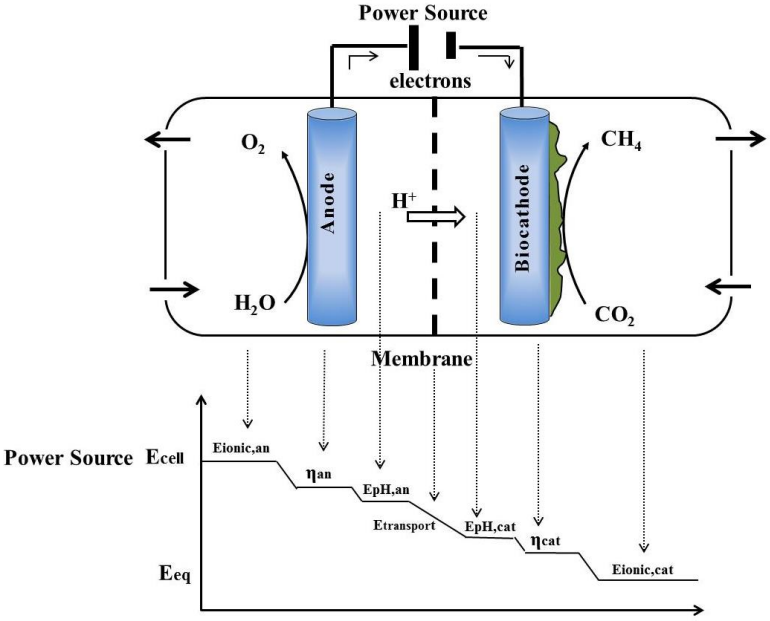

Figure 8. Overview of the voltage loss in a dual-chamber methane-producing BES. E_{cell} is the applied voltage from the power source. E_{eq} is the equilibrium voltage for conversion of CO_2 and H_2O into CH_4 and O_2. The difference between E_{cell} and E_{eq} represents irreversible losses, consisting: ionic loss divided into anodic ($E_{ionic,an}$) and cathodic part ($E_{ionic,an}$), anode overpotential (η_{an}), cathode overpotential (η_{cat}), transport loss at membrane ($E_{transport}$), and pH gradient loss separated into anodic ($E_{\Delta pH,an}$) and cathodic part ($E_{\Delta pH,cat}$).

1.6 Research objective and thesis outline

The objective of this thesis is ***to achieve an efficient methane production in methane-producing BESs and investigate its applicability in full-scale power-to-gas projects***. The efficient methane production means producing methane at high-rate with limited energy loss. We focus on improving the biocathode performance by exploring suitable cathode materials and discovering the distribution of energy loss to optimize the energy efficiency of our methane-producing BESs.

In Chapter 2, the use of heat-treated stainless steel felt as a novel methane-producing cathode is investigated. Comparing with non-treated stainless steel and graphite felt, we suppose to find an alternative metal-based electrode to carbon-based electrodes for methane-producing BESs. In Chapter 3, the high-rate methane production with low cathodic overpotential by using a carbon-based cathode material, i.e. granular activated carbon, under galvanostatic control is discovered and investigated. In Chapter 4, the effect of intermittent electricity supply on the performance of carbon-based biocathodes in methane-producing BESs is investigated. In Chapter 5, integrating methane-producing BES into low-temperature (10 ℃) anaerobic digestion is explored. The outcome is expected to expand the application of methane-producing BESs in wastewater treatment other than renewable electricity conversion and storage system.

Finally, in Chapter 6, we discuss the bottlenecks of methane-producing BESs based on the resutls of this PhD thesis. We evaluated the major issues that will occur when scaling-up methane-producing BESs, by performing a techno-economic analysis of a full-scale methane-producing BES for biogas upgrading. We compared methane-producing BESs with other competing power-to-gas technologies to find a profitable niche market for methane-producing BESs.

Reference

Azari, D., Torbaghan, S.S., Gibescu, M. and Meijden, M.A.M.M.v.d. (2014) The impact of energy storage on long term transmission planning in the North Sea region, pp. 1-6.

Bailera, M., Lisbona, P., Romeo, L.M. and Espatolero, S. (2017) Power to Gas projects review: Lab, pilot and demo plants for storing renewable energy and CO_2. Renewable and Sustainable Energy Reviews 69, 292-312.

Bard, A.J., Parsons, R. and Jordan, J. (1985) Standard Potentials in Aqueous Solution, Taylor & Francis.

Beese-Vasbender, P.F., Grote, J.-P., Garrelfs, J., Stratmann, M. and Mayrhofer, K.J.J. (2015) Selective microbial electrosynthesis of methane by a pure culture of a marine lithoautotrophic archaeon. Bioelectrochemistry 102(0), 50-55.

Cai, W., Liu, W., Yang, C., Wang, L., Liang, B., Thangavel, S., Guo, Z. and Wang, A. (2016) Biocathodic Methanogenic Community in an Integrated Anaerobic Digestion and Microbial Electrolysis System for Enhancement of Methane Production from Waste Sludge. ACS Sustainable Chemistry & Engineering 4(9), 4913-4921.

Chauhan, A. and Saini, R.P. (2014) A review on Integrated Renewable Energy System based power generation for stand-alone applications: Configurations, storage options, sizing methodologies and control. Renewable and Sustainable Energy Reviews 38, 99-120.

Chen, H., Cong, T.N., Yang, W., Tan, C., Li, Y. and Ding, Y. (2009) Progress in electrical energy storage system: A critical review. Progress In Natural Science 19(3), 291-312.

Cheng, S.A., Xing, D.F., Call, D.F. and Logan, B.E. (2009) Direct Biological Conversion of Electrical Current into Methane by Electromethanogenesis. Environmental Science & Technology 43(10), 3953-3958.

Decourt, B. and Debarre, R. (2013) Electricity storage. Leading the enrgy transition factbook. Schlumberger Business Consulting (SBC) Energy Institute, Gravenhage.

Demirbas, A. (2009) Global Renewable Energy Projections. Energy Sources, Part B: Economics, Planning, and Policy 4(2), 212-224.

Deutzmann, J.S., Sahin, M. and Spormann, A.M. (2015) Extracellular Enzymes Facilitate Electron Uptake in Biocorrosion and Bioelectrosynthesis. Mbio 6(2).

Ellabban, O., Abu-Rub, H. and Blaabjerg, F. (2014) Renewable energy resources: Current status, future prospects and their enabling technology. Renewable and Sustainable Energy Reviews 39, 748-764.

Fares, R.L. and Webber, M.E. (2017) The impacts of storing solar energy in the home to reduce reliance on the utility. Nature Energy 2, 17001.

Galán, E.M., Zhai, Y., Giner-Reichl, I., Hamilton, K., Salgado, R. and Sbroiavacca, N.R.D. (2016) renewables 2016-Global status report.

Geppert, F., Liu, D., van Eerten-Jansen, M., Weidner, E., Buisman, C. and Ter Heijne, A. (2016) Bioelectrochemical Power-to-Gas: State of the Art and Future Perspectives. Trends In Biotechnology.

Hashimoto, K. (1994) Metastable metals for "green" materials for global atmosphere conservation and abundant energy supply. Materials Science and Engineering: A 179, 27-30.

He, Z. and Mansfeld, F. (2009) Exploring the use of electrochemical impedance spectroscopy (EIS) in microbial fuel cell studies. Energy & Environmental Science 2(2), 215-219.

Huskinson, B., Marshak, M.P., Suh, C., Er, S., Gerhardt, M.R., Galvin, C.J., Chen, X., Aspuru-Guzik, A., Gordon, R.G. and Aziz, M.J. (2014) A metal-free organic-inorganic aqueous flow battery. 505(7482), 195-198.

Ibrahim, H., Ilinca, A. and Perron, J. (2008) Energy storage systems—characteristics and comparisons. Renewable and Sustainable Energy Reviews 12(5), 1221-1250.

Jeremiasse, A.W., Hamelers, H.V.M. and Buisman, C.J.N. (2010) Microbial electrolysis cell with a microbial biocathode. Bioelectrochemistry 78(1), 39-43.

Jourdin, L., Grieger, T., Monetti, J., Flexer, V., Freguia, S., Lu, Y., Chen, J., Romano, M., Wallace, G.G. and Keller, J. (2015) High Acetic Acid Production Rate Obtained by Microbial Electrosynthesis from Carbon Dioxide. Environmental Science & Technology 49(22), 13566-13574.

Kim, J.-H., Woo, H., Choi, J., Jung, H.-W. and Kim, Y.-T. (2017) CO_2 Electroreduction on Au/TiC: Enhanced Activity Due to Metal–Support Interaction. ACS Catalysis 7(3), 2101-2106.

Kim, J.R., Cheng, S., Oh, S.-E. and Logan, B.E. (2007) Power Generation Using Different Cation, Anion, and Ultrafiltration Membranes in Microbial Fuel Cells. Environmental Science & Technology 41(3), 1004-1009.

Kuramochi, Y., Fu, Q., Kobayashi, H., Ikarashi, M., Wakayama, T., Kawaguchi, H., Vilcaez, J., Maeda, H. and Sato, K. (2013) Electromethanogenic CO_2 Conversion by Subsurface-reservoir Microorganisms. Energy Procedia 37(0), 7014-7020.

LaBarge, N., Yilmazel, Y.D., Hong, P.-Y. and Logan, B.E. (2017) Effect of pre-acclimation of granular activated carbon on microbial electrolysis cell startup and performance. Bioelectrochemistry 113, 20-25.

Leonzio, G. (2016) Process analysis of biological Sabatier reaction for bio-methane production. Chemical Engineering Journal 290, 490-498.

Lozano, F.J., Lozano, R., Freire, P., Jiménez-Gonzalez, C., Sakao, T., Ortiz, M.G., Trianni, A., Carpenter, A. and Viveros, T. (2018) New perspectives for green and sustainable chemistry and engineering: Approaches from sustainable resource and energy use, management, and transformation. Journal of Cleaner Production 172, 227-232.

Lund, P.D., Lindgren, J., Mikkola, J. and Salpakari, J. (2015) Review of energy system flexibility measures to enable high levels of variable renewable electricity. Renewable and Sustainable Energy Reviews 45, 785-807.

Müller, K., Städter, M., Rachow, F., Hoffmannbeck, D. and Schmeißer, D. (2013) Sabatier-based CO_2-methanation by catalytic conversion. Environmental Earth Sciences 70(8), 3771-3778.

Molenaar, S.D., Mol, A.R., Sleutels, T.H.J.A., ter Heijne, A. and Buisman, C.J.N. (2016) Microbial Rechargeable Battery: Energy Storage and Recovery through Acetate. Environmental Science & Technology Letters 3(4), 144-149.

Park, D.H., Laivenieks, M., Guettler, M.V., Jain, M.K. and Zeikus, J.G. (1999) Microbial Utilization of Electrically Reduced Neutral Red as the Sole Electron Donor for Growth and Metabolite Production. Applied and Environmental Microbiology 65(7), 2912-2917.

Rabaey, K. and Rozendal, R.A. (2010) Microbial electrosynthesis - revisiting the electrical route for microbial production. Nature Reviews Microbiology 8(10), 706-716.

Rader, G.K. and Logan, B.E. (2010) Multi-electrode continuous flow microbial electrolysis cell for biogas production from acetate. International Journal Of Hydrogen Energy 35(17), 8848-8854.

Sato, K., Kawaguchi, H. and Kobayashi, H. (2013) Bio-electrochemical conversion of carbon dioxide to methane in geological storage reservoirs. Energy Conversion and Management 66, 343-350.

Schaaf, T., Grünig, J., Schuster, M.R., Rothenfluh, T. and Orth, A. (2014) Methanation of CO_2 - storage of renewable energy in a gas distribution system. Energy, Sustainability and Society 4(1), 2.

Siegert, M., Li, X.-f., Yates, M.D. and Logan, B.E. (2015) The presence of hydrogenotrophic methanogens in the inoculum improves methane gas production in microbial electrolysis cells. Frontiers in Microbiology 5.
Siegert, M., Yates, M.D., Call, D.F., Zhu, X., Spormann, A. and Logan, B.E. (2014) Comparison of Nonprecious Metal Cathode Materials for Methane Production by Electromethanogenesis. ACS Sustainable Chemistry & Engineering 2(4), 910-917.
Sleutels, T.H.J.A. (2010) Microbial electrolysis kinetics and cell design, s.n.], [S.l.
Sterner, M. (2009) Bioenergy and Renewable Power Methane In Integrated 100% Renewable Energy Systems: Limiting Global Warming By Transforming Energy Systems, Kassel University Press.
ter Heijne, A., Hamelers, H.V.M., de Wilde, V., Rozendal, R.A. and Buisman, C.J.N. (2006) A Bipolar Membrane Combined with Ferric Iron Reduction as an Efficient Cathode System in Microbial Fuel Cells. Environmental Science & Technology 40(17), 5200-5205.
Van Eerten-Jansen, M.C.A.A., Heijne, A.T., Buisman, C.J.N. and Hamelers, H.V.M. (2012) Microbial electrolysis cells for production of methane from CO_2: long-term performance and perspectives. International Journal Of Energy Research 36(6), 809-819.
van Eerten-Jansen, M.C.A.A., Jansen, N.C., Plugge, C.M., de Wilde, V., Buisman, C.J.N. and ter Heijne, A. (2015) Analysis of the mechanisms of bioelectrochemical methane production by mixed cultures. Journal of Chemical Technology & Biotechnology 90(5), 963-970.
Van Eerten-Jansen, M.C.A.A., Veldhoen, A.B., Plugge, C.M., Stams, A.J.M., Buisman, C.J.N. and Ter Heijne, A. (2013) Microbial Community Analysis of a Methane-Producing Biocathode in a Bioelectrochemical System. Archaea 2013, 12.
Villano, M., Aulenta, F., Ciucci, C., Ferri, T., Giuliano, A. and Majone, M. (2010) Bioelectrochemical reduction of CO_2 to CH_4 via direct and indirect extracellular electron transfer by a hydrogenophilic methanogenic culture. Bioresource Technology 101(9), 3085-3090.
Wei, J., Liang, P. and Huang, X. (2011) Recent progress in electrodes for microbial fuel cells. Bioresource Technology 102(20), 9335-9344.
Zeppilli, M., Lai, A., Villano, M. and Majone, M. (2016) Anion vs cation exchange membrane strongly affect mechanisms and yield of CO_2 fixation in a microbial electrolysis cell. Chemical Engineering Journal 304, 10-19.

Zervos, A., Lins, C. and Muth, J. (2010) RE-thinking 2050: a 100% renewable energy vision for the European Union, EREC.

Chapter 2. Heat-treated Stainless Steel Felt as a New Cathode Material in a Methane-producing Bioelectrochemical System

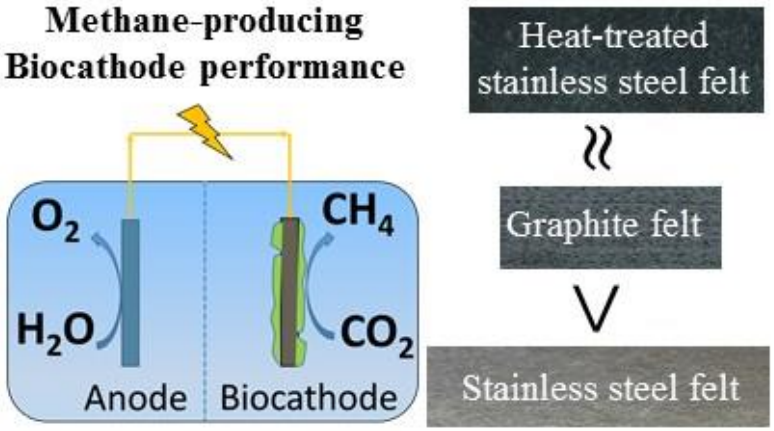

Heat-treated Stainless Steel Felt as a New Cathode Material in a Methane-producing Bioelectrochemical System

ABSTRACT

Methane-producing Bioelectrochemical Systems (BESs) is a promising technology to convert renewable surplus electricity into the form of storable methane. One of the key challenges for this technology is the search for suitable cathode materials with improved biocompatibility and low cost. Here, we study heat-treated stainless steel felt (HSSF) for its performance as biocathode. The HSSF had superior electrocatalytic properties for hydrogen evolution compared to untreated stainless steel felt (SSF) and graphite felt (GF), leading to a faster start-up of the biocathodes. At cathode potentials of -1.3 and -1.1 V, the methane production rates for HSSF biocathodes were higher than the SSF, while its performance was similar to GF biocathodes at -1.1 V and lower than GF at -1.3 V. The HSSF biocathodes had a current-to-methane efficiency of 60.8% and energy efficiency of 21.9% at -1.3 V. HSSF is an alternative cathode material with similar performance compared to graphite felt, suited for application in methane-producing BESs.

This chapter has been published as: Liu, D.; Zheng, T.; Buisman, C.; ter Heijne, A., Heat-Treated Stainless Steel Felt as a New Cathode Material in a Methane-Producing Bioelectrochemical System. *ACS Sustainable Chemistry & Engineering* **2017**.10.1021/acssuschemeng.7b02367.

INTRODUCTION

Renewable energy plays an important role in addressing the global energy crisis and environmental pollution, as it can reduce the demand for fossil fuels, and thus counteract the global warming caused by greenhouse gas (GHG) emissions (Twidell and Weir 2015). Renewable energy supplies, such as the wind and solar, are fluctuating and intermittent (Weitemeyer et al. 2015). Therefore, energy storage systems for integrating renewable energy into a balancing energy grid are essential (Weitemeyer et al. 2015). Power-to-Gas is an emerging renewable energy storage technology which can convert electrical energy into gas fuel (H_2 or CH_4) (Götz et al. 2016, Walker et al. 2016). This technology balances the grid with high flexibility and stability by creating a connection of electrical and gas networks (Bailera et al. 2017). A potentially convenient Power-to-Gas technology is methane-producing bioelectrochemical systems (BESs) which convert electricity and CO_2 into methane in one processing step(Eerten-Jansen et al. 2012, Geppert et al. 2016b). In methane-producing BESs, CO_2 serves as the sole carbon source at the biocathode and is reduced to CH_4 via direct and/or indirect pathways (via H_2) by microorganisms (Villano et al. 2010, Liu et al. 2016a).

Hydrogenotrophic methanogens that utilize hydrogen for their growth, such as *Methanobacterium* and *Methanobrevibacter*, are known to dominate on the cathode electrode(Cai et al. 2016a, Siegert et al. 2014b, van Eerten-Jansen et al. 2015, Van Eerten-Jansen et al. 2013b). To drive CH_4 production at reasonable rates, a cathode potential that is more negative than the theoretical hydrogen evolution potential (-0.61 V vs. Ag/AgCl, at pH 7, 1M solute concentration (Logan et al. 2008)) is usually applied. The additional cathode potential, i.e. the overpotential, reflects the extra energy investment at the cathode to drive the reaction. By introducing cathode materials that catalyze hydrogen evolution in methane-producing BESs, methane production could be enhanced, possibly at lower energy input.

Metal-based electrodes are known to catalyze hydrogen evolution reaction (HER)(Cai et al. 2016b), thereby stimulating methane production rate via hydrogenotrophic methanogenesis. Siegert et al. (2014) showed that a platinum electrode resulted in the highest biotic methane production rate (250±90 nmol cm^{-3} d^{-1}), and also abiotic hydrogen production rate (1600 ± 200 nmol cm^{-3} d^{-1}), compared with several different carbon-based and metal-based cathode

materials (Siegert et al. 2014a). However, platinum is an expensive material, which is a foreseeable practical barrier for implementing methane-producing BESs (Siegert et al. 2014a). Inexpensive metal-based electrode, e.g. stainless steel, are more cost-effective and applicable in methane-producing BESs.

Stainless steel has been found to be a good cathode material for hydrogen-producing biocathodes, with the performance comparable to platinum (Kundu et al. 2013). In addition, high durability and low cost of stainless steel compared with graphite felt are desirable in practical application(Wei et al. 2011). Recently, several strategies have been applied to enhance the performance of stainless steel as an electrode, e.g. surface modification (Kundu et al. 2013). Recently, Guo et al. (2015) demonstrated a simple and economical way to obtain 3D nanostructure stainless steel felt by applying heat treatment (Guo et al. 2015a). The presence of 3D iron oxide nanoparticles increased the biocompatibility of stainless steel materials, which resulted in several-fold enhancement in current density (up to about 1.5 ± 0.13 mA/cm^2) for bioanodes. These iron minerals can potentially enhance methane evolution by facilitating electron transfer between electrode and methanogens (Venzlaff et al. 2013). Heat-treated stainless steel felt may, therefore, be an attractive cathode material for methane-producing BESs. To our best knowledge, although stainless steel felt has been widely used as cathode material in methane-producing BESs, there are no studies investigating the potential of heat-treated stainless steel felt as cathode material in methane-producing BESs.

In this study, we examined the use of heat-treated stainless steel felt (HSSF) in a methane-producing BES and compared the performance of the HSSF with untreated stainless steel felt (SSF) and graphite felt (GF). The performance was investigated in terms of CH_4 production rate, current-to-methane efficiency, current-to-hydrogen efficiency, and energy efficiency at different cathode potentials of -1.3 V, -1.1 V and -0.8 V vs. Ag/AgCl. Polarization curves were used to determine the catalytic activity of different cathode electrode materials.

MATERIALS AND METHODS

Electrode Preparation. Three materials were tested as cathodes: Heat-treated stainless steel felt (HSSF), stainless steel felt (SSF) and graphite felt (GF). 0.28 cm thick GF (CGT Carbon GmbH, Germany) and 0.1 cm thick 316 L SSF (Lier Filter Ltd., China) were cut into a circle with a diameter of 5 cm. The projected surface area of each electrode was 20 cm^2. To obtain heat-treated stainless steel felt (HSSF), SSFs were treated in the same way as described by Guo et al.: placing SSFs into a muffle furnace at 600 °C for 5 minutes, and then taking out SSFs from the muffle furnace, and finally cooling them down under air to ambient temperature overnight (Guo et al. 2015b). Platinum foil (5 cm length × 2.5 cm width) with a projected surface area of 12.5 cm^2 was used as anode material for each reactor. Titanium wires (0.1 cm in diameter) served as current collector for both the anode and the cathode electrode.

Reactor Setup. Each reactor system consisted of 3 chambers, one anodic chamber in the middle facing two cathodic chambers (Figure 1). Each chamber had a cylindrical volume of 25 mL (5 cm diameter× 1.26 cm thickness) and the three chambers were separated by two Nafion® 117 cation exchange membranes (Sigma-Aldrich, Sigma, St, Louis, MO, USA) pretreated by boiling in H_2O_2 (30%), deionized (DI) water, 0.5 M H_2SO_4 and DI water, each solution for 1 hour at 80 °C(Oh and Logan 2006). In each reactor, two separate platinum foils were inserted in the middle anodic chamber to serve as anodes; the same cathode electrode material was used in these two cathodic chambers in order to perform duplicate testing. Each cathode chamber contained an Ag/AgCl reference electrode (3M KCl, ProSenseQiS, Netherlands). All potentials were measured and reported against the Ag/AgCl reference electrode.

The catholyte of each cathode chamber was connected via are circulation bottle (total catholyte volume of 500 mL) at a pump speed of 1.0 mL/min. The pH was measured daily and controlled in the range of 7.1 and 7.6 manually. Gasbags (500 mL, Cali-5-Bond™, Calibrated Instruments INC) were connected to the headspace (25 mL) of the recirculation bottle. All anodic chambers shared the same anolyte (in total 5 L) that was recirculated at a pump speed of 4.0 mL/min.

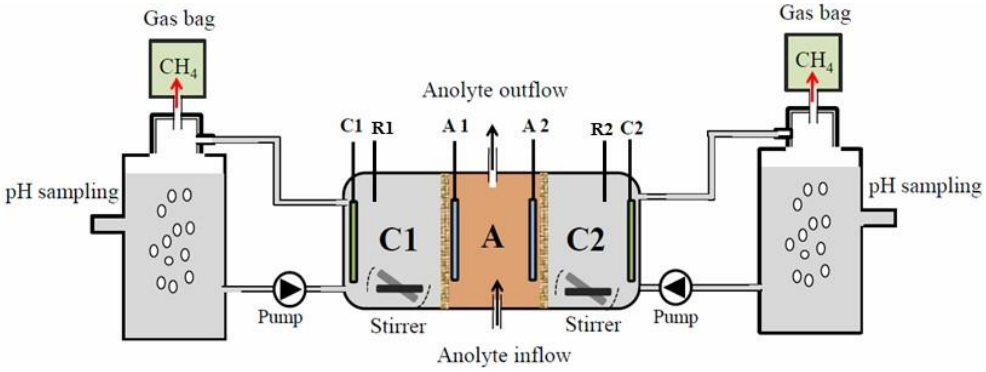

Figure1. Schematic overview of the methane-producing bioelectrochemical reactor. Each cathode material was tested in duplicate and was connected to one of the anodes in the anode chamber. Gas production was collected in the headspace of the recirculation bottle in combination with the 500 mL of the gas bag.

Inoculum and Electrolytes. Each cathode chamber was inoculated with 50 mL anaerobic sludge with a volatile suspended solids (VSS) concentration of 5.7 g/L, from the wastewater treatment plant in Ede, the Netherlands. The procedure of VSS measurement was according to the Standard Method 2540-E(Gilcreas 1966). The catholyte contained 0.2 g/L NH_4Cl, 0.13 g/L KCl, 1 mL/L vitamin and 1 mL/L mineral solution (Wolin et al. 1963a) and 50 mM phosphate buffer solution (4.58 g/L Na_2HPO_4 and 2.77 g/L $NaH_2PO_4 \cdot 2H_2O$). The catholyte was flushed with N_2 gas for 30 minutes before feeding to all cathode chambers of all cells and afterward, 5 g/L $NaHCO_3$ was added to the catholyte as a carbon source. The anolyte contained the same phosphate buffer (50 mM) as the catholyte solution. The anolyte was flushed with N_2 continuously to minimize dissolved oxygen diffusion across the membrane from anodic to cathodic chamber.

Reactor Operation. The cell voltage of each reactor was controlled by an FP-AO-210 module (National Instruments Field Point system, Austin, Texas). The applied voltage was controlled and adapted to reach a certain cathode potential. The current was measured by the voltage difference over a 10 Ω resistor in the electrical circuit between the anode (counter electrode) and the power source. The cathode potentials (measured versus the Ag/AgCl reference electrode) and voltages over the resistor were recorded every minute

using LabVIEW, supported by an FP-AI-110 module (National Instruments Field Point system, Austin, Texas).

For a start-up, all biocathodes were controlled at -0.9 ± 0.03 V for three weeks to allow methanogenic growth, as -0.9 V is a typical cathode potential for methane-producing biocathode(van Eerten-Jansen et al. 2015, Van Eerten-Jansen et al. 2013b). After the start-up phase, each cathode was controlled for 4 weeks first at -1.1 ± 0.03 V, afterward at -0.8 ± 0.03 V and finally at -1.3 ± 0.03 V. When the cathode potential deviated more than 30 mV from the desired cathode potential, the cell voltage was adjusted to reach the desired cathode potential. Each reactor was operated in batch with a length of 168 hours. Four batches were performed at each cathode potential to achieve stable performance (at least two similar batches). Each batch was started by replacing half of the catholyte with fresh medium to ensure sufficient HCO_3^-, nutrients, and buffer.

Gas Analysis. Two or four measurements were done per batch to analyze the methane production rates. The gas volume was determined by emptying the gas bags with a syringe. A gas sample of each cathode chamber was taken from the headspace through the butyl rubber stopper. The gas composition in the headspace was identical to that in the gas bag because the headspace was connected with the gas bag. The gas composition produced at the cathode by two types of gas chromatography: the HP 5890A gas chromatograph and the Finsons Instruments GC 8340 gas chromatograph. The HP 5890A gas chromatograph measured H_2 by injecting 100 µL of a gas sample into a molecular sieve column with thermal conductivity detection (TCD); the Finsons Instruments GC 8340 gas chromatograph measured CH_4, CO_2, O_2, and N_2 by injecting 50 µL of a gas sample into a molecular sieve column with TCD 90 ºC.

The cumulative methane yield was calculated as follows:

$$V_{CH_{4,t}} = (V_{T,t} + V_{hs}) \times C_{CH_{4,t}} \quad (1)$$

Where $V_{CH_{4,t}}$ was the cumulative methane production (mL) at sampling time t; $V_{T,t}$ was the total gas production collected in the gas bag (mL); V_{hs} is the headspace volume (mL); $C_{CH_{4,t}}$ represented the methane concentration (%).

The methane production rate was calculated over the entire batch and normalized to the cathode electrode projected surface area:

$$\gamma_{CH4-A} = \frac{V_{CH4,total}}{A_{proj} \times t} \quad (2)$$

Where γ_{CH4-A} represents methane production rate (L $CH_4/m^2cat_{proj}/d$); $V_{CH4,total}$ is the total amount of methane yield over the entire batch (L); A_{proj} is the projected surface area of the cathode electrode (20 cm^2); t is the experimental time between each sample (day).

VFA Analysis. The volatile fatty acids (VFA), herein including formate, acetate, and lactate, were measured by High-Performance Liquid Chromatography (HPLC) (Lindeboom et al. 2016). Each Liquid sample was centrifuged for 10 min at 10000 RCF, and then 1 mL of the supernatant was directly put into the sample vial. Samples were injected by an autosampler and separated with an Alltech OA-1000 column at 60 °C and 6.0-6.5 MPa.

Dissolved CH_4 Analysis. The dissolved CH_4 was measured by following procedures (Zhang et al. 2013a): 1) adding 5.3 g NaCl into a 50 mL tube sealed by a stopper; 2) extracting 20 mL of air from the tube using a syringe with a needle; 3) slowly injecting 15 mL of the catholyte into the tube; 4) shaking the tube for fully mixing the salt and catholyte; 5) waiting for 30 min to make sure CH_4 get out to the gas phase; 6) measuring the pressure by the pressure meter (GMH 3150, Germany); 7) measuring gas composition by the gas chromatography (Finsons Instruments GC 8340); 8) The amount of dissolved CH_4 was calculated by following formula:

$$n_{CH4-dissovled} = \frac{P \times C \times V}{R \times T} \quad (3)$$

Where $n_{CH4-dissovled}$ represents the moles of dissolved methane; P is the pressure of headspace in the sample tube (kPa); C is the methane percentage (%) in the headspace of the tube; V is headspace volume in the tube (0.035 L); R is the gas constant value (8.314 $J \cdot mol^{-1} \cdot K^{-1}$) ; T is 293 K.

Cathodic Efficiency (η_{CE}). The efficiency of capturing electrons from the electric current in products is the sum of current-to-methane efficiency (η_{CH4}) and current-to-hydrogen efficiency (η_{H2}). The efficiency of capturing the electrons from the electric current in methane or hydrogen was calculated via:

$$\eta_{CH4} = \frac{N_{CH4} \times 8 \times F}{\int_{t=0}^{t} I \, dt} \quad (4)$$

$$\eta_{H2} = \frac{N_{H2} \times 2 \times F}{\int_{t=0}^{t} I \, dt} \quad (5)$$

$$\eta_{CE} = \eta_{CH4} + \eta_{H2} \quad (6)$$

Where N_{CH4} is the total moles of methane produced; N_{H2} is the total moles of hydrogen produced; F is the Faraday constant (96485 C/mole e^-); I is the current (A), and t is the time (s).

Voltage Efficiency ($\eta_{voltage}$) is described as the part of the applied cell voltage that ends up in methane, and was calculated as:

$$\eta_{voltage} = \frac{-\Delta G_{CH_4}}{E_{cell} \times 8 \times F} \quad (7)$$

Where ΔG_{CH_4} is the Gibb's free energy of methane oxidation (-890.4 kJ/mol CH_4)(Eerten-Jansen et al. 2012); E_{cell} is the applied cell voltage (V), F is the Faraday constant (96485 C/mole e^-)

Energy efficiency (η_{energy}) was calculated by taking the product of η_{CH4} and $\eta_{voltage}$, which represents the part of the external electrical energy that ends up in methane(Eerten-Jansen et al. 2012).

Electrochemical Analysis. Polarization tests were performed every two weeks using a potentiostat (Ivium Technologies, Eindhoven, the Netherlands). For the polarization test,

the cathode potential was decreased from -0.7 V to -1.1 V with steps of 0.1 V. Each step lasted for 10 minutes while the catalytic current was recorded was plotted according to the literature (Liu et al. 2016a).

Scanning electron microscopy. Surface morphology of the biofilms on different cathode materials was analyzed by a scanning electron microscope (SEM, FEI Magellan 400). All samples were pretreated in the same method according to the standard procedure (Postma et al. 2013). Processing of SEM images was performed at Wageningen Electron Microscopy Center (WemC, The Netherlands).

RESULTS

Methane Yields and Methane Production Rates. To achieve stable performance, each biocathode underwent four batches (one week per batch) at -1.3 V, -1.1 V and -0.8 V. The average methane production rates for the duplicates achieved in the last two stable cycles are shown in Figure 2. When cathode potentials were controlled at -1.3 V, the methane production rate of HSSF was 7.2 L $CH_4/m^2cat_{proj}/d$, which was 1.4 times higher than that of SSF. It was lower than the methane production rate of 8.8 L $CH_4/m^2cat_{proj}/d$ for GF. At a cathode potential of -1.1 V, HSSF and GF had similar methane production rates of 1.0 L $CH_4/m^2cat_{proj}/d$, which was higher than that of SSF with 0.7 L $CH_4/m^2cat_{proj}/d$. At a cathode potential of -0.8 V, methane production for all three materials was low. The highest methane production rate was in the SSF of around 0.08 L $CH_4/m^2cat_{proj}/d$, followed by the HSSF of 0.02 L $CH_4/m^2cat_{proj}/d$, while methane production rates of the GF were below 0.0015 L $CH_4/m^2cat_{proj}/d$. As the thickness of the electrodes could affect the availability of substrate, proton diffusion (from catholyte to electrode) and biofilm development on the electrode, the different thickness electrodes between (GF 3 cm and SSF 1cm) could affect the results of our study. On the other hand, Sleutels, T et al. has shown that anode electrode(felt) thickness between 1 mm to 3 mm did not affect the current density (normalized to projected surface area) in Microbial Electrolysis Cells(Sleutels et al. 2009a). From an engineering perspective, we normalized each methane production rate by the volume of its cathode electrode (GF 5.6 cm^3; SSF/HSSF 2 cm^3). HSSF showed the superiority over GF, for example, the methane production rate in HSSF at -1.3 V was 2.3 times higher than that in GF.

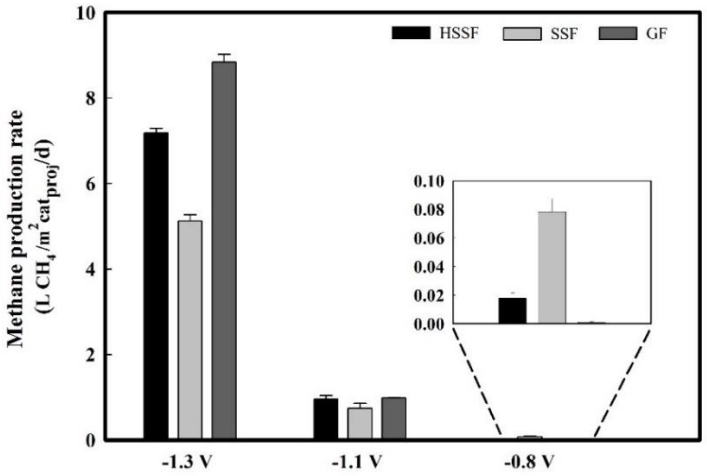

Figure 2. Methane production rate calculated at cathode potentials of -1.3 V, -1.1 V and -0.8 V by taking an average of the cycle 3 and 4. Highest methane production rate was achieved at the most negative potential. Error bars indicate the standard deviation, calculated from duplicate reactors of the last two stable cycles.

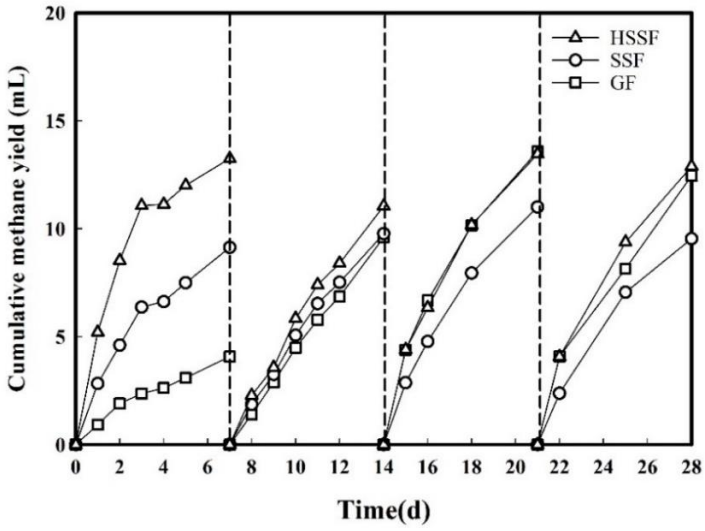

Figure 3. Cumulative methane yields over four consecutive batches for all the three cathode materials at the cathode potential of -1.1 V. The dashed lines indicate 50 % medium replacement at the end of each batch.

Cumulative methane yields over four consecutive batches for all three cathode electrodes at -1.1 V are shown in Figure 3. Within each batch, a clear increase in cumulative methane yield over time was observed for all cathode materials. Within each batch, the HSSF had a stable methane yield between 11 and 13 mL. The SSH had a stable but lower methane yield of around 9 mL. The GF had the lowest methane yield (4 mL) in the first batch, however, it increased to the same level (12 mL) as HSSF in batch 3 and batch 4.

System Efficiency. The total cathodic efficiency (η_{CE}) represents the part of electrons that end up in products (CH_4 and/or H_2) and is shown in Figure 4. The highest total cathodic efficiency (including CH_4 and H_2), between 60 and 80%, was found for the biocathodes controlled at -1.3 V, which had highest current densities. At less negative cathode potentials (-0.8 V and -1.1 V), the cathodic efficiency decreased to below 35%. Slight differences were observed between the materials, with no clear relation between material and η_{CE}. In addition to methane and hydrogen, dissolved methane (Zhang et al. 2013a) and volatile fatty acids (VFAs) (Fernandes et al. 2015) were analyzed to see if these could explain the low cathodic efficiencies. However, neither dissolved methane nor VFAs were detected in any of the experiments.

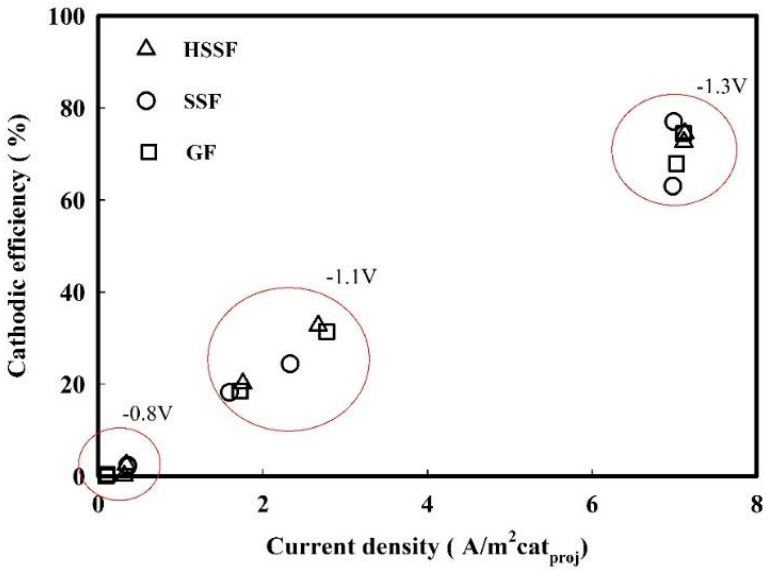

Figure 4. Total cathodic efficiency versus current density of the GF, the SSF and the HSSF at different cathode potentials of -0.8 V, -1.1 V and -1.3 V.

To further analyze the system efficiency, the results of the current-to-methane(η_{CH4}), current-to-hydrogen (η_{H2}) and energy efficiency (η_{energy}) for the different potentials of these different electrode materials are shown in Table 1. Highest current-to-methane efficiency was 60.8% for HSSF at -1.3 V, 56.9% for SSF at -1.3 V and 69.4% for GF at -1.3 V. Hydrogen was only detected at -1.3 V for all cathode materials. HSSF and the GF obtained a similar current-to-hydrogen efficiency of around 40% at the beginning of the batch (Day 1-2), which was higher than that of SSF (30%). However, the HSSF reached a current-to-hydrogen efficiency of 23% at the end of the batch (Day 4-7), which was similar as that of SSF but higher than that of GF (16%). In general, the current-to-hydrogen efficiency decreased with increasing current-to-methane efficiency within each batch, for all cathode materials at the cathode potential of -1.3 V.

The applied voltage in methane-producing BESs can be divided into two parts: a reversible potential loss recovered in CH_4, and an irreversible potential loss dissipated in the form of electrode overpotential, ionic losses and pH gradient over the membrane (Sleutels et al. 2009b). The irreversible potential is the lost energy and reflects the extra voltage required in addition to the thermodynamical equilibrium voltage of CH_4 generation from CO_2 and H_2O (1.06 V at standard conditions, which is 1 mole 1 bar for all chemicals involved in the reaction, pH 7 and 298 K)(Geppert et al. 2016b). Thus, the higher the applied voltage, the lower the voltage efficiency. In this study, the cell voltages were similar for all three cathode materials at each cathode potential, which were around 2.1 ± 0.2 V, 2.8 ± 0.1 V and 3.5 ± 0.3 V for cathode potential of -0.8 V, -1.1 V and -1.3 V, respectively. Therefore, the voltage efficiency was similar for all three cathode materials. The voltage efficiency was 33% at -1.3 V, 41% at -1.1 V, and 55% at -0.8 V. The energy efficiency was calculated as the product of voltage efficiency and current efficiency. The highest energy efficiency was found for HSSF: 22% at -1.3 V, decreasing to 14% at -1.1 V, and further decreasing to 1% at -0.8 V. At each cathode potential of -1.3 V, -1.1 V and -0.8 V, the energy efficiency of HSSF was similar to the energy efficiency of GF and higher than that of SSF.

Table 1. Overview of the average current-to-methane efficiency, current-to-hydrogen efficiency, and energy efficiency of each cathode material at different cathode potentials. The average and standard deviation (less than 5%, not shown) were calculated based on 4 separate samples, which were taken from 2 weeks of stable performance (Batch 3 and Batch 4) with duplicate cathode electrodes for each cathode material. The current-to-hydrogen efficiencies for all reactors were zero at -1.1 V and -0.8 V, which are not included in this table.

	Relative Period in	**-1.3V**			**-1.1V**		**-0.8V**	
Material	**Batch 3 and 4[a]**	**η_{CH4} (%)**	**η_{H2} (%)**	**η_{energy} (%)**	**η_{CH4} (%)**	**η_{energy} (%)**	**η_{CH4} (%)**	**η_{energy} (%)**
GF	Day 0-1	-	-	-	31.8	13.1	2.6	1.4
	Day 1-2	33.6	41.4	11.1	20.3	8.4	1.4	0.8
	Day 2-4	-	-	-	19.2	7.9	1.1	0.6
	Day 4-7	69.4	15.5	22.9	14.5	6.0	0.5	0.3
SSF	Day 0-1	-	-	-	22.9	9.4	10.0	5.5
	Day 1-2	28.2	30.6	8.1	18.6	7.7	5.2	2.9
	Day 2-4	-	-	-	17.7	7.3	4.7	2.6
	Day 4-7	56.9	22.9	16.4	12.7	5.2	2.4	1.3
HSSF	Day 0-1	-	-	-	32.9	13.6	2.4	1.3
	Day 1-2	27.8	43.8	10.0	18.7	7.7	1.1	0.6
	Day 2-4	-	-	-	17.7	7.3	0.9	0.5
	Day 4-7	60.8	22.8	21.9	13.7	5.6	0.2	0.1

a. For example, Day 0-1 refer to Day 14-15 and Day 21-22 within 4 consecutive operational batches at each cathode potential.

Electrochemical Analysis. Polarization curves of the three different cathode materials were analyzed before inoculation and after the operation at the cathode potential of -0.8 V (Figure 5). For the abiotic test, there was a clear difference between the three cathode materials in terms of catalytic behavior for the hydrogen evolution reaction (HER). The onset potential of the HER of HSSF started already at -0.6 V, which was less negative than that of SSF (-0.8 V). The GF, however, showed almost no catalytic current for the HER in the chosen potential range. After biofilm growth, there was hardly any difference in polarization behavior between the three cathode materials. The onset potential of the reaction (hydrogen or methane production) for all the cathode materials was around -0.8 V. The cathodic current of HSSF was similar before and after inoculation. However, after inoculation, the cathodic current of GF and SSF increased to values almost the same as the HSSF, showing that the biofilm catalyzed either hydrogen or methane production more effectively than the bare material (Rozendal et al. 2008). At cathode potentials, less negative than -0.8 V, a small positive current was observed for HSSF and SSF in the polarization curves. This indicates that these materials may be prone to corrosion if used under typical anode conditions (Ledezma et al. 2015), although this effect was not observed in our study as biocathode.

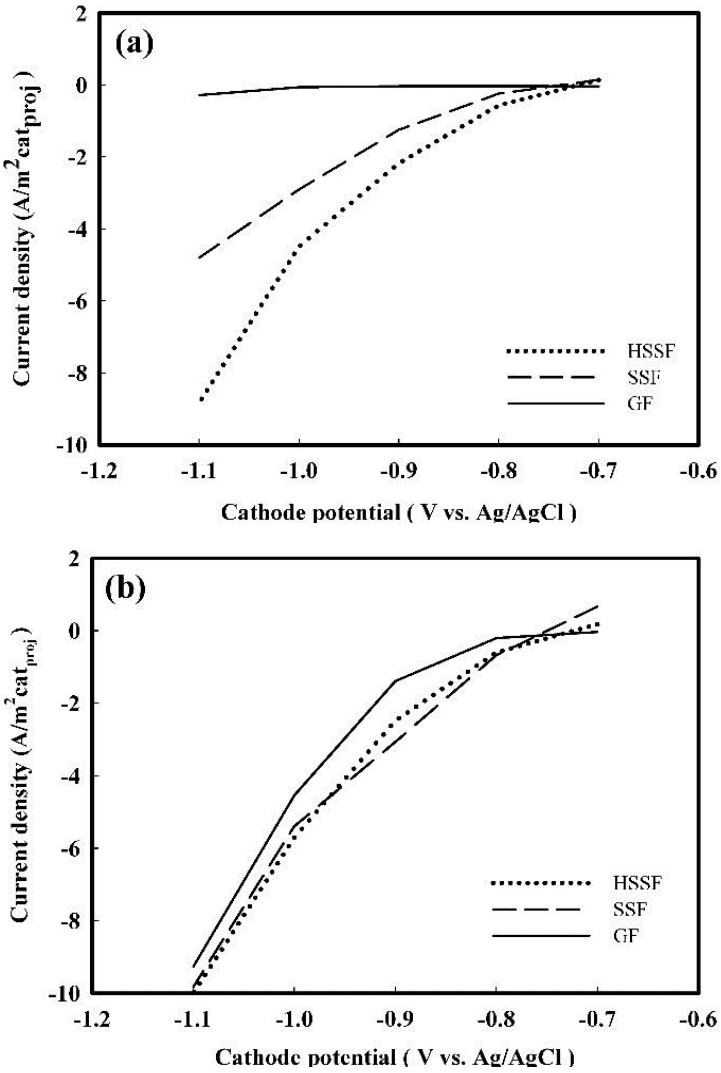

Figure 5. Polarization curves of three different cathode materials before inoculum (a) and after growth at the cathode potential of -0.8 V (b).

Morphology of Biofilm. SEM images of three different biocathodes showed the presence of microorganisms on the surface of the three cathode materials (Figure 6). In general, good coverage of biofilm on the GF electrode was observed, whereas for SSF and HSSF, biofilm coverage was less dense.

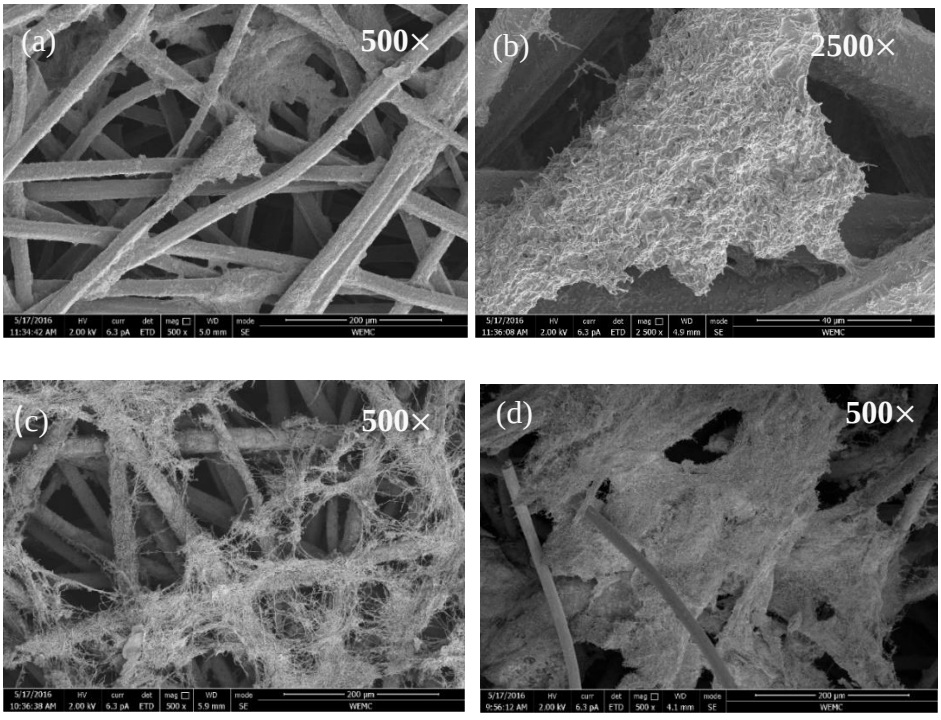

Figure 6. SEM images of microorganisms' attachment on the surface of the HSSF (a and b), SSF (c), and GF (d) after growth at the cathode potential of -1.3 V for almost one month.

DISCUSSION

After the start-up phase, all reactors were poised at a cathode potential of -1.1 V, which could be sufficient to drive the hydrogen evolution reaction (HER), especially for HSSF and SSF, as shown in the polarization curves (Figure 5a). The HER in the HSSF and the SSF probably promoted methane production with a faster start-up process, whereas the poor HER of GF resulted in lower methane production yield in the first biotic batch. In the absence of H_2, the growth of methanogens may be slower because hydrogenotrophic methanogenesis (indirect via H_2) has been suggested as a vital pathway for the methane-producing BESs(Siegert et al. 2014b). The heat treatment process enhanced the performance of the SSF both in abiotic HER (Figure 5a) and in methane production yield at more negative cathode potentials, i.e. -1.1 V and -1.3 V (Figure 2). This can be attributed to the formation of 3D iron oxide nanoparticles on the surface of the HSSF. It has been found that nano-structured electrodes could increase the abiotic reaction rate by enlarging the electro-active surface area, and also stimulate the development of an electro-active biofilm by proving additional anchoring points for microbial adhesion (Guo et al. 2015a). The SEM images showed that microorganisms on the HSSF seemed to form a matrix of extracellular polymeric substances (EPS) which allowed adhesion of cell-to-cell and cell-to-electrode surface (Figure 6b), whereas the microorganisms on the SSF formed a loose matrix (Figure 6c). It has also found that the HSSF bioanode could facilitate a robust electro-active biofilm formation and increased current generation in BESs: current densities achieved for bioanodes on HSSF were several-fold higher than for SSF and the carbon-based felt (Guo et al. 2014, Guo et al. 2015c). When applied as biocathode for methane production, however, HSSF had similar performance to GF at the cathode potential of -1.1 V, and its performance was slightly lower than GF at the cathode potential of -1.3 V. The fact that HSSF showed lower improvement compared to GF when used as cathode than as anode could be due to different mechanisms for electron transfer between microorganisms and the electrode. At a cathode potential of -0.8 V, the low methane production rates obtained in all the biocathodes was in line with the results from polarization curve (Figure 5b), which indicated that cathode potential of -0.8 V was not negative enough to obtain a substantial current in all these biocathodes. It is worth noticing that the methane yield for GF gradually increased, and reached similar and stable performance as HSSF during Batch 3 and Batch 4 at the cathode potential of -1.1 V (Figure 3). Furthermore, polarization curves changed after the biofilm developed on GF (Figure 5): (a) current density increased considerably after

biofilm formation (biotic GF) compared to abiotic tests at the same potential, and b) the onset potential for hydrogen evolution was less negative in the biotic case compared to the abiotic experiments. These results suggest that the presence of biofilm on the GF could play a role by catalyzing hydrogen evolution that enhances methane production (Siegert et al. 2014a, Batlle-Vilanova et al. 2014). Although no hydrogen was detected in the headspace, it might have been directly consumed by the methanogens(Geppert et al. 2016b). As GF is a material with good biocompatibility (Wei et al. 2011), there was evidence for a dense biofilm formation on the GF in one of the SEM images (Figure 6d).

Concerning cathodic efficiency, the impact of dissolved methane and volatile fatty acids (VFAs) was eliminated as neither dissolved methane or VFAs were detected. However, it is confirmed by Van Eerten-Jansen et al. that using water as anolyte can lower cathodic efficiency compared to other anolytes(Eerten-Jansen et al. 2012), e.g. hexacyanoferrate (II) or acetate. Oxygen diffusion through the membrane from the anode to the cathode can lead to a lower cathodic efficiency, as oxygen was the most favorable compound to be reduced at the cathode(Eerten-Jansen et al. 2012, Min and Logan 2004). In this study, around one percent of oxygen was found in the headspace of cathode circulation bottle, which suggested oxygen diffusion and its reduction was occurring continuously at the cathode. This process can consume electrons and lower cathodic efficiencies. A low cathodic efficiency (below 35% at cathode potentials of both -0.8 V and -1.1 V) can also be caused by other factors that vary with studies: inoculum, catholyte, biomass growth, membrane, system configuration and duration of the experiment(Siegert et al. 2014b, Sleutels et al. 2011, Zeppilli et al. 2016b).

Furthermore, we observed that the cathodic efficiency was related to the current densities rather than to the cathode materials, with higher efficiencies found for higher current densities. In contrast, the voltage efficiency decreased with the increased current density because of the higher applied voltages. Therefore, there is a trade-off between the two, with somewhere an optimum at which the highest energy efficiency is achieved. This study is one of the first ones analyzing the energy efficiency of methane-producing BES in more detail, with maximum values of 22% (Table 1), values similar as those determined for short term yield tests in another study utilizing water as the electron donor(Eerten-Jansen et al. 2012). The energy efficiency is a crucial factor to determine the performance of the

methane-producing BESs and to assess its capability as an energy storage system(Geppert et al. 2016b). Further increase in energy efficiency is required, which need to be achieved by further improvements in system's performance, to bring methane-producing BESs closer to the application.

CONCLUSIONS

Heat treatment of stainless steel felt improved methane production rates of SSF in the methane-producing BESs when operated at -1.1 V and -1.3 V vs. Ag/AgCl, with performance similar to GF. HSSF had a maximum current-to-methane efficiency of 60.8% and energy efficiency of 21.9% at -1.3 V. These values were similar to the ones found for GF, and higher than those for untreated SSF. Moreover, HSSF had better electrocatalytic property for hydrogen evolution, leading to a fast start-up of the biocathode. HSSF is an alternative cathode material with similar performance compared to graphite felt, suited for application in methane-producing BESs.

ASSOCIATED CONTENT

Supporting Information. Cumulative methane yields over four consecutive batches for all the three cathode materials at the cathode potential of -1.3 V (Figure S1.) and -0.8 V (Figure S2.).

ACKNOWLEDGMENT

The authors would like to thank Kun Guo for supplying the electrode material of stainless steel felt, and thank Marijke Hamelers for her help with setting up the reactors. Besides, we thank Marcel Giesbers for his efforts for biocathode sample pretreatment and execution of scanning electron microscopy. The project was sponsored by two Dutch companies (Alliander, DMT Environmental Technology), together with Chinese Scholarship Council (File No.201306120043).

REFERENCES

Bailera, M., Lisbona, P., Romeo, L.M. and Espatolero, S. (2017) Power to Gas projects review: Lab, pilot and demo plants for storing renewable energy and CO_2. Renewable and Sustainable Energy Reviews 69, 292-312.

Batlle-Vilanova, P., Puig, S., Gonzalez-Olmos, R., Vilajeliu-Pons, A., Bañeras, L., Balaguer, M.D. and Colprim, J. (2014) Assessment of biotic and abiotic graphite cathodes for hydrogen production in microbial electrolysis cells. International Journal Of Hydrogen Energy 39(3), 1297-1305.

Cai, W., Liu, W., Han, J. and Wang, A. (2016a) Enhanced hydrogen production in microbial electrolysis cell with 3D self-assembly nickel foam-graphene cathode. Biosensors and Bioelectronics 80, 118-122.

Cai, W., Liu, W., Yang, C., Wang, L., Liang, B., Thangavel, S., Guo, Z. and Wang, A. (2016b) Biocathodic methanogenic community in an integrated anaerobic digestion and microbial electrolysis system for enhancement of methane production from waste sludge. ACS Sustainable Chemistry & Engineering 4(9), 4913-4921.

Eerten-Jansen, V., Mieke, C., Heijne, A.T., Buisman, C.J. and Hamelers, H.V. (2012) Microbial electrolysis cells for production of methane from CO_2: long-term performance and perspectives. International Journal of Energy Research 36(6), 809-819.

Fernandes, T.V., van Lier, J.B. and Zeeman, G. (2015) Humic Acid-Like and Fulvic Acid-Like Inhibition on the Hydrolysis of Cellulose and Tributyrin. BioEnergy Research 8(2), 821-831.

Geppert, F., Liu, D., van Eerten-Jansen, M., Weidner, E., Buisman, C. and ter Heijne, A. (2016) Bioelectrochemical power-to-gas: State of the art and future perspectives. Trends in Biotechnology 34(11), 879-894.

Gilcreas, F. (1966) Standard methods for the examination of water and waste water. American Journal of Public Health and the Nations Health 56(3), 387-388.

Götz, M., Lefebvre, J., Mörs, F., McDaniel Koch, A., Graf, F., Bajohr, S., Reimert, R. and Kolb, T. (2016) Renewable Power-to-Gas: A technological and economic review. Renewable Energy 85, 1371-1390.

Guo, K., Donose, B.C., Soeriyadi, A.H., Prévoteau, A., Patil, S.A., Freguia, S., Gooding, J.J. and Rabaey, K. (2014) Flame Oxidation of Stainless Steel Felt Enhances Anodic Biofilm Formation and Current Output in Bioelectrochemical Systems. Environmental Science & Technology 48(12), 7151-7156.

Guo, K., Prévoteau, A., Patil, S.A. and Rabaey, K. (2015a) Engineering electrodes for microbial electrocatalysis. Current Opinion In Biotechnology 33(0), 149-156.
Guo, K., Soeriyadi, A.H., Feng, H., Prévoteau, A., Patil, S.A., Gooding, J.J. and Rabaey, K. (2015b) Heat-treated stainless steel felt as scalable anode material for bioelectrochemical systems. Bioresource Technology 195, 46-50.
Guo, K., Soeriyadi, A.H., Feng, H., Prévoteau, A., Patil, S.A., Gooding, J.J. and Rabaey, K. (2015c) Heat-treated stainless steel felt as scalable anode material for bioelectrochemical systems. Bioresource Technology (0).
Kundu, A., Sahu, J.N., Redzwan, G. and Hashim, M.A. (2013) An overview of cathode material and catalysts suitable for generating hydrogen in microbial electrolysis cell. International Journal Of Hydrogen Energy 38(4), 1745-1757.
Ledezma, P., Donose, B.C., Freguia, S. and Keller, J. (2015) Oxidised stainless steel: a very effective electrode material for microbial fuel cell bioanodes but at high risk of corrosion. Electrochimica Acta 158, 356-360.
Lindeboom, R.E.F., Shin, S.G., Weijma, J., van Lier, J.B. and Plugge, C.M. (2016) Piezo-tolerant natural gas-producing microbes under accumulating CO_2. Biotechnology for Biofuels 9(1), 236.
Liu, D., Zhang, L., Chen, S., Buisman, C. and ter Heijne, A. (2016) Bioelectrochemical enhancement of methane production in low temperature anaerobic digestion at 10 °C. Water Research 99, 281-287.
Logan, B.E., Call, D., Cheng, S., Hamelers, H.V.M., Sleutels, T.H.J.A., Jeremiasse, A.W. and Rozendal, R.A. (2008) Microbial Electrolysis Cells for High Yield Hydrogen Gas Production from Organic Matter. Environmental Science & Technology 42(23), 8630-8640.
Min, B. and Logan, B.E. (2004) Continuous electricity generation from domestic wastewater and organic substrates in a flat plate microbial fuel cell. Environmental Science & Technology 38(21), 5809-5814.
Oh, S.-E. and Logan, B.E. (2006) Proton exchange membrane and electrode surface areas as factors that affect power generation in microbial fuel cells. Applied Microbiology and Biotechnology 70(2), 162-169.
Postma, J., Clematis, F., Nijhuis, E.H. and Someus, E. (2013) Efficacy of four phosphate-mobilizing bacteria applied with an animal bone charcoal formulation in controlling Pythium aphanidermatum and Fusarium oxysporum f.sp. radicis lycopersici in tomato. Biological Control 67(2), 284-291.

Rozendal, R.A., Jeremiasse, A.W., Hamelers, H.V.M. and Buisman, C.J.N. (2008) Hydrogen production with a microbial biocathode. Environmental Science and Technology 42(2), 629-634.
Siegert, M., Li, X.-F., Yates, M.D. and Logan, B.E. (2014a) The presence of hydrogenotrophic methanogens in the inoculum improves methane gas production in microbial electrolysis cells. Frontiers in microbiology 5, 778.
Siegert, M., Yates, M.D., Call, D.F., Zhu, X., Spormann, A. and Logan, B.E. (2014b) Comparison of Nonprecious Metal Cathode Materials for Methane Production by Electromethanogenesis. ACS Sustainable Chemistry & Engineering 2(4), 910-917.
Sleutels, T.H., Darus, L., Hamelers, H.V. and Buisman, C.J. (2011) Effect of operational parameters on Coulombic efficiency in bioelectrochemical systems. Bioresource Technology 102(24), 11172-11176.
Sleutels, T.H.J.A., Hamelers, H.V.M., Rozendal, R.A. and Buisman, C.J.N. (2009a) Ion transport resistance in Microbial Electrolysis Cells with anion and cation exchange membranes. International Journal Of Hydrogen Energy 34(9), 3612-3620.
Sleutels, T.H.J.A., Lodder, R., Hamelers, H.V.M. and Buisman, C.J.N. (2009b) Improved performance of porous bio-anodes in microbial electrolysis cells by enhancing mass and charge transport. International Journal of Hydrogen Energy 34(24), 9655-9661.
Twidell, J. and Weir, T. (2015) Renewable Energy Resources, Taylor & Francis.
Van Eerten-Jansen, M.C., Veldhoen, A.B., Plugge, C.M., Stams, A.J., Buisman, C.J. and Ter Heijne, A. (2013) Microbial community analysis of a methane-producing biocathode in a bioelectrochemical system. Archaea 2013 (Article ID 481784).
van Eerten-Jansen, M.C., Jansen, N.C., Plugge, C.M., de Wilde, V., Buisman, C.J. and ter Heijne, A. (2015) Analysis of the mechanisms of bioelectrochemical methane production by mixed cultures. Journal of Chemical Technology and Biotechnology 90(5), 963-970.
Venzlaff, H., Enning, D., Srinivasan, J., Mayrhofer, K.J.J., Hassel, A.W., Widdel, F. and Stratmann, M. (2013) Accelerated cathodic reaction in microbial corrosion of iron due to direct electron uptake by sulfate-reducing bacteria. Corrosion Science 66, 88-96.
Villano, M., Aulenta, F., Ciucci, C., Ferri, T., Giuliano, A. and Majone, M. (2010) Bioelectrochemical reduction of CO_2 to CH_4 via direct and indirect extracellular electron transfer by a hydrogenophilic methanogenic culture. Bioresource Technology 101(9), 3085-3090.

Walker, S.B., Mukherjee, U., Fowler, M. and Elkamel, A. (2016) Benchmarking and selection of Power-to-Gas utilizing electrolytic hydrogen as an energy storage alternative. International Journal Of Hydrogen Energy 41(19), 7717-7731.
Wei, J., Liang, P. and Huang, X. (2011) Recent progress in electrodes for microbial fuel cells. Bioresource Technology 102(20), 9335-9344.
Weitemeyer, S., Kleinhans, D., Vogt, T. and Agert, C. (2015) Integration of Renewable Energy Sources in future power systems: The role of storage. Renewable Energy 75, 14-20.
Wolin, E.A., Wolin, M.J. and Wolfe, R.S. (1963) FORMATION OF METHANE BY BACTERIAL EXTRACTS. The Journal of biological chemistry 238, 2882-2886.
Zeppilli, M., Lai, A., Villano, M. and Majone, M. (2016) Anion vs cation exchange membrane strongly affect mechanisms and yield of CO 2 fixation in a microbial electrolysis cell. Chemical Engineering Journal 304, 10-19.
Zhang, L., Hendrickx, T.L.G., Kampman, C., Temmink, H. and Zeeman, G. (2013) Co-digestion to support low temperature anaerobic pretreatment of municipal sewage in a UASB–digester. Bioresource Technology 148(0), 560-566.

SUPPORTING INFORMATION

Heat-treated Stainless Steel Felt as a New Cathode Material in a Methane-producing Bioelectrochemical System

1 Table, 2 Figures.

Table S1. Overview of operational conditions during the experiment.

Experimental condition	HSSF (weeks)		SSF (weeks)		GF (weeks)	
	Reacotr 1		Reactor 2		Reactor 3	
	Ⅰ	Ⅱ	Ⅰ	Ⅱ	Ⅰ	Ⅱ
-0.9 V	3		3		3	
-1.1 V	4		4		4	
-0.8 V	4		4		4	
-1.3 V	4		4		4	

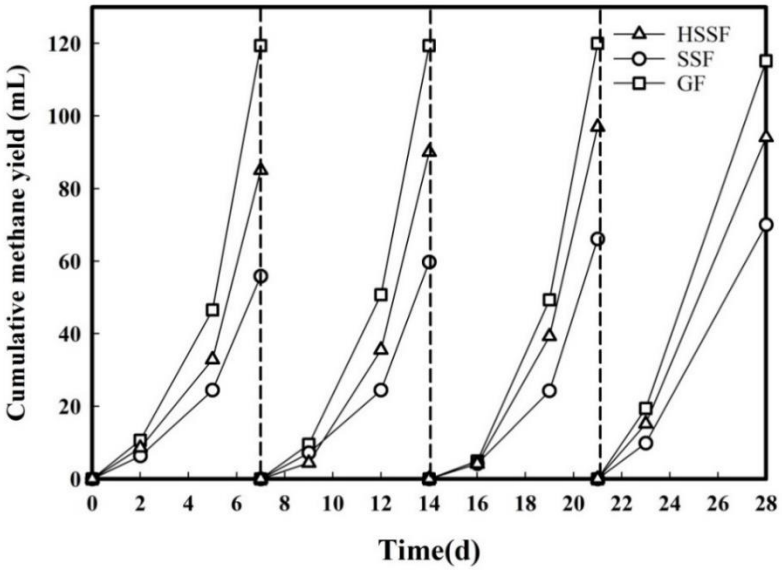

Figure S1. Cumulative methane yields over four consecutive batches for all the three cathode materials at the cathode potential of -1.3 V. The dashed lines indicate 50 % medium replacement at the end of each batch.

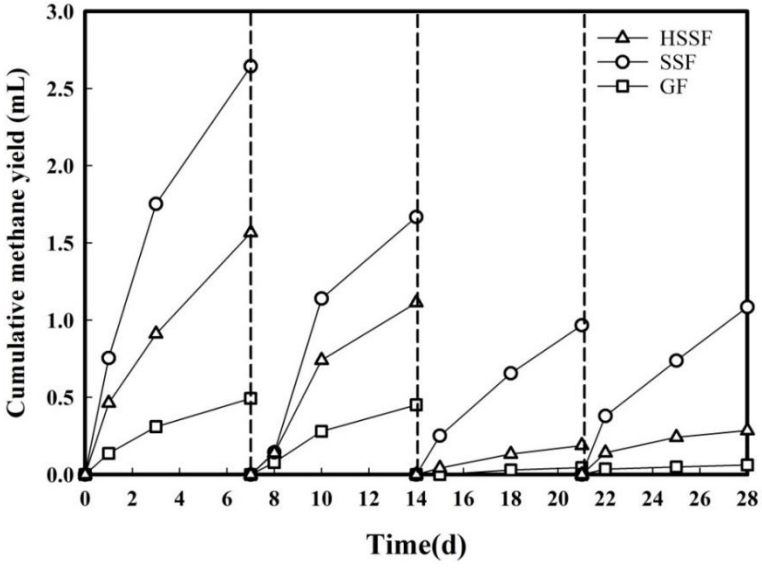

Figure S2. Cumulative methane yields over four consecutive batches for all the three cathode materials at the cathode potential of -0.8 V. The dashed lines indicate 50 % medium replacement at the end of each batch.

Chapter 3. Granular Activated Carbon as Cathode Material in Methane-Producing Bioelectrochemical Systems

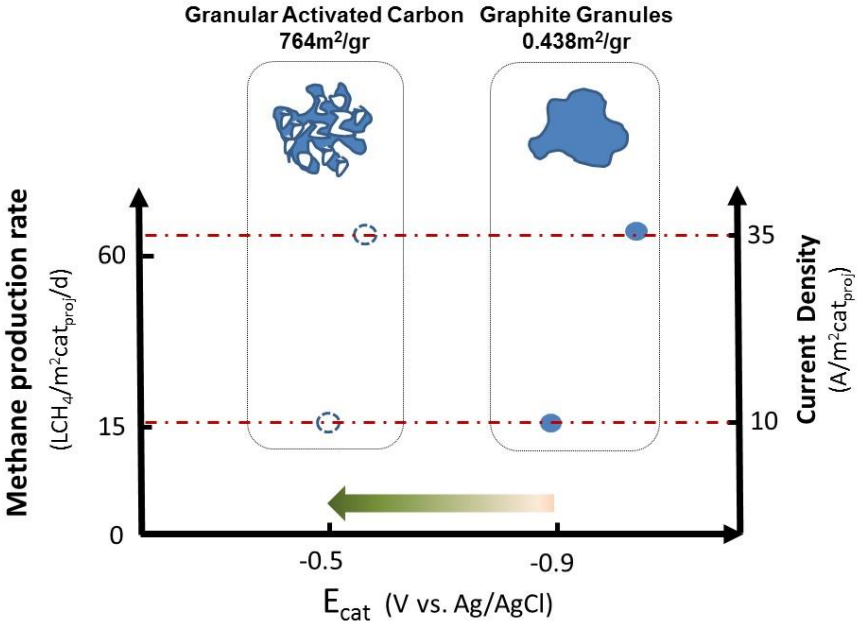

Granular Activated Carbon as Cathode Material in Methane-Producing Bioelectrochemical Systems

ABSTRACT

Methane-producing bioelectrochemical systems generate methane by using microorganisms to reduce carbon dioxide at the cathode. However, current densities and methane production rates have remained low so far. We have used granular activated carbon (GAC) as a carbon-based cathode material with a high specific surface area and compared its performance with that of graphite granules (GG) as carbon-based cathode material with a low specific surface area. Under galvanostatic control, the reactors in our study achieved methane production rates of around 65 L $CH_4/m^2cat_{proj}/d$ at 35 A/m^2cat_{proj}. The GAC biocathodes had a lower overpotential than the GG biocathodes, with methane generation occurring at -0.52 V vs. Ag/AgCl for GAC and at -0.92 V for GG at a current density of 10 A/m^2cat_{proj}, and still at only -0.58 V for GAC at 35 A/m^2cat_{proj}. Upon addition of methanogenesis inhibitor 2-BES, all biocathodes produced mainly acetate, at a cathode potential of -0.58 V for GAC and -0.92 V for GG. 16S rRNA gene analysis showed that *Methanobacterium* was the dominant methanogen and that the GAC biocathodes experienced a higher abundance of *Proteobacteria* than the GG biocathodes. These results are promising for the practical application potential of methane-producing BESs.

INTRODUCTION

The worldwide economic growth and the need for alternative energy sources drive the increase of electricity generation from renewables (such as solar, wind, and geothermal power) (Cheng et al. 2009, Administration 2016). The intermittent production of these newer types of energy, in combination with the fluctuating need for electricity, requires innovative technologies for electricity storage. Methane-producing bioelectrochemical systems (BESs) are a promising electricity conversion and storage technology (Van Eerten-Jansen et al. 2012) with the advantage that methane can be integrated into the natural gas grid (Sato et al. 2013b). In methane-producing BESs, H_2O is typically used as an electron donor, and oxidized at the anode (Van Eerten-Jansen et al. 2012). At the cathode, microorganisms reduce CO_2 to CH_4. This reduction can be direct (via electrons) and/or indirect (via H_2 formed at the cathode) (Villano et al. 2010, Liu et al. 2016a). The assembly of cathode and microorganisms is called biocathode.

Methane production rates achieved so far have remained low at values of 0.13-30 L $CH_4/m^2cat_{proj}/day$ (Geppert et al. 2016a), which limits the applicability of methane-producing BESs. Several studies have looked at cathode materials (Siegert et al. 2014a, Zhang et al. 2013b), inoculum sources (Siegert et al. 2015, Beese-Vasbender et al. 2015a) and operating conditions (Van Eerten-Jansen et al. 2012) with the aim of stimulating methane production. One effective method is to enhance microorganism attachment by increasing the available area for biofilm growth on the cathode surface (Jourdin et al. 2015, Guo et al. 2015a). The material and structural properties of the cathode are therefore of the utmost importance. Siegert et al. (Siegert et al. 2014a) investigated several cathode materials with different surface areas to optimize methane generation by a mixed culture. They showed that methane production rates can be enhanced with carbon-based electrodes (e.g. carbon brush), especially with materials providing a high surface area per volume of cathodic chamber (m^2/m^3). The reason behind this may be that these 3D electrodes can provide benefits for the attachment of microorganisms and biofilm development, but it is also possible that they increase mass transfer of substrate and product. Carbon-based electrodes are generally biocompatible and attractive candidates for use in scaled-up BESs. Examples of 3D carbon-based electrode materials are carbon granules (Freguia et al. 2007), activated carbon felt (Deng et al. 2010) or carbon cloth/felt modified with carbon nanotubes (Guo et al. 2015a, Zhang et al. 2013b).

Recently, it has been shown that the presence of granular activate carbon (GAC) in anaerobic digestion stimulates methane production. In these studies, GAC was not used as cathode material, as no current or potential was applied. Methane production was, in presence of GAC, probably enhanced by promoting direct interspecies electron transfer from *Geobacter* (Liu et al. 2012), *Sporanaerobacter*, and *Enterococcus* (Dang et al. 2016) species to methanogens. One of these studies (Dang et al. 2016) found that using a graphite rod, to the contrary, does not affect performance, for reasons not yet understood. Another study showed that adding pre-acclimated GAC can enhance methane production and decrease start-up times in the methane-producing BESs that use carbon brushes as cathode electrodes (LaBarge et al. 2017). GAC therefore appears to provide effective growth support for pre-acclimation of electrophilic methanogenic communities with exocellular electron transfer (LaBarge et al. 2017). This makes GAC an attractive electrode material for enhancing methanogenesis relative to other carbon-based electrodes, but to the best of our knowledge, GAC has not yet been used as the cathode electrode material in methane-producing BESs.

In this paper, we report methane production rates in an methane-producing BES of up to 65 L $CH_4/m^2cat_{proj}/d$ from CO_2. This was achieved by using GAC in a packed bed as the cathode electrode. The performance of the methane-producing BES with GAC was compared with that of an methane-producing BES with a packed bed of graphite granules (GG) as the cathode. We tested both granule types in duplicate reactors during 90 days at two different current densities and assessed performance in terms of methane production rate, current-to-methane efficiency and energy efficiency. We also analyzed the microbial community composition.

MATERIALS AND METHODS

Experimental Setup. We operated four bioelectrochemical reactors (Figure S1 in the Supporting Information). As cathode materials, we used granular activated carbon (GAC) with a specific surface area of 764 m^2/g (Cabot Norit Nederland B.V., Zaandam, the Netherlands; 1-3 mm diameter) and graphite granules (GG) with a specific surface area of 0.438 m^2/g (Carbone Lorraine Benelux BV, Wemmel, Belgium; 3-5 mm).(Borsje et al. 2016)

Each reactor contained an anodic and cathodic chamber, each with a volume of 33 cm^3 (11cm×2cm×1.5cm). A cation exchange membrane (FumaTech GmbH, Ingbert, Germany) was used with a projected surface area of 22 cm^2 (11cm×2cm). Two cathodic chambers were packed with GAC granules (GAC_1 with 8.5 g and GAC_2 with 8.4 g). The other two cathodic chambers were packed with GG granules (GG_1 with 26 g and GG_2 with 29.2 g). The current collector at the cathode was a plain graphite plate. The granule bed was tightly packed to ensure good contact between granules and current collector. The anodic chambers contained a 22-cm^2 platinum-iridium-coated titanium plate as electrode (Magneto Special Anodes BV, Schiedam, the Netherlands). The anodic chambers were filled with glass beads with a 7-mm diameter (Hecht-Assistent, Sondheim v. d. Rhön, Germany) to further ensure tight packing of the carbon granules. The reference electrodes (3M KCl Ag/AgCl, QM710X, QIS, Oosterhout, the Netherlands, +0.205 V vs. standard hydrogen electrode) were connected to the anolyte and catholyte solutions. Throughout this paper, all potentials are expressed against Ag/AgCl reference electrode.

Each cathodic chamber was connected to a liquid-gas separation bottle (60 mL) with a gas bag of 2 L (Cali-5-Bond™). After the separation bottle, the catholyte was channeled into the recirculation bottle (500 mL), where it was sparged with CO_2 for 2 hours/day during weekdays. After day 71, the catholyte was sparged with CO_2 continuously. All four anode chambers shared the same anolyte that was pumped via a recirculation bottle (5 L). Anolyte and catholyte flow rates were 7 mL/min.

Electrolytes and Microorganisms. The catholyte consisted of a 50mM phosphate buffer (2.77 g/L $NaH_2PO_4 \cdot 2H_2O$ and 4.58 g/L Na_2HPO_4) with 0.2 g/L NH_4Cl, 0.13 g/L KCl, 1 mL/L Wolfe's vitamin solution and 1 mL/L Wolfe's modified mineral solution (Wolin et

al. 1963b). The catholyte was flushed with N_2 gas for 30 minutes before each use. The pH in both anolyte and catholyte were 7.1 ± 0.2 at the start of each experiment.

All cathode chambers were inoculated at the same time with 10 mL of an anaerobic mixed culture (volatile suspended solids = 12.9±1.3 g/L), which contained 50% anaerobic granular sludge from the paper industry wastewater treatment facility in Eerbeek (the Netherlands) and 50% anaerobic sludge from the municipal wastewater treatment facility in Ede (the Netherlands).

The anolyte consisted of a 50 mM phosphate buffer. The anolyte was continuously flushed with N_2 gas in the recirculation bottle to keep O_2 levels at a minimum.

System Operation. To obtain a successful methane-producing biocathode, all reactors were galvanostatically controlled (at a fixed current) by a potentiostat (Ivium n-Stat, Eindhoven, the Netherlands), which collected the cathode potential data from all reactors at intervals of 1 minute. In this way, methane production rates can be regulated more directly than with cathode potential control, as the current determines the electrochemical reaction rate (Jörissen and Speiser 2015). After inoculation, all reactors were operated at a fixed current of 5 A/m^2cat_{proj} during the startup period. The current of all reactors was increased from 5 to 10 A/m^2cat_{proj} on day 37 and from 10 to 35 A/m^2cat_{proj} on day 71. All cathodes were operated in batch. Half of the catholyte was replaced on days 31 and 70 to replenish buffer, nutrients and vitamins. The pH of each reactor was monitored daily by pH measurement of liquid samples (0.5 mL per sample) taken from anode and cathode chamber. All reactors were operated inside a temperature-controlled cabinet at 30 ºC.

At the end of each experiment, methanogenesis of each biocathode was inhibited by spiking each catholyte with 15 mM of sodium 2-bromoethanesulfonate (2-BES). The possible generation of products like hydrogen, acetate and formate was investigated for each biocathode under galvanostatic control at a current density of 10 A/m^2 cat_{proj}.

Electrochemical Analysis. Polarization curves were acquired before inoculation and on day 30 and day 90 after inoculation. For the polarization curve before inoculation, the cathode potential was controlled from -0.5 V to -1.0 V with steps of 0.1 V; for the polarization curve after inoculation, the cathode potential was controlled from -0.1 V to -

0.7 V with steps of 0.05 V. Each potential step lasted 600 s for the GAC biocathodes but 300 s for the GG biocathodes, as the latter required a shorter equilibrium time.

Chemical Analyses. The liquid and gas samples were taken from each reactor twice a week, each sample representing 3 to 4 days. Volatile fatty acids (VFAs), including formate, acetate and lactate, were determined in the liquid phase by high-performance liquid chromatography (HPLC),(Lindeboom et al. 2016) whereas the gas composition was measured by gas chromatography (GC) (Liu et al. 2016a), both as described elsewhere. The gas volume was quantified by emptying the gas bags with a syringe. The methane production rate was calculated and normalized to the projected surface area of the cathode (Eq. 1) and the volume of the cathodic chamber (Eq. 2), as follows:

$$\gamma_{CH4-A} = \frac{V_T \times C_{CH4}}{A_{proj} \times t} \quad (1)$$

$$\gamma_{CH4-V} = \frac{V_T \times C_{CH4}}{V_{electrode} \times t} \quad (2)$$

Here, γ_{CH4-A} (L CH_4/m^2 cat_{proj} /d) and γ_{CH4-V} (L CH_4/m^3 cat /d) represent methane production rates; V_T (L) is the total volume by summing up the volume of the gas bag and the headspace (0.015 L); C_{CH_4}(%) is the methane fraction in the headspace; $A_{proj}(m^2)$ is the projected surface area of the cathode; $V_{electrode}(m^3)$ is the cathodic chamber volume; t (d) is the experimental time between each headspace measurement (d).

Current-to-methane efficiency. This indicates which percentage of the electrons ended up in the form of methane.

$$\eta_{CH4} = \frac{N_{CH4} \times n_{CH4} \times F}{\int_{t=0}^{t} I \, dt} \quad (3)$$

F is the Faraday constant (96485 C/mol e^-); N_{CH4} (mol) is total moles of CH_4 produced; n_{CH4} is moles of electrons per mole of CH_4 (8); I (A) is the current.

Voltage efficiency and energy efficiency. These describe how much of the applied voltage and applied energy ended up in CH_4.

$$\eta_{voltage,CH4} = \frac{-\Delta G_{CH_4}}{E_{cell} \times n_{CH4} \times F} \quad (4)$$

$$\eta_{\text{energy,CH}_4} = \eta_{\text{CH}_4} \times \eta_{\text{voltage,CH4}} \quad (5)$$

Here, ΔG_{CH_4} is the Gibb's free energy of methane oxidation (-890.4 kJ/mol) and E_{cell} is the applied cell voltage (V).

Microbial community analysis. After operation at a current density of 35 A/m^{2}cat$_{proj}$, we disassembled all reactors inside an anaerobic chamber, and 0.5 g (wet weight) of the granules was taken from each cathode. In addition, we took 300 mL of the used catholyte from each reactor and filtered it over a 0.22 μm MF-MilliPore filter. Genomic DNA was extracted from each reactor samples with a Mo Bio PowerSoil DNA isolation kit for 0.5 g of the granular electrode and a Mo Bio PowerWater DNA isolation kit for the filter, according to the manufacturer's instructions. To investigate both bacteria and archaea, we carried out amplification of 16S rRNA gene fragments by using a two-step PCR protocol (see Supportive Information, under B). We also calculated Bray-Curtis similarities between reactors (biocathodes and used catholytes) from the microbial community relative abundance data with Primer-E software, version 7 (LaBarge et al. 2017).

RESULTS AND DISCUSSION

High Methane Production Rates Directly Linked to Current Density. We determined methane production rates at two different current densities, namely 10 and 35 A/m^{2}cat$_{proj}$. At the current density of 35 A/m^{2}cat$_{proj}$, the methane production rates were around 65 L CH_4 /m^{2}cat$_{porj}$/d for both GAC and GG reactors. As these methane production rates were directly related to current density, they were almost four times higher than the methane production rates at 10 A/m^{2}cat$_{proj}$ (Figure 1a). The current-to-methane efficiencies for the GAC and GG reactors were also similar (Figure 1b); they increased from 55% at 10 A/m^{2}cat$_{proj}$ to 67% at 35 A/m^{2}cat$_{proj}$. We detected no H_2 and volatile fatty acids in any of the reactors when they were controlled at these two current densities, which suggests that during the stable performance period, the methanogenic activity was high enough to utilize them if they were produced. The lost electrons were probably used for oxygen reduction, as oxygen was also generated at a high rate in the anodic chamber and can diffuse through the membrane to the cathodic chamber.(Van Eerten-Jansen et al. 2012) Also, the low current-to-methane efficiency might be due to other factors, e.g. electrons used for biomass growth (Geppert et al. 2016a), or loss of methane via membrane, tubes, and connections within the reactor (Skovsgaard and Jacobsen 2017), especially considering our relatively long sampling intervals (3 to 4 days). In terms of energy efficiency (see the Supporting Information, under D), all reactors achieved a similar result of around 20% at a current density of 10 A/m^2 cat$_{proj}$, while the energy efficiencies of all reactors decreased to around 15% when operated at the higher current density of 35 A/m^2 cat$_{proj}$. Although applying a higher current density resulted in a higher current-to-methane efficiency, i.e. an increase from 55% to 67%, the energy efficiency decreased as a result of lower voltage efficiency.

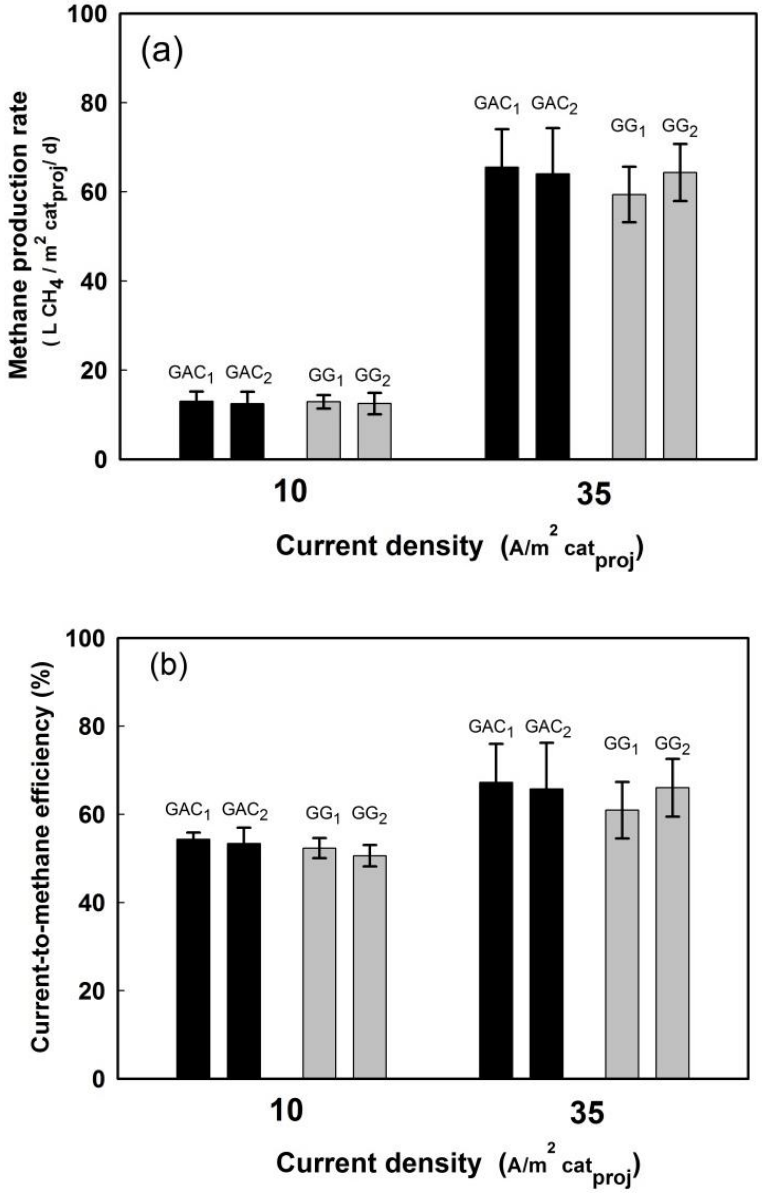

Figure 1. (a) Methane production rates and (b) current-to-methane efficiencies at current densities of 10 A/m^{2}cat$_{proj}$ and 35 A/m^{2}cat$_{proj}$ for GAC and GG reactors. Data were collected throughout a period of 2 weeks with stable performance for every reactor. Shown are the average value and standard deviation of four samples for each reactor and current density.

Biocathodes with Granular Activated Carbon Produced Methane at Low Overpotentials. Directly after inoculation, all the reactors had similar cathode potentials of about -0.90 V (Figure 2). The cathode potential of GAC_1 changed from -0.90 V to -0.52 V between day 7 and 10, whereas the cathode potential of GAC_2 changed from -0.80 V to -0.52 V between day 30 and 37 (Later in this section, we give a possible explanation for this difference). The cathode potentials of the GG reactors remained stable around -0.92 V long after inoculation (and became slightly more negative around day 37 and day 70 due to the increases in current density). These potential differences between GAC and GG biocathodes were also seen in the polarization curves at day 30 (Figure S2-b in the Supporting Information) and day 90 (Figure S2-c in the Supporting Information). These polarization curves show that the onset of current for GAC biocathodes occurred at a more positive potential from -0.5 V to even -0.4 V during operation, whereas the current densities of GG biocathodes were negligible in the whole range of cathode potentials tested (-0.7 V to -0.3 V). Nevertheless, the onset potentials of the bare GAC electrodes (Figure S2-a in the Supporting Information) were around -0.7 V, the difference indicating the catalytic effect of the growth of cathodic micoorganisms on the GAC electrodes.

To further strengthen our experiment findings, we started two methane-producing BESs with new and clean GAC electrodes (R_1 and R_2, detailed information in SI, section E). Again, the cathode potentials of both GAC biocathodes became less negative after 10 days of inoculation and finally reached similar values of -0.53 V for R_1 and -0.6 V for R_2, supporting the observations reported here.

These cathode potentials for GAC are the least negative ones (i.e. lowest overpotential) reported in the literature for methane-producing BESs, to our knowledge (Geppert et al. 2016a). To exclude that the measurement of cathode potential was influenced by the fact that the reference electrode was placed just outside the cathode compartment, we inserted a new Ag/AgCl reference electrode into the cathodic chamber close to the granular bed. The cathode potential was -0.43 V, which was 100 mV less negative than the cathode potential (-0.54 V) measured just outside the cathode chamber, pointing out that the cathode potential was even more positive than measured. The thermodynamic equilibrium potential for hydrogen evolution being -0.62 V, under the conditions applied here (T=30ºC, P=1 bar, pH=7) (Beese-Vasbender et al. 2015b) methane formation via hydrogen produced at the cathode (possibly catalyzed by microorganisms) seems thermodynamically unfavourable,

although hydrogen could still be an intermediate in the reaction, as the local hydrogen pressures may be extremely low and local pH value may be extremely high. To further study the mechanisms of methane production, biocathodes were flushed with a mixture of N_2 and CO_2, and thereafter with only N_2. In presence of CO_2, cathode potential was similar to the one measured during normal operation. In absence of CO_2, however, cathode potential decreased to more negative values of -0.9V, Thus, when CO_2 is available, it is likely that methane is produced directly, without hydrogen as intermediate, whereas hydrogen formation occurs at more negative potentials in absence of CO_2.

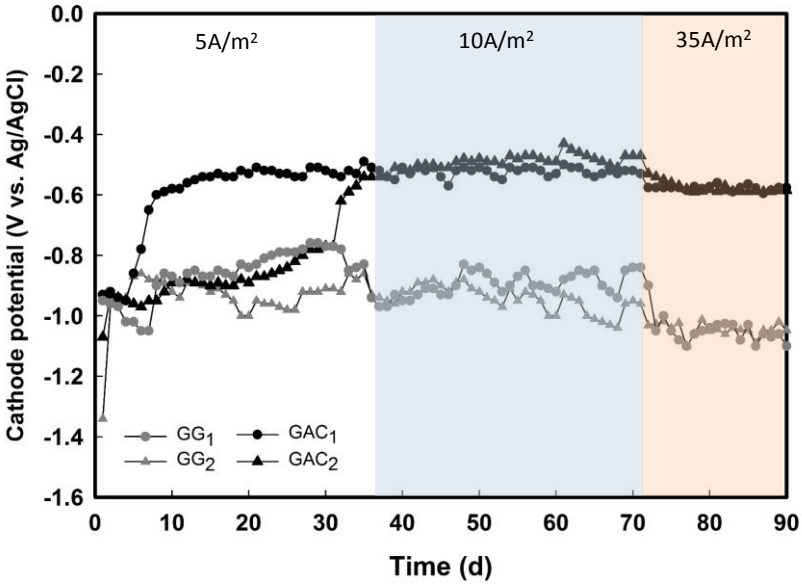

Figure 2. Average daily cathode potentials of all the reactors after inoculation. Both GAC biocathodes showed a steep increase in cathode potential, whereas the cathode potential for both GG biocathodes remained constant, and decreased with increased current density.

Key question is why methane production on GAC occurred at a cathode potential of -0.52 V, while methane production on GG occurred at -0.90 V. The high specific surface area of GAC (764 m2/g) and average smaller size (1-3 mm) relative to GG (0.438 m2/g, 3-5 mm) may have played a role, but does not explain the mechanism of methane formation. It is likely that methane production at a cathode potential of -0.52 V has not been reported before due to the fact that all methane-producing biocathodes in other studies were operated at a constant potential rather than at a constant current. In fact, most of the studies have

used cathode potentials more negative than -0.7 V vs. Ag/AgCl to supply a sufficiently high overpotential for methane generation (LaBarge et al. 2017, Siegert et al. 2014a, Villano et al. 2016). To explore if there would be a difference in methane production between potential control and current control, we switched the biocathodes from galvanostatic control to potentiostatic control with an active biocathode. After this switch to cathode potential control, the current as well as methane production rates and efficiencies remained similar (results not shown).

The abrupt changes in the biocathode potentials of the GAC reactors occurred on different days (Figure 2). The reason for that may be that in GAC_1, which had been operated and adjusted during 2 months before inoculation to perform electrochemical measurements, the catholyte and/or electrode may already have contained methanogens before inoculation. Indeed, a minor amount of CH_4 was already detected in the headspace of GAC_1 during the phase before inoculation (data not shown). The fluctuations of the cathode potentials, especially at current densities of 5 A/m^2cat_{proj} and 10 A/m^2cat_{proj}, were probably the result of fluctuations in catholyte pH due to intermittent CO_2 supply (Jourdin et al. 2015). After changing to continuous CO_2 supply and a current density of 35 A/m^2cat_{proj} on day 71, the pH of the catholyte and the cathode potentials remained more stable. Figure S3 in the Supporting Information contains detailed pH data.

Inhibition of Methanogens Resulted in Acetate Formation for Both GG and GAC Biocathodes. At the end of our experiment, we performed two weeks of methanogenic inhibition tests with 15 mM sodium 2-bromoethanesulfonate (2-BES) for all biocathodes. We operated the cells at a constant current density of 10 A/m^2cat_{proj} and compared product formation and cathode potentials before and after 2-BES addition (Figure 3). For both the GAC and GG biocathodes, acetate was the main product after 2-BES addition and methane formation still accounted for 11% (GG) and 5.7% (GAC) of the supplied charge. For the GAC biocathodes, some hydrogen was measured as well (accounting for 4%). The cathode potentials for the GAC biocathodes became slightly more negative (from -0.52 V to -0.58 V). It is interesting that acetate and hydrogen formation occurred at those low potentials for the GAC biocathodes as well; reported cathode potentials for a current density of 10 A/m^2cat_{proj} for acetate production are more negative than -1.0 V (Jourdin et al. 2015, Jourdin et al. 2016) and those for hydrogen production are more negative than -0.9 V (Rozendal et al. 2008). The cathode potentials for GG hardly changed (about -0.93 V vs.

Ag/AgCl) after 2-BES addition, showing that the electrons were diverted to acetate when the methane production pathway was inhibited.

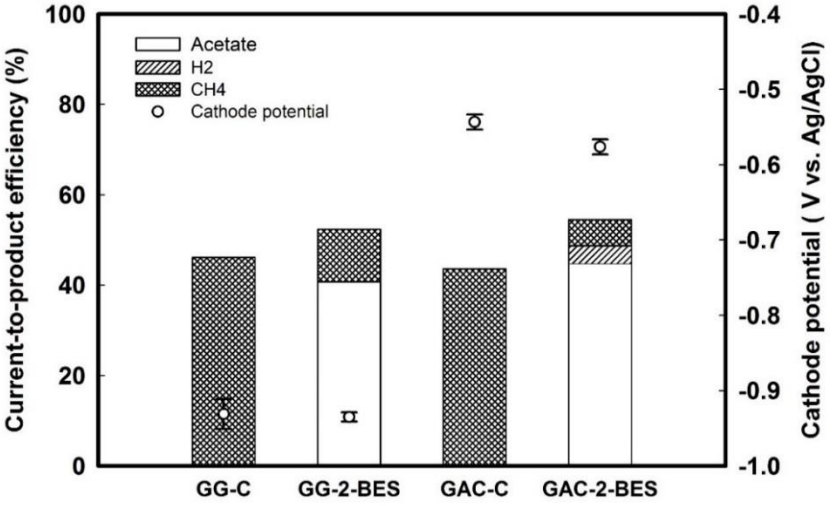

Figure 3. Performance comparison for GAC and GG biocathodes at a current density of 10 A/m^2 cat_{proj}, between the period without inhibition (average value from duplicate reactors for each biocathode material: GG-C and GAC-C) and the period with 15 mM 2-BES (average value from duplicate reactors for each biocathode material: GG-2-BES and GAC-2-BES). The average current-to-product efficiency data for each biocathode material are shown as a stacked bar chart and are based on 4 samples (2 samples for each reactor × 2 reactors for each biocathode material). The average cathode potential for each biocathode material is represented as a black circle with standard deviation (error bar).

Microbial Community Analysis Revealed *Methanobacterium* as the Dominant Genus. Microbial community characterization of biofilm and catholyte was performed for all reactors to investigate whether different microbial communities developed on the two cathode materials. Table S1 in the Supporting Information shows the community similarity results for all granules. All cathodic communities (both in biofilm and catholyte) were dominated by hydrogenotrphic methanogen (*Methanobacterium*), which has been found in many other studies (Cai et al. 2016a, LaBarge et al. 2017, Van Eerten-Jansen et al. 2013a), regardless of electrode material and inoculum source (Figure 4). Another hydrogenotrphic methanogen, namely *Methanocorposculum*, was detected 21 % in the catholyte of GG_1. The GAC electrode samples showed a greater relative abundance of *Proteobacteria* (*Deltaproteobacteria and Betaproteobacteria*) with 14% for GAC_1 and 47% for GAC_2, relative to 8.7% for GG_1 and 3.4 % for GG_2, which may be related to the lower overpotentials measured for GAC. Exoelectrogens like *Geobacter* sp. belong to the *Proteobacteria*, the most common phylum of bacteria found on the anode of microbial fuel cells (Hasany et al. 2016). In another study (Liu et al. 2012), GAC has been proven to promote direct interspecies electron transfer in anaerobic microbial communities, although the mechanism was not explained. The question remains if direct electron transfer at the GAC biocathodes is the mechanism occurring here.

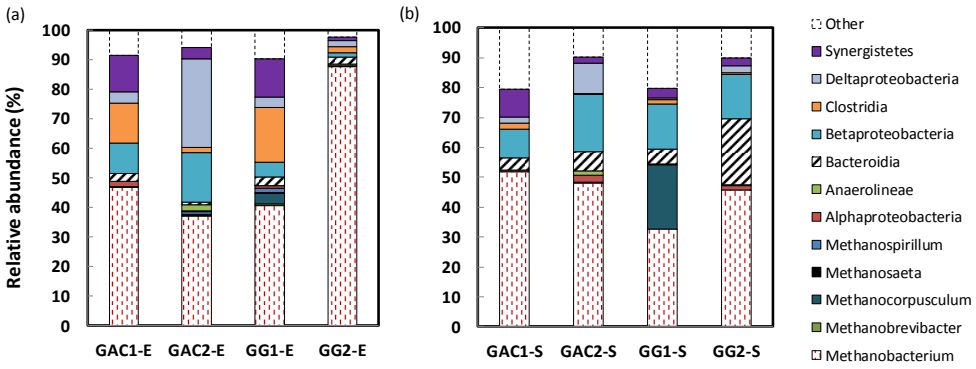

Figure 4. Taxonomic distribution of microbial populations with >2% relative abundance by 16S rRNA gene sequences. Samples from all four reactors were taken from: (a) biofilm on granular biocathodes (GAC_1-E, GAC_2-E, GG_1-E, GG_2-E); (b) suspended cells within the catholyte (GAC_1-S, GAC_2-S, GG_1-S, GG_2-S).

OUTLOOK

In this paper, we have shown that both GAC and GG are suitable cathode materials for high methane production rates in methane-producing BESs. The methane production rates achieved with GAC and GG at constant current were several times higher than the rates obtained with similar carbon-based electrodes in other studies(Geppert et al. 2016a) (Table 1). In addition, the low overpotentials for GAC biocathodes indicate that mixed-culture biomes can effectively catalyze the production of methane and/or intermediates without the need for expensive electrode materials modified with special enzymes or chemicals. In general, the high methane production rates and low overpotentials observed in the current-controlled systems with GAC biocathodes in our study hold great promise for the practical application of methane-producing BESs.

ASSOCIATED CONTENT

The Supporting Information is available at the end of this chapter.

ACKNOWLEDGEMENTS

The authors thank Nurul Azyyati Sabri for her help with DNA extraction, and Caroline Plugge for facilitating the microbial community analyses. The authors are also grateful for financial support from Dutch companies (Alliander, DMT Environmental Technology), the Chinese Scholarship Council (File No. 201306120043) and the Cluster of Excellence RESOLV (EXC 1069), which is funded by the Deutsche Forschungsgemeinschaft.

Table 1. Comparison of methane production rates for similar carbon-based electrodes in methane-producing BESs.

Electrode Material	Current Density		Methane Production Rate		Current-to-CH_4 Efficiency (%)	Cathode Potential (V vs. Ag/AgCl)	Reference
	(A/m^2cat_{proj})	(kA/m^3cat)	($LCH_4/m^2cat_{proj}/d$)	(m^3 $CH_4/m^3cat/d$)			
Activated carbon granules	10	0.67	15	1.0	54	-0.52	This study
Activated carbon granules	35	2.3	65	4.3	66	-0.58	This study
Graphite felt	0.21	0.070	0.13	0.045	23	-0.75	(Van Eerten-Jansen et al. 2012)
Graphite felt	2.9	0.97	5.1	1.7	73	-0.9	(van Eerten-Jansen et al. 2015)
Graphite granules	10	0.67	15	0.97	52	-0.9	This study
Graphite granules	35	2.3	62	4.1	67	-1.05	This study
Graphite granules	3.81	0.13	17	0.56	79	-1.13	(Villano et al. 2013)

REFERENCES

Administration, U.S.E.I. (2016) <Annual energy outlook 2016 with projections to 2040.pdf>.

Beese-Vasbender, P.F., Grote, J.-P., Garrelfs, J., Stratmann, M. and Mayrhofer, K.J.J. (2015a) Selective microbial electrosynthesis of methane by a pure culture of a marine lithoautotrophic archaeon. Bioelectrochemistry 102(Supplement C), 50-55.

Beese-Vasbender, P.F., Grote, J.-P., Garrelfs, J., Stratmann, M. and Mayrhofer, K.J.J. (2015b) Selective microbial electrosynthesis of methane by a pure culture of a marine lithoautotrophic archaeon. Bioelectrochemistry 102, 50-55.

Borsje, C., Liu, D., Sleutels, T.H.J.A., Buisman, C.J.N. and ter Heijne, A. (2016) Performance of single carbon granules as perspective for larger scale capacitive bioanodes. Journal of Power Sources 325, 690-696.

Cai, W., Liu, W., Yang, C., Wang, L., Liang, B., Thangavel, S., Guo, Z. and Wang, A. (2016) Biocathodic methanogenic community in an integrated anaerobic digestion and microbial electrolysis system for enhancement of methane production from waste sludge. ACS Sustainable Chemistry & Engineering 4(9), 4913-4921.

Cheng, S.A., Xing, D.F., Call, D.F. and Logan, B.E. (2009) Direct Biological Conversion of Electrical Current into Methane by Electromethanogenesis. Environmental Science & Technology 43(10), 3953-3958.

Dang, Y., Holmes, D.E., Zhao, Z., Woodard, T.L., Zhang, Y., Sun, D., Wang, L.-Y., Nevin, K.P. and Lovley, D.R. (2016) Enhancing anaerobic digestion of complex organic waste with carbon-based conductive materials. Bioresource Technology 220, 516-522.

Deng, Q., Li, X., Zuo, J., Ling, A. and Logan, B.E. (2010) Power generation using an activated carbon fiber felt cathode in an upflow microbial fuel cell. Journal Of Power Sources 195(4), 1130-1135.

Freguia, S., Rabaey, K., Yuan, Z. and Keller, J. (2007) Non-catalyzed cathodic oxygen reduction at graphite granules in microbial fuel cells. Electrochimica Acta 53(2), 598-603.

Geppert, F., Liu, D., van Eerten-Jansen, M., Weidner, E., Buisman, C. and Ter Heijne, A. (2016) Bioelectrochemical Power-to-Gas: State of the Art and Future Perspectives. Trends In Biotechnology.

Guo, K., Prévoteau, A., Patil, S.A. and Rabaey, K. (2015) Engineering electrodes for microbial electrocatalysis. Current Opinion In Biotechnology 33(0), 149-156.

Hasany, M., Mardanpour, M.M. and Yaghmaei, S. (2016) Biocatalysts in microbial electrolysis cells: A review. International Journal Of Hydrogen Energy 41(3), 1477-1493.
Jörissen, J. and Speiser, B. (2015) Organic Electrochemistry, Fifth Edition, pp. 263-330, CRC Press.
Jourdin, L., Freguia, S., Flexer, V. and Keller, J. (2016) Bringing high-rate, CO_2-based microbial electrosynthesis closer to practical implementation through improved electrode design and operating conditions. Environmental Science & Technology 50(4), 1982-1989.
Jourdin, L., Grieger, T., Monetti, J., Flexer, V., Freguia, S., Lu, Y., Chen, J., Romano, M., Wallace, G.G. and Keller, J. (2015) High Acetic Acid Production Rate Obtained by Microbial Electrosynthesis from Carbon Dioxide. Environmental Science & Technology 49(22), 13566-13574.
LaBarge, N., Yilmazel, Y.D., Hong, P.-Y. and Logan, B.E. (2017) Effect of pre-acclimation of granular activated carbon on microbial electrolysis cell startup and performance. Bioelectrochemistry 113, 20-25.
Lindeboom, R.E.F., Shin, S.G., Weijma, J., van Lier, J.B. and Plugge, C.M. (2016) Piezo-tolerant natural gas-producing microbes under accumulating CO_2. Biotechnology for Biofuels 9(1), 236.
Liu, D., Zhang, L., Chen, S., Buisman, C. and ter Heijne, A. (2016) Bioelectrochemical enhancement of methane production in low temperature anaerobic digestion at 10 °C. Water Research 99, 281-287.
Liu, F., Rotaru, A.-E., Shrestha, P.M., Malvankar, N.S., Nevin, K.P. and Lovley, D.R. (2012) Promoting direct interspecies electron transfer with activated carbon. Energy & Environmental Science 5(10), 8982-8989.
Rozendal, R.A., Jeremiasse, A.W., Hamelers, H.V.M. and Buisman, C.J.N. (2008) Hydrogen production with a microbial biocathode. Environmental Science and Technology 42(2), 629-634.
Sato, K., Kawaguchi, H. and Kobayashi, H. (2013) Bio-electrochemical conversion of carbon dioxide to methane in geological storage reservoirs. Energy Conversion and Management 66(0), 343-350.
Siegert, M., Li, X.-f., Yates, M.D. and Logan, B.E. (2015) The presence of hydrogenotrophic methanogens in the inoculum improves methane gas production in microbial electrolysis cells. Frontiers in Microbiology 5.

Siegert, M., Yates, M.D., Call, D.F., Zhu, X., Spormann, A. and Logan, B.E. (2014) Comparison of Nonprecious Metal Cathode Materials for Methane Production by Electromethanogenesis. ACS Sustainable Chemistry & Engineering 2(4), 910-917.
Skovsgaard, L. and Jacobsen, H.K. (2017) Economies of scale in biogas production and the significance of flexible regulation. Energy Policy 101, 77-89.
Van Eerten-Jansen, M.C.A.A., Heijne, A.T., Buisman, C.J.N. and Hamelers, H.V.M. (2012) Microbial electrolysis cells for production of methane from CO_2: long-term performance and perspectives. International Journal of Energy Research 36(6), 809-819.
van Eerten-Jansen, M.C.A.A., Jansen, N.C., Plugge, C.M., de Wilde, V., Buisman, C.J.N. and ter Heijne, A. (2015) Analysis of the mechanisms of bioelectrochemical methane production by mixed cultures. Journal of Chemical Technology & Biotechnology 90(5), 963-970.
Van Eerten-Jansen, M.C.A.A., Veldhoen, A.B., Plugge, C.M., Stams, A.J.M., Buisman, C.J.N. and Ter Heijne, A. (2013) Microbial Community Analysis of a Methane-Producing Biocathode in a Bioelectrochemical System. Archaea 2013, 12.
Villano, M., Aulenta, F., Ciucci, C., Ferri, T., Giuliano, A. and Majone, M. (2010) Bioelectrochemical reduction of CO_2 to CH_4 via direct and indirect extracellular electron transfer by a hydrogenophilic methanogenic culture. Bioresource Technology 101(9), 3085-3090.
Villano, M., Ralo, C., Zeppilli, M., Aulenta, F. and Majone, M. (2016) Influence of the set anode potential on the performance and internal energy losses of a methane-producing microbial electrolysis cell. Bioelectrochemistry 107, 1-6.
Villano, M., Scardala, S., Aulenta, F. and Majone, M. (2013) Carbon and nitrogen removal and enhanced methane production in a microbial electrolysis cell. Bioresource Technology 130, 366-371.
Wolin, E.A., Wolin, M.J. and Wolfe, R.S. (1963) Formation of Methane by Bacterial Extracts. Journal Of Biological Chemistry 238(8), 2882-2886.
Zhang, T., Nie, H.R., Bain, T.S., Lu, H.Y., Cui, M.M., Snoeyenbos-West, O.L., Franks, A.E., Nevin, K.P., Russell, T.P. and Lovley, D.R. (2013) Improved cathode materials for microbial electrosynthesis. Energy & Environmental Science 6(1), 217-224.

SUPPORTING INFORMATION

Granular Activated Carbon as Cathode Material in Methane-Producing Bioelectrochemical Systems

5 Figures, 3 Tables

A. Methane-producing BES setup

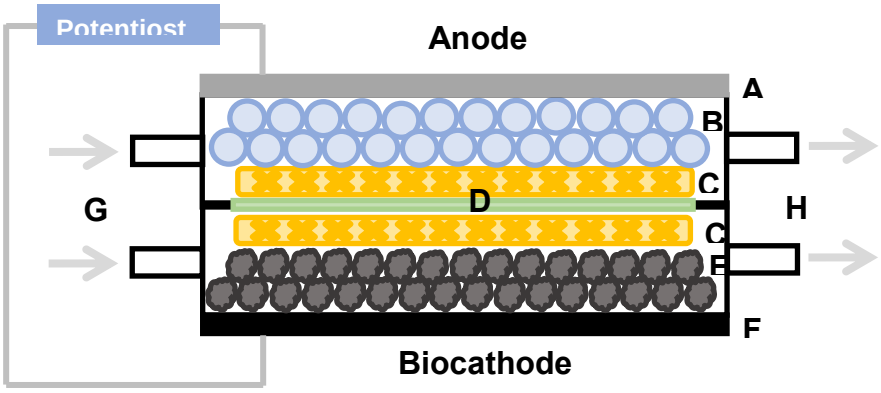

Figure S1. Schematic depiction of the methane-producing BES in our study. Each reactor contained an anodic and a biocathodic chamber. The anode was a titanium plate covered with platinum-iridium (A). The anode chamber was filled with glass beads of a 7-mm diameter (Hecht-Assistent, Sondheim v. d. Rhön, Germany) (B) and a plastic spacer (Sefar Nitex 06-3300/59, Buffalo, NY, USA) (C) to protect the cation exchange membrane (D). The cathode chamber was fully filled with the cathode, GG or GAC (E), together with a plastic spacer (C). The electrons were supplied to the bed of granules from the external circuit via a graphite plate (working area of 22 cm^2) (F). Both chambers had an inlet (G) and an outlet (H) with anolyte and catholyte flowing through the anodic and cathodic chamber, respectively.

B. 16S rRNA Miseq Sequencing Analysis

Extracted DNA from selected samples was kept at -20 ºC for bacterial and archaeal community analyses. DNA was measured with a DeNovix DS-11 FX spectrophotometer/fluorometer (DENovix Inc., Wilmington, DE, USA) and the DNA concentrations (ca. 20 ng/µl) were used as PCR templates.

The amplification of bacterial and archaeal 16S rRNA gene fragments was performed using a two-step PCR protocol. For the bacterial gene fragments, first PCR was done with universal primers 515f and 806r (Parada et al. 2015), while for the archaeal gene fragments universal primers 518f (Wang and Qian 2009) and 905r (Kvist et al. 2007) were used. The first PCR for both bacterial and archaeal 16S rRNA gene fragments was performed in a total volume of 50 µl, containing 2.5 µl of each forward and reverse primer, 0.5 µl (2 unit) of the DNA polymerase, 10 µl of 5 x HF-buffer, 1 µl (200 µM) dNTP mix, 1 µl of DNA template, and 32.5 µl of nuclease-free sterile water. The PCR program for bacterial amplification was as follows: a pre-denaturing step at 98 ºC for 3 min, followed by 25 cycles at 98 ºC for 10 s, 50 ºC for 20 s, 72 ºC for 20 s, and a post-elongation step of 10 min at 72 ºC. For archaeal amplification, the PCR program was as follows: a pre-denaturing step at 98 ºC for 30 s, followed by 25 cycles at 98 ºC for 10 s, 60 ºC for 20 s, 72 ºC for 20 s, and a post-elongation step of 10 min at 72 ºC. PCR amplifications were carried out in technical duplicates.

After positive amplification, the second PCR for both bacterial and archaeal 16S rRNA gene fragments was separately done using the same protocol in 100 µl, containing 10 µl of the bar-coded primer mix, 1 µl (2 units) of the DNA polymerase, 20 µl of 5 x HF-buffer, 2 µl (200 µM) dNTP mix, 5 µl of DNA template, and 62 µl of nuclease free sterile water. The second PCR for both the bacterial and the archaeal gene fragments was carried out with eight-base specific barcodes as previously described (Hamady et al. 2008), using Phusion Hot start II High-Fidelity DNA polymerase (Themo Fisher Scientific, Waltham, MA, USA). PCR amplification was performed using a G-Storm cycler (G-storm, Essex, UK). The second PCR program was as follows: a pre-denaturing step at 98 ºC for 30 s, followed by 5 cycles at 98 ºC for 10 s, 52 ºC for 20 s, 72 ºC for 20 s, and a post-elongation step of 10 min at 72 ºC. Bar-coded PCR products were checked for positive amplification on an

agarose gel and then were purified using CleanPCR kit system according to the manufacturer's instructions (CleanNA, Alphen aan den Rijn, the Netherlands).

DNA was quantified using a Qubit® dsDNA BR Assay Kit and a DeNovix DS-11 FX spectrophotometer/fluorometer (DENovix Inc., Wilmington, DE, USA). All samples were pooled in equimolar amounts (200 ng of DNA per sample) to create a library, which was then purified again with the CleanPCR kit to a final volume of 35 µl. The library was dispatched for paired-end Illumina MiSeq sequencing at GATC Biotech (Konstanz, Germany).

16S rRNA gene Miseq sequencing data were analyzed using Galaxy/NG-Tax, an in-house pipeline, as previously described by Ramiro-Garcia et al. (Ramiro-Garcia et al. 2016). Paired-end libraries were filtered to obtain only read pairs with perfectly matching barcodes and those barcodes were then used to detach reads by the sample. The Silva 16S rRNA gene reference database (release 128) was used for the taxonomic classification (Quast et al. 2012).

Bray-Curtis Similarities

The Bray-Curtis similarity is a useful coefficient to measure the resemblance between samples containing multivariate data (Somerfield 2008). Table S1 shows the Bray-Curtis similarities for the methane-producing BES reactors in our study.

Table S1. Bray-Curtis similarities (%) between electrodes samples (E) and catholyte samples (S), taken from all the reactors after the operation at a current density of 35 A/m^2cat_{proj}. Darker shades indicate greater resemblance between samples.

	GAC1-E	GAC2-E	GG1-E	GG2-E	GAC1-S	GAC2-S	GG1-S	GG2-S
GAC1-E		**64**	**87**	**58**	**81**	**76**	**60**	**74**
GAC2-E	**64**		**59**	**47**	**60**	**75**	**60**	**65**
GG1-E	**87**	**59**		**52**	**76**	**65**	**60**	**65**
GG2-E	**58**	**47**	**52**		**63**	**58**	**42**	**56**
GAC1-S	**81**	**60**	**76**	**63**		**76**	**72**	**75**
GAC2-S	**76**	**75**	**65**	**58**	**76**		**66**	**83**
GG1-S	**60**	**60**	**60**	**42**	**72**	**66**		**66**
GG2-S	**74**	**65**	**65**	**56**	**75**	**83**	**66**	

C. Additional Information on Performance

(a)

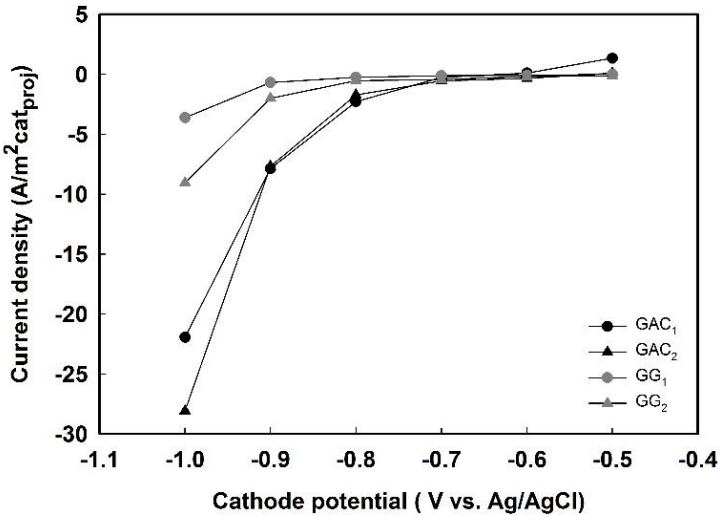

(b)

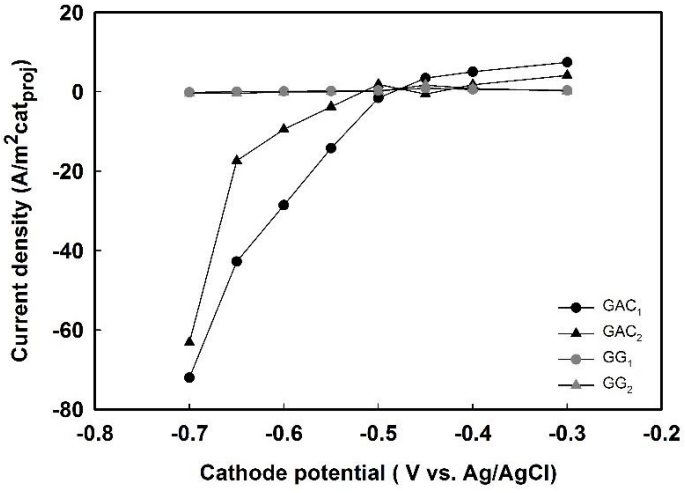

(c)

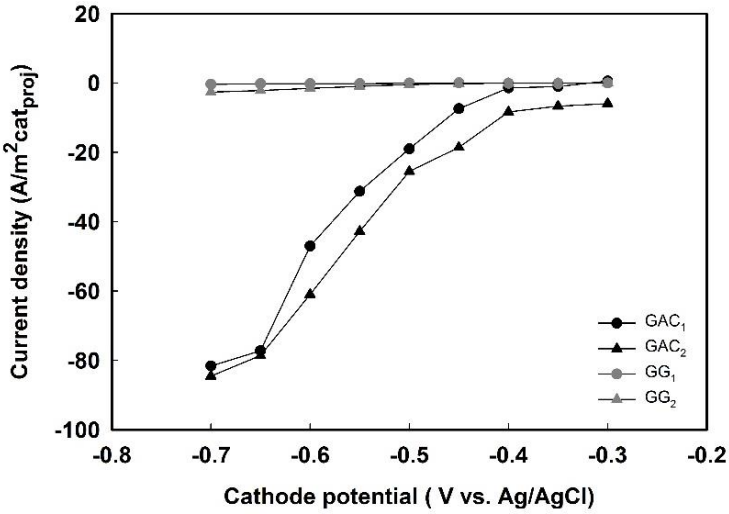

Figure S2. Polarization curves acquired before inoculation (a), after inoculation on day 30 (b) and day 90 (c) for all reactors**.** For bare electrode materials (Figure S2a), GAC had a less negative onset potential (about -0.7 V vs. Ag/AgCl) than GG (about -0.8 V vs. Ag/AgCl). In the presence of the catalytic effect of microorganisms on electrodes (Figures S2b and S2c), the onset potentials of the GAC biocathodes became more positive during operation. The current densities reached values that are in line with the results obtained during galvanostatically controlled operation.

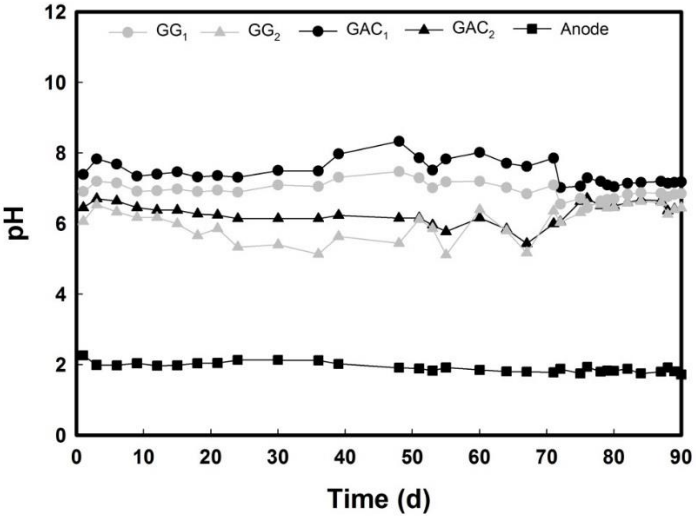

Figure S3. pH values for anolyte and catholyte in all reactors after inoculation. Catholyte pH of all reactors fluctuated between 6 and 8 during the period with intermittent CO_2 supply, but became stable at 7 during the period with constant CO_2 supply. All reactors shared the same anolyte with a stable pH of 2 throughout the whole experiment.

D. Energy Efficiencies for All Reactors

Table S2. Measured anode and cathode potentials, cell voltages, current-to-methane efficiencies, voltage efficiencies and energy efficiencies for all four reactors at current densities of 10 and 35 $A/m^2cat_{proj.}$ Data represent the average ± standard deviation of four separate samples taken from each reactor within a period of 2 weeks.

Current density (A/m^2cat_{proj})	**Reactor**	$E_{an,measured}$ **(V vs. Ag/AgCl)**	$E_{cat,measured}$ **(V vs. Ag/AgCl)**	E_{cell} **(V)**	η_{CH4} **(%)**	$\eta_{voltage,CH4}$ **(%)**	η_{energy,CH_4}**(%)**
10	**GG_1**	1.73 ± 0.01	-0.92 ± 0.02	-3.09 ± 0.04	51.34 ± 2.08	37.29 ± 0.05	19.14 ± 0.75
	GG_2	2.35 ± 0.04	-0.91 ± 0.01	-3.27 ± 0.03	53.31 ± 2.02	35.24 ± 0.34	18.78 ± 0.53
	GAC_1	1.83 ± 0.01	-0.52 ± 0.01	-2.94 ± 0.02	54.48 ± 0.89	39.26 ± 0.33	21.38 ± 0.17
	GAC_2	2.40 ± 0.01	-0.51 ± 0.01	-2.98 ± 0.06	54.15 ± 1.99	38.72 ± 0.84	20.98 ± 1.22
35	**GG_1**	2.44 ± 0.10	-1.03 ± 0.06	-4.67 ± 0.07	65.37 ± 6.46	24.78 ± 0.50	15.99 ± 1.49
	GG_2	2.61 ± 0.04	-1.07 ± 0.01	-5.02 ± 0.04	69.55 ± 7.23	22.70 ± 0.48	15.79 ± 1.67
	GAC_1	2.64 ± 0.08	-0.58 ± 0.01	-4.76 ± 0.13	67.25 ± 8.72	23.77 ± 1.00	15.96 ± 2.02
	GAC_2	2.55 ± 0.05	-0.59 ± 0.02	-4.78 ± 0.13	65.78 ± 10.51	23.55 ± 1.22	15.53 ± 2.70

E. Repeatability Tests for Achieving Low Cathode Overpotentials

We restarted two new methane-producing BES reactors, using the same setups and operational conditions as the experiment described in this manuscript: clean packed bed of GAC cathode electrodes, anolyte and catholyte, inoculum, operational conditions (i.e., galvanostatically controlled operation with a current density of 5 A/m^2cat_{proj}, continuous sparging with CO_2, the circulating pump speed with 7 min/L for both anolyte and catholyte). During the experiment, the cathode potentials of these two GAC biocathodes (R_1 and R_2) were monitored, and the pH of the catholyte and anolyte was measured without controlling. Figure S4 (a) showed that both R_1 and R_2 again changed to less negative cathode potentials, which were similar as those results reported herein.

To verify the measurement of cathode potential, another new Ag/AgCl reference electrode was inserted into the cathode chamber of the R_1 as close as possible to the activated carbon granular bed. The cathode potential of R_1 was about -0.43 V vs. Ag/AgCl (inside cathode compartment), which was even less negative than the cathode potential when the reference electrode was placed outside the cathode compartment: -0.54 V vs. Ag/AgCl. Such potential discrepancy might be due to the resistance of the catholyte and/or the resistance of the granular bed.

After cathode potentials of these two GAC biocathodes were stable, these GAC biocathodes were tested under galvanostatically controlled operation at 5 A/m^2cat_{proj}, firstly supplying them with a CO_2/N_2 gas mixture (20/80 by volume) at day 50, and then with pure N_2 at day 51. The pure N_2 was used to flush away all dissolved CO_2. With CO_2 supply, methane is expected to be the main product for the GAC biocathodes, however, without CO_2 supply, methane production would not be feasible, and hydrogen would be the main product. For the GAC biocathodes shown in Figure S4 (b), in absence of CO_2, the cathode potential changed from -0.6 to -0.9 V, pointing out the low overpotential is related to methane production and not to hydrogen production. This decrease in cathode potential cannot be explained by the increase of catholyte pH, as there was only a minor change in pH (Figure S5 (b)). These results indicate that methane produced in our GAC biocathodes probably occurred via direct electron transfer rather than via indirect electron transfer (H_2).

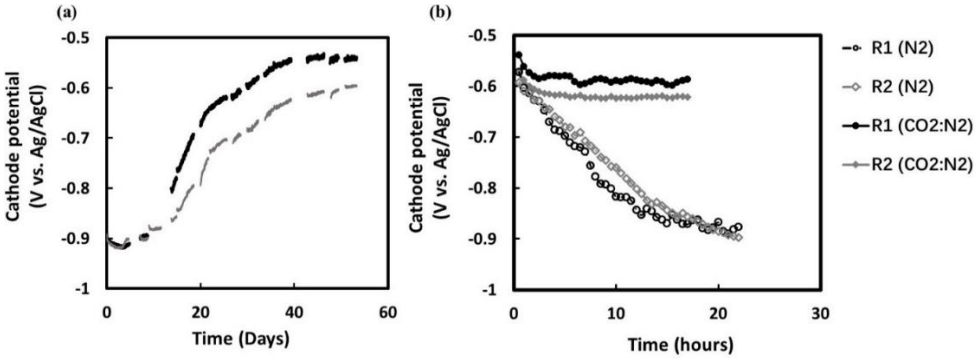

Figure S4. Overview of cathode potentials for two GAC biocathodes (a) during 50 days after inoculation; (b) during the test with CO_2/N_2 gas mixture at day 50 or the test only N_2 gas at day 51 (b).

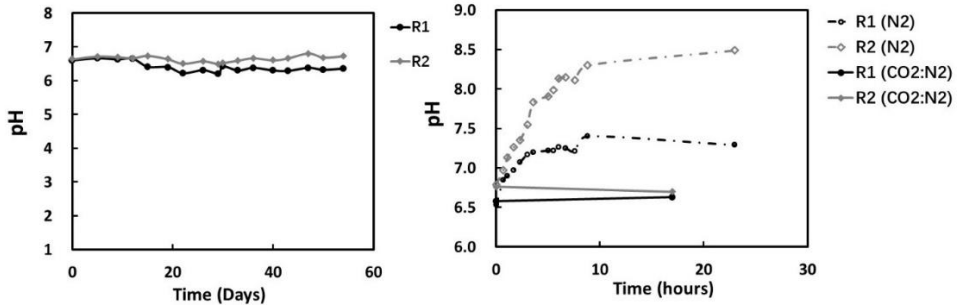

Figure S5. Overview of pH for two GAC biocathodes (a) during 50 days after inoculation; (b) during the test with CO_2/N_2 gas mixture at day 50 or the test only N_2 gas at day 51.

REFERENCES

Hamady, M., Walker, J.J., Harris, J.K., Gold, N.J. and Knight, R. (2008) Error-correcting barcoded primers allow hundreds of samples to be pyrosequenced in multiplex. Nature methods 5(3), 235.

Kvist, T., Ahring, B.K. and Westermann, P. (2007) Archaeal diversity in Icelandic hot springs. Fems Microbiology Ecology 59(1), 71-80.

Parada, A.E., Needham, D.M. and Fuhrman, J.A. (2015) Every base matters: assessing small subunit rRNA primers for marine microbiomes with mock communities, time series and global field samples. Environmental Microbiology.

Quast, C., Pruesse, E., Yilmaz, P., Gerken, J., Schweer, T., Yarza, P., Peplies, J. and Glöckner, F.O. (2012) The SILVA ribosomal RNA gene database project: improved data processing and web-based tools. Nucleic Acids Research, gks1219.

Ramiro-Garcia, J., Hermes, G.D., Giatsis, C., Sipkema, D., Zoetendal, E.G., Schaap, P.J. and Smidt, H. (2016) NG-Tax, a highly accurate and validated pipeline for analysis of 16S rRNA amplicons from complex biomes. F1000Research 5.

Somerfield, P.J. (2008) Identification of the Bray-Curtis similarity index: Comment on Yoshioka (2008). Marine Ecology Progress Series 372, 303-306.

Wang, Y. and Qian, P.-Y. (2009) Conservative fragments in bacterial 16S rRNA genes and primer design for 16S ribosomal DNA amplicons in metagenomic studies. PLoS One 4(10), e7401.

Chapter 4. Effect of Intermittent Current on the Performance of Methane-producing Bioelectrochemical Systems

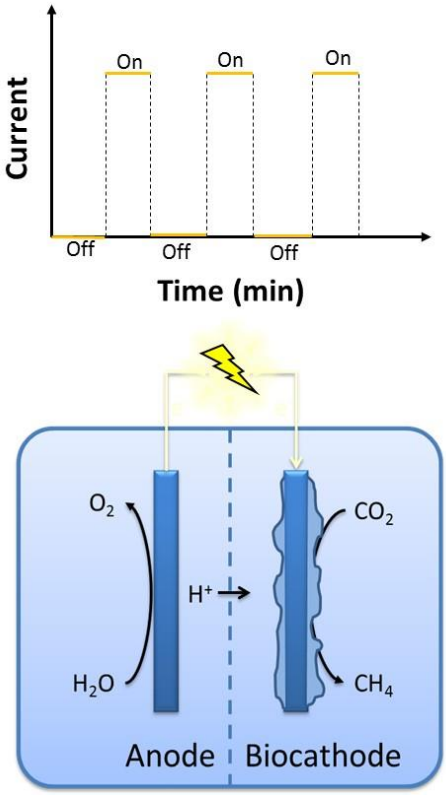

Effect of Intermittent Current on the Performance of Methane-producing Bioelectrochemical Systems

ABSTRACT

Methane-producing bioelectrochemical systems (BESs) convert carbon dioxide into methane when supplied with external electricity. This technology provides an innovative approach for renewable electricity conversion and storage. Renewable electricity is known to be intrinsically intermittent. The effect of intermittent electricity supply on the performance of methane-producing BESs has only been scarcely investigated. This study investigated the effect of intermittent current on four mature biocathodes of methane-producing BESs, by operating them under three different current supply modes (time-ON/time-OFF: 4'- 2', 3'- 3', 2'- 4'), at two current densities (10 and 35 A/m^2 cat_{proj}). Two cathode materials were used: graphite and activated carbon granules, both in a packed bed, to assess if electrode capacitance improves performance at intermittent current. Methane production rate was calculated during both time-ON and time-OFF periods, while current-to-methane efficiency was only calculated by taking into account the time-ON period. Our results showed that methane production rates increased with longer time-ON modes for both materials. The current-to-methane efficiencies of all biocathodes at intermittent current were similar to those under constant current, with 50-60 % at 10 A/m^2 cat_{proj} and 80-90 % at 35 A/m^2 cat_{proj}. After switching to continuous current supply, the biocathodes recovered their original performance directly. Our results show that methane-producing biocathodes are robust and can operate under intermittent current and no effect of capacitance on performance was observed. The capability of dealing with intermitttent current supply provides promise for methane-producing BESs as a renewable electricity conversion and storage technology.

INTRODUCTION

The expansion of global energy demand results in an increasing utilization of fossil fuels, which leads to unwanted CO2 emissions (Rogelj et al. 2016). To mitigate CO2 emissions, the energy transition from fossil fuels to renewable energy is necessary. In the Energy Roadmap 2050 released by European Commission in 2011, the share of renewable energy in the final gross energy consumption will grow from 10% of today, to 30% in 2030, and at least 55% in 2050 (Roadmap 2011). The substantial rise of renewable electricity use, requires development of energy storage technologies (Roadmap 2011, Administration 2016, Weitemeyer et al. 2015), because large part of renewable electricity produced is fluctuating and intermittent due to the intermittent nature of wind and sun (Ellabban et al. 2014, Twidell and Weir 2015).

Power to Gas (PtG) technologies have been reported as a flexible option to convert and store excess renewable electricity from the power grid (electricity) into the gas grid (CH4) (Bailera et al. 2017). CH4 can be generated by reduction of CO2 through thermochemical or biological methanation (Bailera et al. 2017). Methane-producing bioelectrochemical systems (BESs) are one form of biological methanation (Geppert et al. 2016). At the cathode of a methane-producing BES, CO2 is reduced to methane by methanogens. At the anode, water is oxidized to protons with electrons transferred to cathode through an electric circuit when electrical energy is supplied.

Since the concept of methane-producing BESs has been shown in 2009 (Cheng et al. 2009), research has aimed at increasing the methane production rate and conversion efficiency. A variety of electrode materials with a wide range of properties have been compared for growing biocathode to optimize methane production (Siegert et al. 2014, Liu et al. 2017). Microbial community analyses suggest that methane-producing biocathodes are typically dominated by hydrogenotrophic methanogens (Van Eerten-Jansen et al. 2013, Cai et al. 2016, Bretschger et al. 2015), e.g. *Methanobacterium*. Therefore, biocathodes inoculated with these hydrogenotrophic methanogens can promote fast start-up of biocathode and improve methane production rates (Siegert et al. 2015). Methane producing BESs have mainly been studied at constant external electricity supply. The electricity generated by the renewable sources (e.g. wind turbine) is, however, intermittent. Therefore, it is necessary to investigate whether methane-producing BESs can cope with intermittent electricity supply.

So far, one study has addressed methane generation after an open circuit period of 45 minutes (Bretschger et al. 2015). It was found that the methane production rate decreased by 87% after this open circuit period, and it took 4 months before performance was back at the original level (Bretschger et al. 2015). To our best knowledge, no systematic research has been performed to study the effect of intermittent electricity supply on the performance of methane-producing BESs.

Intermittent operation has been performed with capacitive anode electrode materials in the form of activated carbon granules for wastewater microbial fuel cells (MFCs) (Deeke et al. 2015, Deeke et al. 2013) (Borsje et al. 2016). These capacitive bioanodes can store electrons generated by electroactive microorganisms in the charging period (open circuit), and afterwards, these stored electrons could be harvested in the discharging cell (closed circuit). Introducing biocathodes with this capacitive property (storage of electrons) might also benefit methane-producing BESs operated with intermittent electricity supply. The possible advantages of capacitive electrodes for biocathodes could be: (i) storage of electrons in the electrical double layer during the current time-ON, that can be used when current is switched off, so that capacitance acts as an electron buffer when current peaks occur; (ii) providing high surface area for biofilm growth, which could mitigate the overpotential in biocathodes, as shown in Chapter 3 in this thesis.

The aim of this research is to investigate the effect of intermittent current supply on the performance of the methane-producing BESs. Three intermittent current supply modes with time-ON/time-OFF (4'- 2', 3'- 3' and 2'- 4') were performed at two different current densities (10 and 35 A/m2 catproj). These experiments were performed on two types of packed bed of materials: activated carbon granules (GAC) and graphite granules (GG), to compare the effect of intermittent current supply on capacitive electrodes versus non-capacitive electrodes. Methane production rate (L CH4 /m2 catproj/d) and current-to-methane efficiency (%) were analysed to assess the performance of methane-producing BESs.

MATERIALS AND METHODES

Methane-producing BES set-up

In this study, four bioelectrochemical reactors were operated. Each reactor had two chambers separated by a cation exchange membrane (FumaTech GmbH, Germany) with a working surface area of 22 cm^2. Each anodic or cathodic chamber had a working volume of 33 cm^3 (11 cm × 2 cm × 1.5 cm). Two types of carbon granules were used as cathode electrode materials, each material operationed in duplicate: activated carbon granules (Norit® PK, 1-3 mm diameter; cathode compartment of cell 1 (PK_1) containing a total weight of 8.5 g and PK_2 8.4 g), and graphite granules (Carbone Lorraine Benelux BV, 3-5 mm diameter; cathode compartment of cell 1 (GG_1) containing a total weight of 26 g and GG_2 29.2 g). A platinum and iridium coated titanium plate (Magneto Special Anodes BV, The Netherlands) was used as the anode electrode. To ensure good contact between cathode granules and current collector, the anode chamber was fully filled with glass beads of 7 mm diameter (VWR, Hecht-Assitent, Germany), covered with a plastic spacer on the side of the membrane. A schematic overview of the experiment set-up is shown in Figure 1. The experiment was operated inside a temperature-controlled cabinet at 30℃.

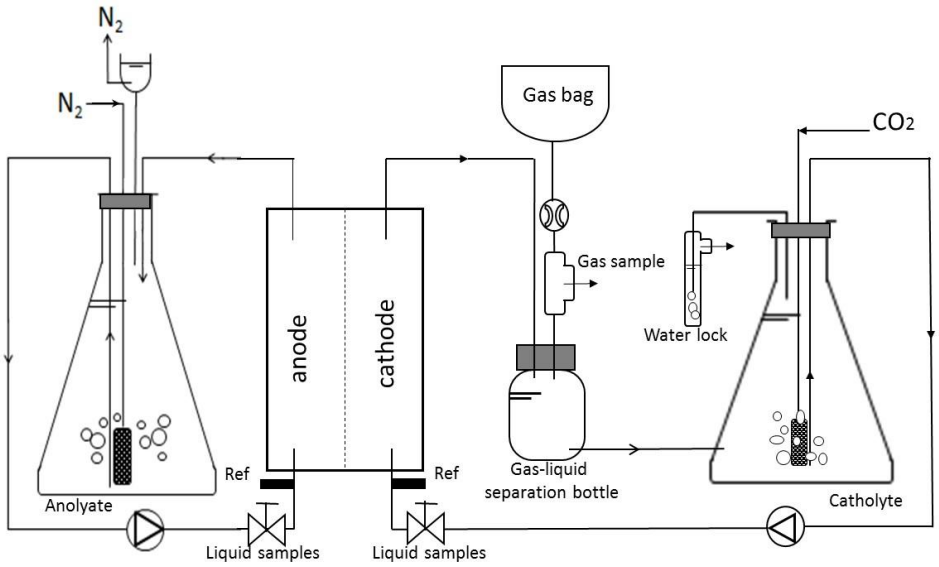

Figure 1. Schematic overview of the experimental set-up.

The cathode chamber of each reactor was connected to a gas-liquid separation bottle (60 mL) where the gas outflow passed through its headspace (15 mL) and was finally collected by a gas bag (2 L, Cali-5-BondTM, Calibrated Instruments INC). The headspace had an open pot fitted with a rubber stopper for gas sampling. The liquid phase of the gas-liquid separation bottle connected with a recirculation bottle (500 mL). In order to keep the catholyte with sufficient CO_2 and stable pH simultaneously, the catholyte in the recirculation bottle was continuously sparged with CO_2. The excess CO_2 went through a water lock and was released into the environment. All anode chambers were connected to the same anolyte recirculation bottle (5 L) which was sparged continuously with N_2 to remove the O_2 produced in the anodes. The inflow of each chamber contained a liquid sampling valve where samples were taken for pH and volatile fatty acid analyses. Reference electrodes (Ag/AgCl 3M KCl, ProSenseQiS, Netherlands) were used in both cathodic and anodic chambers for each reactor.

Source of microorganisms and electrolytes

All cathode chambers were inoculated at the same time with 10 mL of anaerobic sludge (50% granular sludge from the anaerobic treatment of paper industry wastewater in Eerbeek, The Netherlands and 50% granular sludge from the anaerobic treatment plant in Ede, The Netherlands). The volatile suspended solids (VSS) of the inoculum was 12.9 ± 1.3 g/L. The catholyte used in this experiment was composed of 0.2 g/L NH_4Cl, 0.13 g/L KCl, 50 mM phosphate buffer (2.77 g/L $NaH_2PO_4 \cdot 2H_2O$ and 4.58 g/L Na_2HPO_4), 1 mL/L vitamin(Wolin et al. 1963) and 1 mL/L mineral solution(Wolin et al. 1963). The anolyte used in this experiment was composed of 50 mM phosphate buffer (same as used in the catholyte). The anolyte and catholyte in all reactors were constantly recirculated at a rate of 7 mL/min.

Methane-producing BES Operation

All biocathodes were controlled galvanostatically by a potentiostat (Ivium n-stat with IviumSoft v2.462, Eindhoven, The Netherlands), at a current density of 5 A/m^2, afterwards 10 A/m^2 and finally 35 A/m^2. Experimental conditions are shown in Figure 2. For intermittent operations, a cycle time of 6 minutes was carried out using three different current time-ON/time-OFF ratios: 4’ – 2’, 3’ – 3’ and 2’ – 4’. Each intermittent operation

lasted for 20 h and was performed twice. After intermittent operations, all biocathodes were supplied with constant current supply for 20 h again to investigate whether intermittent operation would affect biological activity.

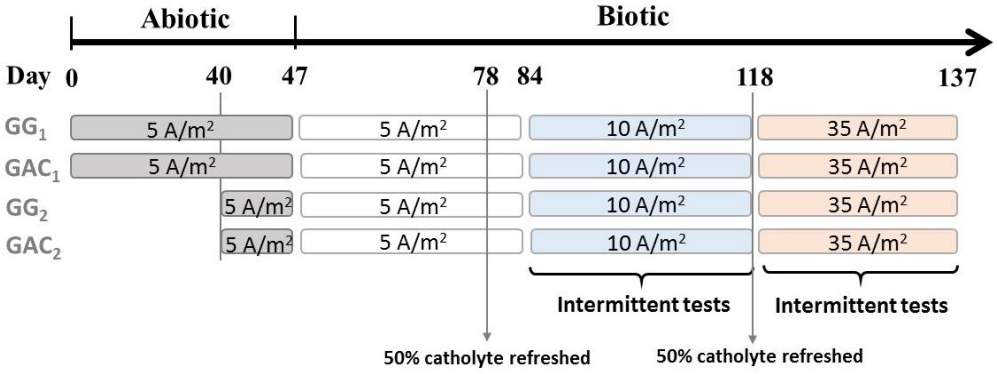

Figure 2. Overview of experimental conditions that were carried out for four methane-producing BES reactors. The numbers inside the box represents current density supplied to the biocathode. During those phases under current densities of 10 and 35 A/m^{2}cat$_{proj}$, the intermittent current supply modes were performed.

Analytical methods

At the end of each operation, the gas composition (i.e. CH_4, H_2, O_2, CO_2 and N_2) in the headspace of each methane-producing BES reactor was quantified by two types of gas chromatography: HP 5890A gas chromatograph (to measure H_2) and Finsons Instruments GC 8340 gas chromatography (to measure CH_4, CO_2, O_2 and N_2). The total gas volume inside the gas bags was quantified by emptying the gas bags with a syringe. The methane production rate of each biocathode during each operation was calculated using the following equation:

$$\gamma_{CH4-A} = \frac{V_T \times C_{CH4}}{A_{proj} \times t} \quad (1)$$

Where γ_{CH4-A} (L CH_4/m^2 cat$_{proj}$ /d) represents methane production rate normalized to the projected surface area of the cathode electrode; V_T (L) is the total volume by summing up the volume of the gas bag (as measured with syringe) and the headspace (0.015 L);

$C_{CH_4}(\%)$ is the methane fraction in the headspace; $A_{proj}(m^2)$ is the projected surface area of the cathode electrode; t (d) is the duration of each operation (including both current time-ON and time-OFF periods).

Current-to-methane efficiency (%) for within each operation indicates which percentage of the electrons consumed to produce methane (Liu et al. 2016).

$$\eta_{CH4} = \frac{N_{CH4} \times n_{CH4} \times F}{\int_{t=0}^{t} I \, dt} \quad (2)$$

F is the Faraday constant (96485 C/mol e^-); N_{CH4} (mol) is total moles of CH_4 produced; n_{CH4} is moles of electrons per mole of CH_4 (n=8); I (A) is the current; t (s) is the total current time-ON period (when the current was supplied to the biocathode) within each operation.

In addition, catholyte samples of 2 mL was taken from each methane-producing BES reactor for VFA analysis. The liquid sample was firstly pre-treated by centrifuged for 10 minutes at 10, 000 RPM, and then diluted with 15% formic acid in the sample vial. Finally, VFA concentration of each liquid sample was measured by using a gas chromatograph (Agilent 7890B) equipped with flame ionization detector and capillary column (HP-FFAP, 25M x 0.32mm x 0.5μm).

RESULTS AND DISCUSSION

Methane production was related to total charge provided. After all the biocathodes achieved a stable methane production rates at a constant current supply of 10 A/m^2cat_{proj}, intermittent current (at the same current density) was supplied to all biocathodes with three different time intervals: 4'-2', 3'-3' and 2'-4'. Methane production rate of each biocathode is shown in Figure 2a, calculations based on the overall period of each operation (20 h). Higher current time-ON/time-OFF interval supplied to the biocathodes resulted in higher methane production rates, with 9.5 L CH_4/m^2 cat_{proj}/d at 4'-2', 5.5 L CH_4/m^2 cat_{proj}/d at 3'-3' and 4.0 L CH_4/m^2 cat_{proj}/d at 2'-4'.

When the current density was increased from 10 to 35 $A/m^2cat_{proj,}$ the methane production rate at continuous current supply increased from 15 L CH_4/m^2 cat_{proj}/d at 10 A/m^2 (Figure 3a) to 90 L CH_4/m^2 cat_{proj}/d at 35 A/m^2 (Figure 3b). As galvanostatic control was used, the current density supplied to the biocathode was directly related to the methane production rate. When current supply was switched from constant to intermittent mode for all biocathodes, an increase in methane production rate was observed along with increasing time-ON/time-OFF ratios, same as for 10 A/m^2. Moreover, we compared our experimental data with the theoretical data calculated according to different current time-ON/time-OFF ratios (Figure S2 in Supporting Information). The close fit between measured and calculated data shows that methane generation is directly linked to the charge provided to the biocathode, for both GG and GAC.

Finally, we operated all biocathodes at constant current density of 60 A/m^2cat_{proj}. Methane was the main product for all biocathodes, but also substantial amounts of hydrogen were found for both GG and GAC biocathodes (Figure S3. in SI section C). These results suggest that when GAC biocathodes receive higher currents, the electrons that could not be diverted to methane were not stored in GAC biocathodes but rather utilized to produce hydrogen.

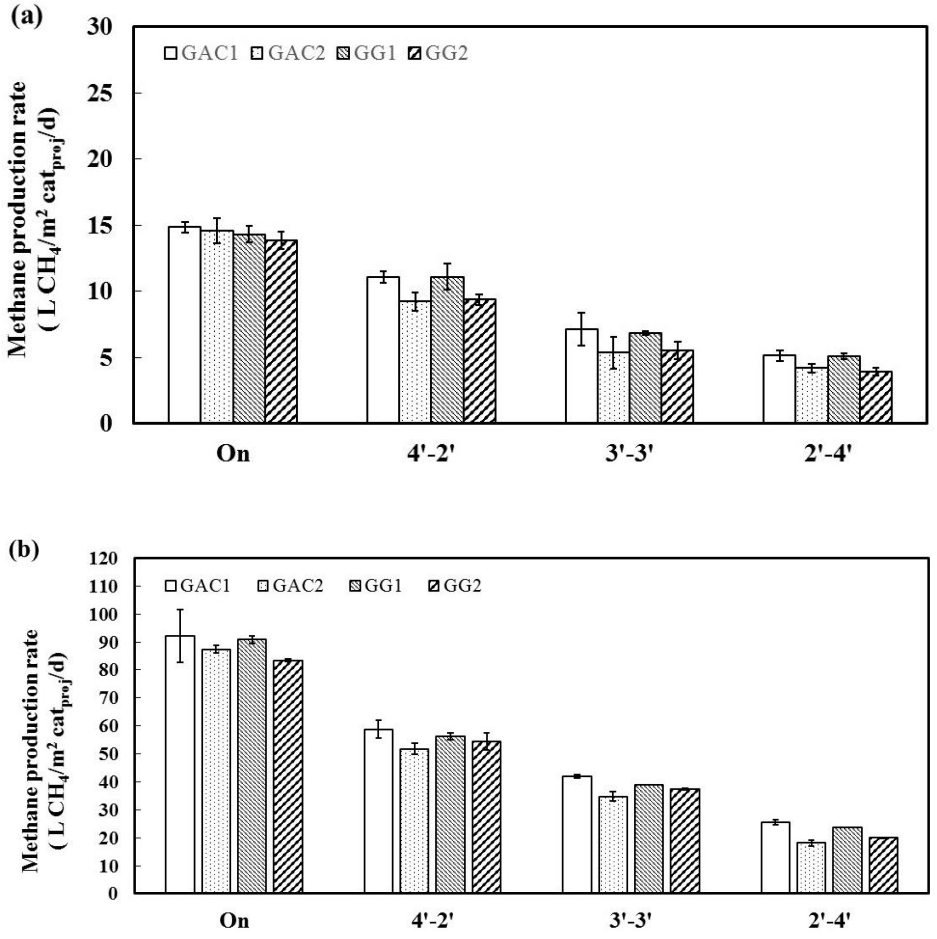

Figure 3. Methane production rates for all biocathodes when they were supplied with constant current and intermittent current. Three different current time-ON/time-OFF intervals (4' – 2', 3' – 3' and 2' – 4') were carried out. The current density during the current time-ON was 10 A/$m^2$$cat_{proj}$ (a) and 35 A/$m^2$$cat_{proj}$ (b). For each operational condition, duplicate experiments were performed. The standard deviations are shown as an error bar, whereas the average value is shown as a column.

Intermittent current operation does not influence biocathode activity. At a current density of 10 A/m^{2}cat$_{proj}$, all biocathodes had a similar current-to-methane efficiency of 50-60% (Figure 4a), at different current time-ON/time-OFF intervals. When the current density was increased from 10 to 35 A/m^{2}cat$_{proj,}$ the current-to-methane efficiency was also constant with a slight decrease along with the longer time-OFF intervals. The current-to-methane efficiency at a continuous current supply with 35 A/m^{2}cat$_{proj}$, was much higher (about 90%) (Figure 4b) than those at 10 A/m^2 (Figure 4a). These high cathodic efficiencies obtained at the current density of 35 A/m^{2}cat$_{proj}$, is also higher than the cathodic efficiency achieved at the same continuous current density reported in Chapter 3. This discrepancy could be due to the different durations between headspace sampling: 20 h in this study and 3-4 days in Chapter 3. Shorter duration between headspace sampling would help mitigate electrons loss via H_2 or O_2 leakage from the joints of the experimental set-up. To conclude, current-to-methane efficiency (%) remained quite stable under the different current supply modes at 10 A/m^2, and showed a slight decrease with increasing OFF-time at 35 A/m^2.

After these intermittent operations, the methane production of each biocathode was quantified, for an additional operation of 20 h with constant current supply, to study if initial activity was restored after intermittent operation. As shown in Figure 4, biocathodes were not seriously affected during the intermittent operation at these two current densities of 10 and 35 A/m^{2}cat$_{proj}$, the current-to-methane efficiencies of all biocathodes after intermittent operations were similar to those at constant current supply.

When comparing performance of GAC to GG, we observed that differences between replicates were larger than differences between cathode materials during these intermittent operations. GAC_1 and GG_1 biocathodes had, consistently, 10-15% higher current-to-methane efficiencies than GAC_2 and GG_2 biocathodes. The reason why duplicate biocathodes were different could be due to the difference in biofilm maturity between the first (GAC_1 and GG_1) and second (GAC_2 and GG_2) set of reactors, as the first set of reactors had been operated 40 days longer than the second set of reactors.

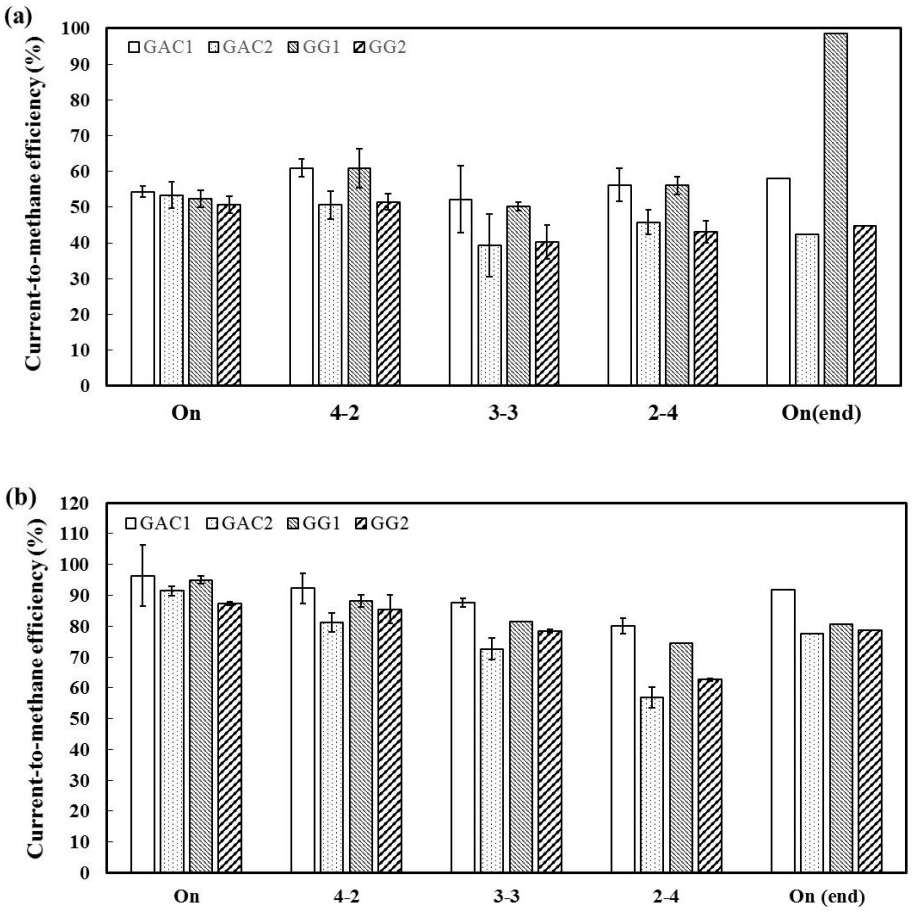

Figure 4. Current-to-methane efficiencies (%) for all reactors when they were supplied with constant and intermittent current. Three different current time-ON/time-OFF ratios (4' – 2', 3' – 3' and 2' – 4') were carried out. The current density during the current time-ON was 10 A/m^2cat_{proj} (a) and 35 A/m^2cat_{proj} (b). For each operational condition, duplicate operations were performed. The standard deviations are shown as an error bar, whereas the average value is shown as a column.

GAC biocathodes did not show advantages over GG under intermittent current supply operations. Studies on bioanodes have shown that GAC can store charge in the electric double layer when used in Microbial Fuel Cells (Deeke et al. 2015, Borsje et al. 2016, Lu et al. 2015, Liu et al. 2014), whereas graphite granules with low capacitance do not show this charge storage behavior. The GAC biocathode was found to have 2000-3000x

higher capacitance than the GG biocathode, as determined from charge-discharge experiments (Figure S1 in supporting information). This higher capacitance of GAC biocathodes could result in less fluctuation in cathode potential, and as a possible electron buffer, than that in GG biocathodes during intermittent operations (Borsje et al. 2016). As shown in Figure 5, the cathode potentials of GAC biocathodes during intermittent current kept stable around -0.5 V, whereas the cathode potentials of GG biocathodes changed in the range from -0.6 V to -1.0 V. Besides the cathode potentials, no considerable differences were observed between the two materials (GAC_1 and GG_1; GAC_2 and GG_2) at intermittent current supply in terms of methane production rate (Figure 3) and current-to-methane efficiency (Figure 4). These results indicated that the fluctuations of cathode potentials, especially in GG biocathodes, did not negatively affect the biological activity of these methane-producing biocathdoes.

Although there is no difference between GAC and GG biocathodes during intermittent operation, the use of GAC as the cathode electrode material for methane-producing BESs still brings advantages in terms of energy efficiency, which is defined as the part of the applied electrical energy that ends up in CH_4. One the one hand, this energy efficiency is higher as a result of the less negative cathode potential of -0.5 V observed for GAC biocathodes compared with GG bicathodes (-0.9 V), On the other hand, GAC biocathodes produced less hydrogen and more methane than GG biocathodes at high current density of 60 A/m^2cat_{proj}. The reason could be that the cathode potentials for GAC biocathodes still kept at around -0.6 V, whereas the cathode potentials for GG biocathdoes became even more negative to about -1.1 V.

Our results show that methane-producing biocathodes were robust under certain intermittent conditions, rather than very sensitive to open-circuit as concluded by Bretschger et al. (Bretschger et al. 2015). The capability of dealing with intermitttent current supply is a promising feature for application of methane-producing BESs for renewable electricity storage.

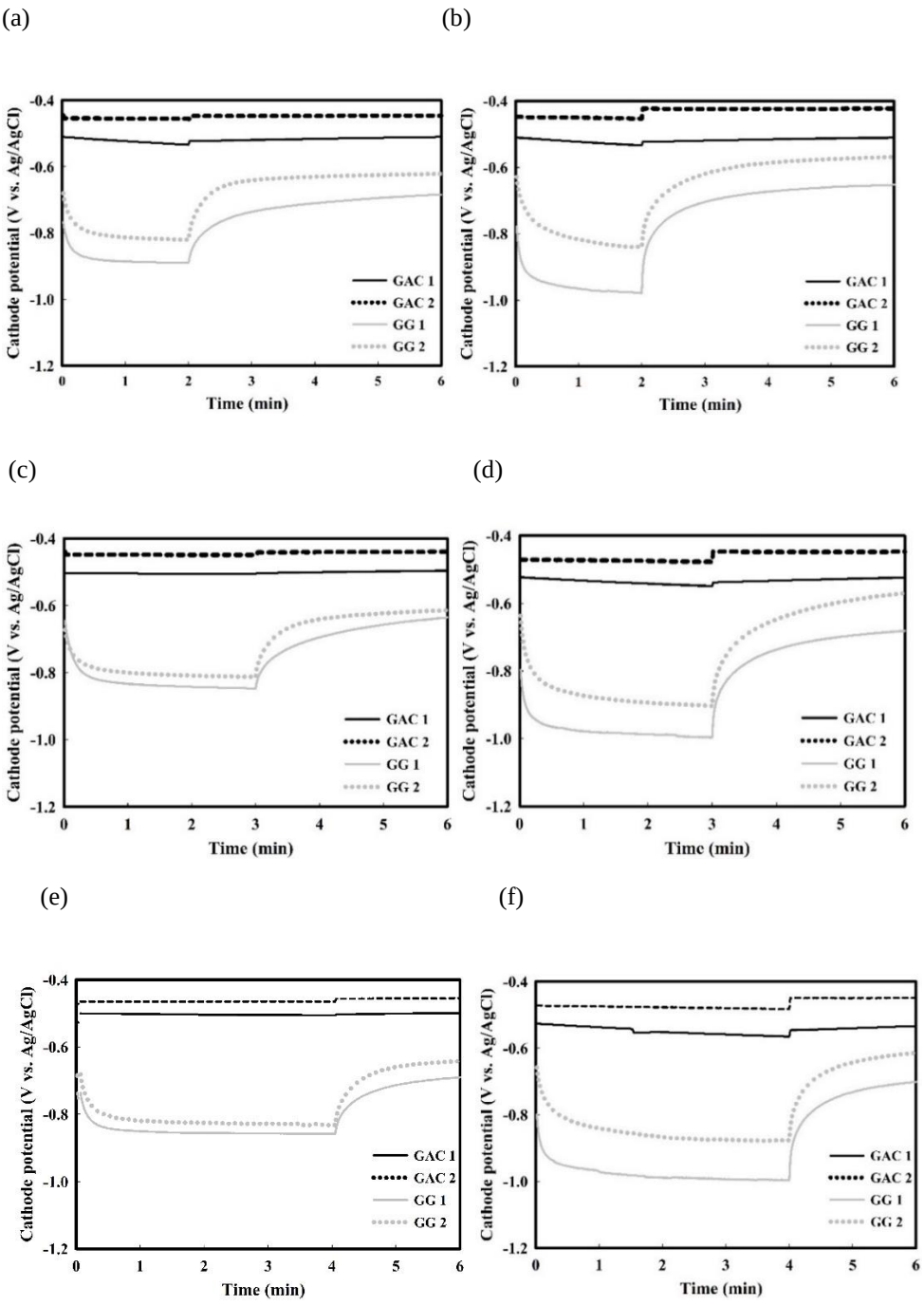

Figure 5. Overview of cathode potentials from all biocathodes within one typical cycle (6 min) of intermittent operations at current density of 10 (a, c and e) and 35 A/m^2cat_{proj} (b, d

and f). During the period with current time-ON, the cathode potentials of GG biocathodes became more negative in the range of -0.8 V to -1.0 V. However, during the period with current time-OFF, the cathode potentials of GG biocathodes became less negative in the range of -0.6 V to -0.7 V. Moreover, higher changed in the cathode potentials was observed at the current density of 35 A/m^2cat_{proj}, instead of 10 A/m^2cat_{proj}. In the intermittent operations, the cathode potentials of GAC biocathodes kept stable around -0.5 V.

ASSOCIATED CONTENT

The Supporting Information is available at the end of this chapter.

AKNOWLEDGEMENT

We thank two Dutch companies: Alliander and DMT Environmental Technology for giving their scientific discussion input and financial support to the research. We also thank the Chinese Scholarship Council for financial support to the author's Ph.D. programme (File No. 201306120043) in Wageningen University & Research.

REFERENCE

Administration, U.S.E.I. (2016) <Annual energy outlook 2016 with projections to 2040.pdf>.

Bailera, M., Lisbona, P., Romeo, L.M. and Espatolero, S. (2017) Power to Gas projects review: Lab, pilot and demo plants for storing renewable energy and CO_2. Renewable and Sustainable Energy Reviews 69, 292-312.

Borsje, C., Liu, D., Sleutels, T.H.J.A., Buisman, C.J.N. and ter Heijne, A. (2016) Performance of single carbon granules as perspective for larger scale capacitive bioanodes. Journal Of Power Sources 325, 690-696.

Bretschger, O., Carpenter, K., Phan, T., Suzuki, S., Ishii, S.i., Grossi-Soyster, E., Flynn, M. and Hogan, J. (2015) Functional and taxonomic dynamics of an electricity-consuming methane-producing microbial community. Bioresource Technology 195, 254-264.

Cai, W., Liu, W., Yang, C., Wang, L., Liang, B., Thangavel, S., Guo, Z. and Wang, A. (2016) Biocathodic methanogenic community in an integrated anaerobic digestion and microbial electrolysis system for enhancement of methane production from waste sludge. ACS Sustainable Chemistry & Engineering 4(9), 4913-4921.

Cheng, S.A., Xing, D.F., Call, D.F. and Logan, B.E. (2009) Direct Biological Conversion of Electrical Current into Methane by Electromethanogenesis. Environmental Science & Technology 43(10), 3953-3958.

Deeke, A., Sleutels, T.H.J.A., Donkers, T.F.W., Hamelers, H.V.M., Buisman, C.J.N. and Ter Heijne, A. (2015) Fluidized Capacitive Bioanode As a Novel Reactor Concept for the Microbial Fuel Cell. Environmental Science & Technology 49(3), 1929-1935.

Deeke, A., Sleutels, T.H.J.A., Heijne, A.T., Hamelers, H.V.M. and Buisman, C.J.N. (2013) Influence of the thickness of the capacitive layer on the performance of bioanodes in Microbial Fuel Cells. Journal Of Power Sources 243(0), 611-616.

Ellabban, O., Abu-Rub, H. and Blaabjerg, F. (2014) Renewable energy resources: Current status, future prospects and their enabling technology. Renewable and Sustainable Energy Reviews 39, 748-764.

Geppert, F., Liu, D., van Eerten-Jansen, M., Weidner, E., Buisman, C. and Ter Heijne, A. (2016) Bioelectrochemical Power-to-Gas: State of the Art and Future Perspectives. Trends In Biotechnology.

Liu, D., Zhang, L., Chen, S., Buisman, C. and ter Heijne, A. (2016) Bioelectrochemical enhancement of methane production in low temperature anaerobic digestion at 10 °C. Water Research 99, 281-287.

Liu, D., Zheng, T., Buisman, C. and ter Heijne, A. (2017) Heat-Treated Stainless Steel Felt as a New Cathode Material in a Methane-Producing Bioelectrochemical System. ACS Sustainable Chemistry & Engineering.

Liu, J., Zhang, F., He, W., Zhang, X., Feng, Y. and Logan, B.E. (2014) Intermittent contact of fluidized anode particles containing exoelectrogenic biofilms for continuous power generation in microbial fuel cells. Journal Of Power Sources 261, 278-284.

Lu, Z., Girguis, P., Liang, P., Shi, H., Huang, G., Cai, L. and Zhang, L. (2015) Biological capacitance studies of anodes in microbial fuel cells using electrochemical impedance spectroscopy. Bioprocess and Biosystems Engineering 38(7), 1325-1333.

Roadmap, E. (2011) Energy Roadmap 2050. Communication from the Commission to the European Parliament, the Council, the European Economic and Social Committee and the Committee of the Regions, Brussels 15, 12.

Rogelj, J., den Elzen, M., Höhne, N., Fransen, T., Fekete, H., Winkler, H., Schaeffer, R., Sha, F., Riahi, K. and Meinshausen, M. (2016) Paris Agreement climate proposals need a boost to keep warming well below 2 °C. Nature 534(7609), 631-639.

Siegert, M., Li, X.-f., Yates, M.D. and Logan, B.E. (2015) The presence of hydrogenotrophic methanogens in the inoculum improves methane gas production in microbial electrolysis cells. Frontiers in Microbiology 5.

Siegert, M., Yates, M.D., Call, D.F., Zhu, X., Spormann, A. and Logan, B.E. (2014) Comparison of Nonprecious Metal Cathode Materials for Methane Production by Electromethanogenesis. ACS Sustainable Chemistry & Engineering 2(4), 910-917.

Twidell, J. and Weir, T. (2015) Renewable energy resources, Routledge.

Van Eerten-Jansen, M.C.A.A., Veldhoen, A.B., Plugge, C.M., Stams, A.J.M., Buisman, C.J.N. and Ter Heijne, A. (2013) Microbial Community Analysis of a Methane-Producing Biocathode in a Bioelectrochemical System. Archaea 2013, 12.

Weitemeyer, S., Kleinhans, D., Vogt, T. and Agert, C. (2015) Integration of Renewable Energy Sources in future power systems: The role of storage. Renewable Energy 75, 14-20.

Wolin, E.A., Wolin, M.J. and Wolfe, R.S. (1963) Formation of Methane by Bacterial Extracts. Journal Of Biological Chemistry 238(8), 2882-2886.

SUPPORTING INFORMATION

Effect of Intermittent Current on the Performance of Methane-producing Bioelectrochemical Systems

3 Figures

A. Capacitance test: methodology and results

The capacitance of granular electrodes was determined by performing galvanostatic charge-discharge test. During the charging phase, a negative current was supplied to the electrode. On the contrary, the discharge phase was done at a positive current in order to extract the electrons. These tests were performed both before and after biofilm growth, respectively. For capacitance test before inoculum, the current used for both GAC and GG cathodes was ± 30 mA within a cathode potential range of -0.5 V to -0.7 V vs. Ag/AgCl. For capacitance test after inoculum, same currents and potential boundaries were used for GG biocathodes, while for GAC biocathodes the charge and discharge currents were -70 mA and 50 mA with potential boundaries of -0.2 V and -0.4 V vs. Ag/AgCl, respectively. That GAC biocathodes need different charge-discharge current and potential windows compared with GG biocahtodes, is due to its high capacitive property and methane production occurs in the range -0.5 V to -0.7 V vs. Ag/AgCl. One the one hand, the high capacitance of GAC biocathodes leads to a longer period of charge-discharge phase, which can be shortened by increasing the current used in charge-discharge phase. On the other hand, the capacitance tests should be performed outside the potential range, without happening any faradic reaction because faradic charge transfer can affect the real value of capacitance.

Specific capacitance (F/g) was calculated from galvanostatic charge-discharge curve, with the following formula in either the charge or discharge phases:

$$\text{Capacitance} = \frac{I \times \text{t}}{\Delta\text{E(t)} \times \text{m}} = \frac{I \times \text{t}}{(\text{E}_\text{f} - \text{E}_\text{i}) \times m} \quad (1)$$

where I is the charge/discharge current (A), t is the charge/discharge time (s). $\Delta\text{E(t)}$ is the potential difference between the final (E_f) and initial time (E_i) of charge/discharge phase (V), m is the mass of the granular electrode bed (g).

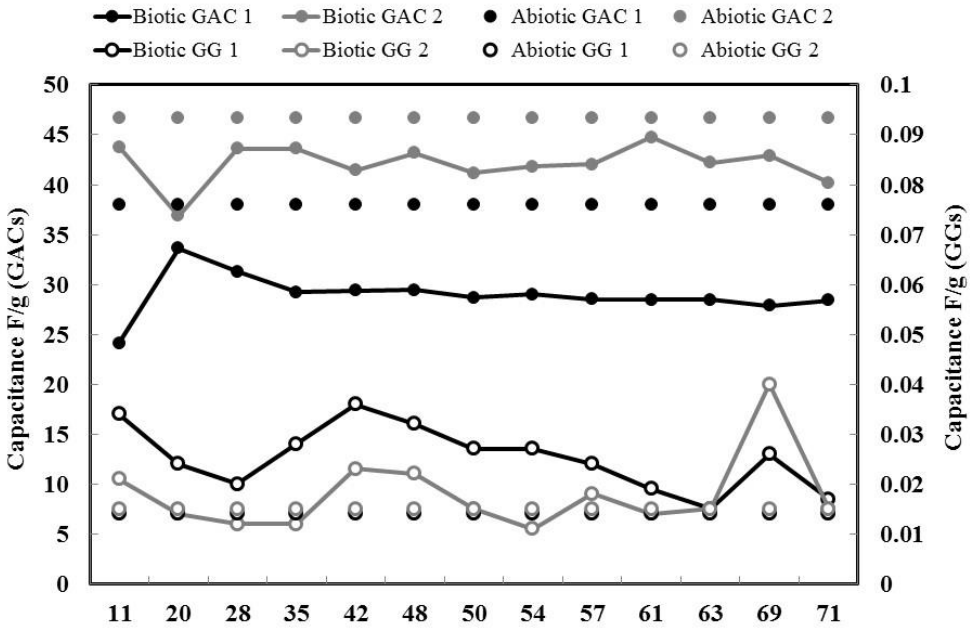

Figure S1. Capacitance values for abiotic and biotic tests with all reactors over a period of 71 days. In general, GAC cathodes had higher capacitances than GG cathodes. When no biofilm was present (abiotic), the values obtained were 38 F/g and 46.7 F/g for GAC_1 and GAC_2 and 0.014 F/g and 0.015 F/g for GG_1 and GG_2 respectively. When biofilm grew on the cathodes (biotic), capacitances of GAC biocathodes were lower under biotic conditions than under abiotic conditions. The average capacitance values for biotic tests were 29 F/g and 42.1 F/g for GAC_1 and GAC_2 and 0.025 F/g and 0.018 F/g for GG_1 and GG_2, respectively. The differences between biotic and abiotic capacitance values in GAC cathodes could be explained by biofilm blockage of inner pores of the GAC. This could probably lead to ion diffusion limitation, preventing the formation of the electrical double layer within the pores.

B. Comparision of methane prouction rates between experimental data and theoretical resutls.

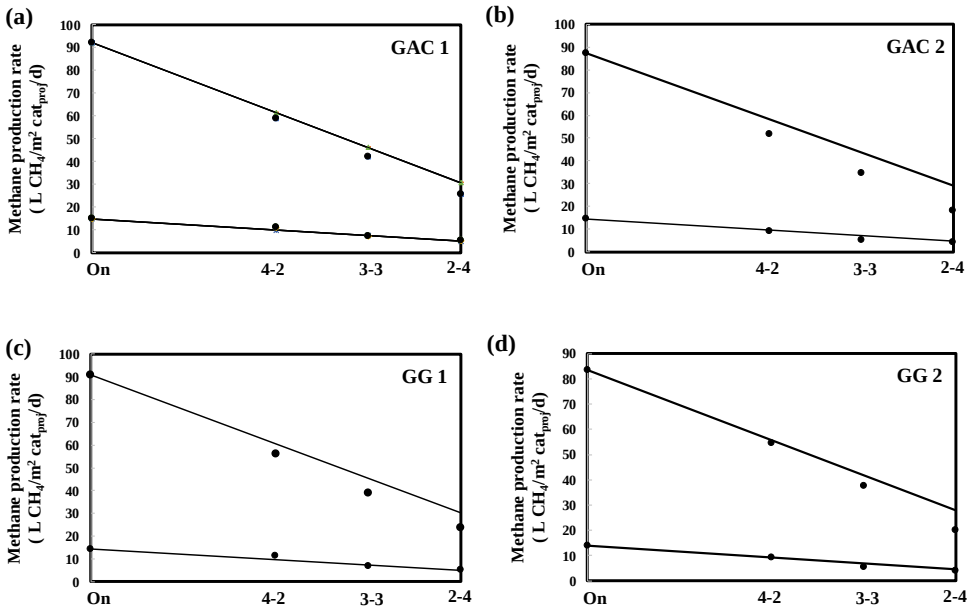

Figure S2. Overview of methane production rates of four biocathodes at different current supply modes: constant current (On) and intermittent current. Three different current time-ON/time-OFF ratios (4 - 2, 3 - 3 and 2 - 4) were carried out. The methane production rates of experimental data are shown as filled circles, while the methane production rates of theoretical data calculated according to different current time-On/time-OFF ratios are decapitated as solid line. The calculation assumed that the methane production rate at constant current supply of 35 A/m^2cat_{proj} was same for both experimental data and theoretical data. The theoretical data meet the experimental data, which indicates a liner relationship between the amount of methane produced in biocathodes and the current time-ON/time-OFF ratios.

C. Substantial hydrogen production at a higher current density of 60 A/m^{2}cat$_{proj}$.

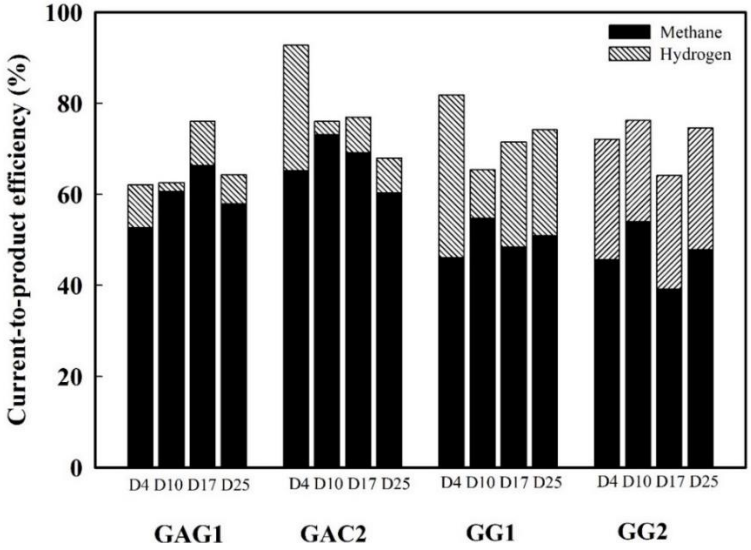

Figure S3. Current-to-product efficiencies (%) of all biocathodes at constant current supply of 60 A/m^{2}cat$_{proj}$. This test lasted for 25 days in total, which was carried out at the end of our experiment. Compared with the results obtained at current densities of 10 and 35 A/m^{2}cat$_{proj}$, GAC biocathodes started to produce detectable hydrogen, whereas GG biocathodes produced substantially at higher current density of 60 A/m^{2}cat$_{proj}$.

Chapter 5. Bioelectrochemical enhancement of methane production in low temperature anaerobic digestion at 10 °C

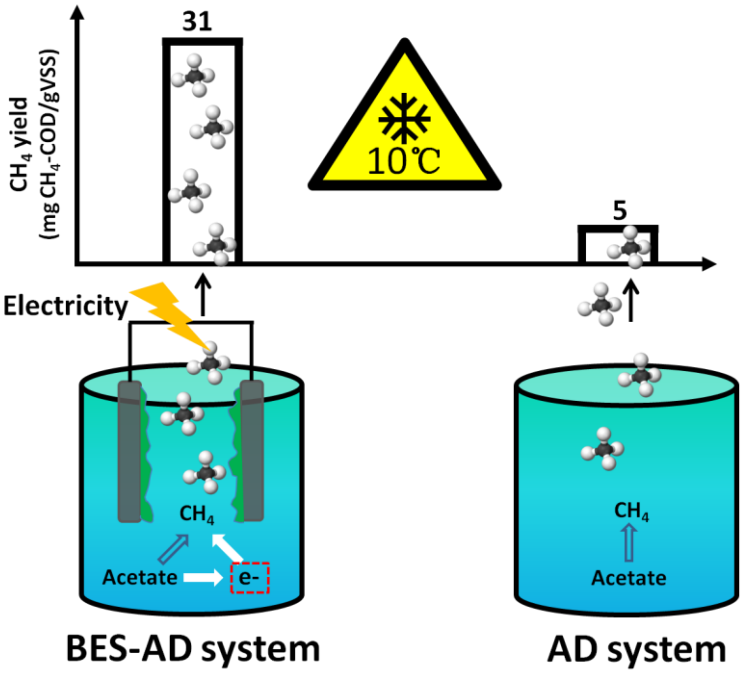

Bioelectrochemical enhancement of methane production in low temperature anaerobic digestion at 10 °C

ABSTRACT

Anaerobic digestion at low temperature is an attractive technology especially in moderate climates, however, low temperature results in low microbial activity and low rates of methane formation. This study investigated if bioelectrochemical systems (BESs) can enhance methane production from organic matter in low-temperature anaerobic digestion (AD). A bioelectrochemical reactor was operated with granular activated carbon as electrodes at 10 ℃. Our results showed that bioelectrochemical systems can enhance CH_4 yield, accelerate CH_4 production rate and increase acetate removal efficiency at 10 ℃. The highest CH_4 yield of 31 mg CH_4-COD/g VSS was achieved in the combined BES-AD system at a cathode potential of -0.90 V (Ag/AgCl), which was 5.3 to 6.6 times higher than that in the AD reactor at 10 ℃. CH_4 production rate achieved in the combined BES-AD system at 10 ℃ was only slightly lower than that in the AD reactor at 30 ℃. The presence of an external circuit between the acetate-oxidizing bioanode and methane-producing cathode provided an alternative pathway from acetate via electrons to methane, potentially via hydrogen. This alternative pathway seems to result in higher CH_4 production rates at low temperature compared with traditional methanogenesis from acetate. Integration of BES with AD could therefore be an attractive alternative strategy to enhance the performance of anaerobic digestion in cold areas.

This chapter has been published as: Liu, D., Zhang, L., Chen, S., Buisman, C. and ter Heijne, A. (2016a) Bioelectrochemical enhancement of methane production in low temperature anaerobic digestion at 10 °C. Water Research 99, 281-287.

INTRODUCTION

Anaerobic wastewater treatment is an attractive technology that recovers energy in the form of CH_4, has low excess sludge production, and low operational cost (Speece 2008). For anaerobic digestion, mesophilic conditions (25-37 ℃) and thermophilic conditions (55-65 ℃) are required to ensure optimal microbial activity (Hussain and Dubey 2015). Many types of wastewater are discharged at low temperature, however, such as wastewater from malting, breweries, soft drink industry and domestic sewage, with typical temperatures around 10-20 ℃ (Lettinga et al. 2001). As low temperature leads to low activity and low growth rate of methanogens, and consequently to low CH_4 production rate, strategies are needed to improve methanogenic activity of anaerobic sludge (Zhang et al. 2013c, Álvarez et al. 2004, Mahmoud et al. 2004). CH_4 production at 10 ℃ is at this moment unfeasible. In order to keep CH_4 production and wastewater treatment at a high rate in a cold area or during cold months, many anaerobic digesters are heated up to mesophilic conditions. However, this requires expensive heating and insulation systems, which makes it not practical and uneconomical (Witarsa and Lansing 2015). Use of electrodes instead of heating up could provide an alternative, cost-effective strategy to enhance performance of anaerobic digesters.

Methane-producing bioelectrochemical systems (BESs) are of special interest as a promising "power to gas" technology for renewable energy storage (Cheng et al. 2009, Villano et al. 2010, Van Eerten-Jansen et al. 2012). In this system, different types of electron donors (e.g. organic matter contained in waste streams) can be oxidized at the anode, and when electrical energy is supplied to the system, the released electrons can be transferred to the cathode to produce CH_4 from CO_2. Reduction of CO_2 to CH_4 can occur via two pathways: direct, using electrons and protons (H^+) and indirect, where protons are first reduced to H_2, and H_2 is used to reduce CO_2 in the presence of hydrogenotrophic methanogens (Villano et al. 2010).

BESs have been integrated with anaerobic digestion to enhance CH_4 formation at mesophilic conditions (20 – 40 ℃). Compared to the digesters without electrodes, integrating these two technologies has been shown to lead to enhanced CH_4 production rates (Feng et al. 2015, Tartakovsky et al. 2011, Zamalloa et al. 2013). Moreover, control

experiments with electrodes but without an additional electrical energy supply also resulted in increasing CH_4 yield and rate, as a result of enhanced biofilm attachment (De Vrieze et al. 2014). Also, it was shown that hydrogenotrophic methanogens and exoelectrogens (e.g. *Geobacter* sp.) were enriched, especially on the cathode electrode, when integrating BES with AD. This also enhanced CH_4 production rate in anaerobic digestion of waste activated sludge at 20-25 ℃ (Liu et al. 2016b). The integration of BES in anaerobic digestion at low temperature (< 20 ℃), however, has not been studied. While bioanodes have been shown to produce current at low temperature (< 20 ℃), albeit at lower rates than at mesophilic conditions, the cathodic production of CH_4 at low temperature has not been reported before.

At low temperature (< 20 ℃), fatty acids are accumulated as a result of low methanogenic activity. Hydrogenotrophic methanogenesis is far less temperature-sensitive than acetoclastic methanogenesis (Enright et al. 2009), and the growth of hydrogenotrophic methanogens can be stimulated by a moderate release of small amount of hydrogen at the cathode electrode (Liu et al. 2016b, Yang et al. 2013). Instead of producing CH_4 through the traditional route of acetoclastic methanogenesis and hydrogenotrophic methanogenesis, including elecrodes in the system could result in a new route for methanogenesis, created via the bio-anode (Figure 1a): acetate is oxidized while generating electrons and protons (Lu et al. 2011), which, with input of electrical energy can be reduced to H_2 or CH_4 at the biocathode(van Eerten-Jansen et al. 2015). The different routes via which CH_4 can be produced from acetate in this combined BES-AD system are summarized in Figure 1b.

(a)

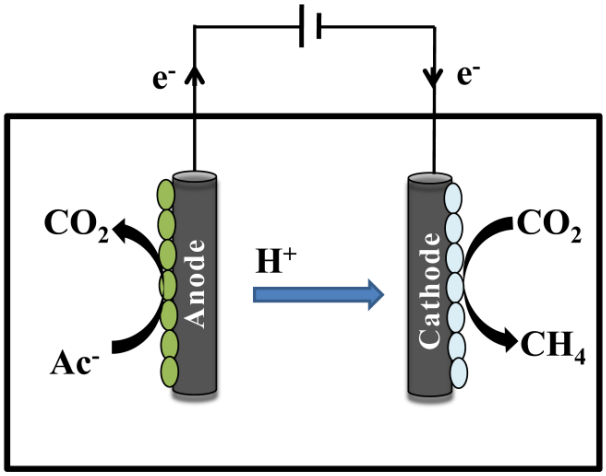

(b)

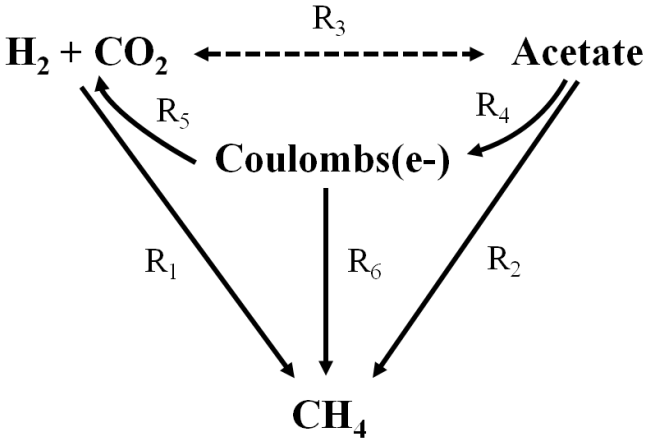

Figure 1. (a) Process scheme of the single chamber BES-AD system. (b) Overview of main reactions involved in BES-AD system. R_1: hydrogenotrophic methanogenesis ($H_2 \rightarrow CH_4$); R_2: Acetoclastic methanogenesis (acetate $\rightarrow CH_4$); R_3: Acetogenesis and homoacetogenesis, which were specially focused on syntrophic oxidation of acetate to CO_2 and H_2, and acetate production from CO_2 and H_2. R_4: Oxidation of organic matter by

Anode-Respiring Bacteria at anode electrode (herein acetate→electrons); R_5: H^+ reduction to H_2 at cathode electrode; R_6: Direct electron up-take by methanogens (electrons→CH_4).

The objective of this study was to investigate whether a methane-producing BES could enhance CH_4 production rate in low-temperature (10 ℃) anaerobic digestion. Energy input in terms of electricity in this combined BES-AD system was also investigated. Acetate was used as a model substrate. The results were compared to reactors without external voltage and in the presence of electrodes at 10 ℃, and to anaerobic digestions alone (control reactors without electrodes) at different operational temperatures (10 ℃, 15 ℃ and 30 ℃).

MATERIALS AND METHODS

BES-AD system. The experiment was carried out in reactors constructed by assembling rectangular Perspex frames. These frames had internal cylindrical volume of 28 mL(dimensions: 3.0 cm diameter×4.0 cm length) , and the reactor had a 8.0 mL gas collection tube (Figure 2.). The solution (20 mL) in each reactor was continuously stirred with a magnet. For the BES-AD reactor, an anode and cathode electrode compartment were made on both sides of the chamber in one reactor. The electrodes were made of granular activated carbon(1.5 g, 875 m^2/g, Norit PK 1-3) and were packed in a cylindrical cage (3.0 cm diameter×6.0 mm length), and were separated from the chamber with a spacer (SEFAR, PROPYLTEX). A graphite rod was inserted in both anode and cathode compartments as a current collector. Potentials were measured and were reported in this paper versus Ag/AgCl reference electrode (Ag/AgCl 3M KCl, ProSenseQiS, QM 710X, Netherlands) placed in the chamber. For the AD reactor, the spacer and electrodes were replaced with the same volume of a rubber sheet leading to the same internal volume as BES-AD system.

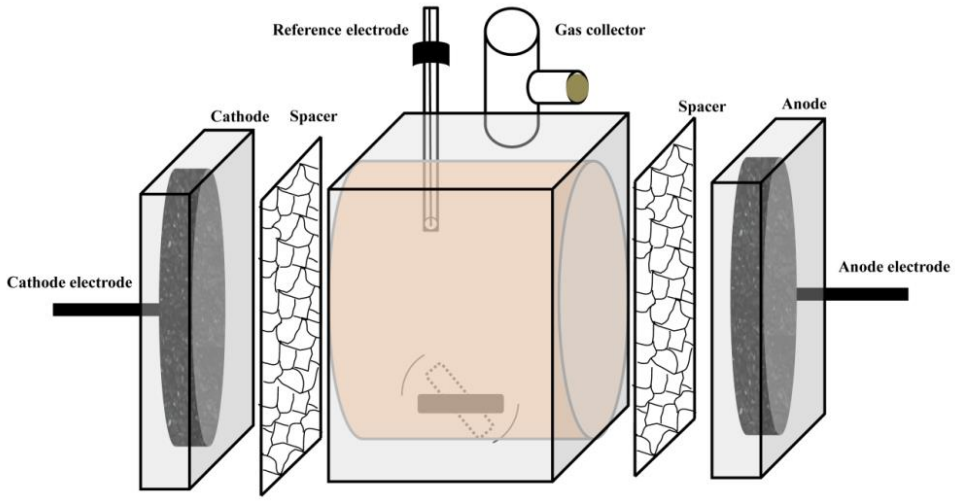

Figure 2. Experimental setup of the BES-AD reactor

Inoculum and medium. Each reactor was filled with 15mL of anaerobic sludge as inoculum. The anaerobic sludge was taken from a digester (35 ℃) in the UASB-digester

system treating domestic sewage (Zhang et al. 2013a). The volatile suspended solids concentration of the inoculum was 5.9±0.20 g VSS/L. Each reactor was filled with 5mL of concentrated medium (12.8 g/L CH3COONa, 0.80 g/L NH4Cl, 0.54 g/L KCL, 18.32 g/L Na2HPO4, 11.08 g/L NaH2PO4·2H2O, 0.80 mL of Wolfe's micronutrients (Clauwaert and Verstraete 2009), including vitamin and mineral solution). After mixing well with the inoculum, the concentration the solution in each reactor was 3.2 g/L CH3COONa, 0.05 g/L NH4Cl, 0.032 g/L KCL, 50mM phosphate buffer (4.58 g/L Na2HPO4, 2.77 g/L NaH2PO4·2H2O), 0.20 mL of Wolfe's micronutrients. All of the chemicals used in this study were from Merck, Germany. The medium was flushed with N2 (99.99%) for 30 minutes prior to each experiment to provide anaerobic conditions.

Operational conditions and start-up. Five anaerobic reactors were operated in the conditions as shown in Table 1. One reactor (BES-AD-10) was operated at 10 ℃ with BES in which the cathode potential was controlled at -0.90 V. One reactor (BES-ADC-10) was operated as a control at 10 ℃, with electrodes but without an electrical connection via the potentiostat (open circuit condition). Three other control reactors (ADC-10, ADC-15, ADC-30) were operated at 10, 15 and 30 ℃ to determine CH4 production rates for AD without electrodes. Low temperature digesters were operated in a fridge at 10 and 15 ℃, and the digester at 30 ℃ was located in a temperature controlled cabinet.

Table 1. Overview of experimental conditions at which the reactors were operated.

Reactor	BES-AD-10	BES-ADC-10	ADC-10	ADC-15	ADC-30
Temperature (℃)	10	10	10	15	30
Electrode materials	+[a]	+	-[b]	-	-
Cathode potential(V)	-0.9	0	0	0	0

a. Reactor was equipped with activated carbon granules.

b. Reactor was without any activated carbon granules.

To start-up the bioanode for the BES-AD-10 reactor, the anode was set at 0 V vs. Ag/AgCl using a potentiostat (Ivium with IviumSoft v2.462, Eindhoven, The Netherlands) to cultivate electroactive bacteria oxidizing acetate. After running for 4 weeks, the anode potential reached around -0.35 V at open circuit conditions, and the cultivation of the bacteria oxidizing acetate was considered to be completed (Wang et al. 2009). In the BES-AD-10 reactor, afterwards, the cathode potential was controlled at -0.90 V with the potentiostat.

No anaerobic sludge was added in the following batches. At the end of each batch, part of the reactor solution (5 mL) was replaced by the same amount of concentrated medium (see section 2.1.2 for the concentrated medium composition). Each batch lasted for 2 weeks. Three sequential batches in total lasted around 41 days.

Gas production. CH_4 and H_2 were analysed by Gas chromatograph with the same conditions as described in the literature (Van Eerten-Jansen et al. 2012). CH_4 yield and production rate were calculated with the following equation:

Cumulative CH_4 yield (mg CH_4-COD/gVSS):

$$Y_{CH_4} = C_{CH_4} \cdot \frac{PV}{RT} \cdot \frac{4 \times M_{CH_4}}{C_{vss} \times V_{sludge} * 1000} \quad (1)$$

Where C_{CH4} is concentration of CH_4 in the headspace (%) which was measured by gas chromatography, same as (Van Eerten-Jansen et al. 2012); *P* is the gas pressure of the reactor (Pa) and it was measured periodically by gas pressure meter (GMH 3151, Germany); *V* is the volume of headspace (16 mL) of each reactor; *R* is gas constant value (8.314 m^3 Pa/mol K); *T* is the temperature in Kelvin; 4: per g of CH_4 equals to 4 g COD; M_{CH_4} is the molecular weight of CH_4 (16 g/mol); C_{vss} is the concentration of volatile suspended solids (5.9±0.20 g/L); V_{sludge} is the volume of sludge in each reactor (15 mL). 1 mg CH_4-COD is equal to 0.35 mL CH_4 at standard conditions with a temperature of 273.15 K and an absolute pressure of 1 bar.

CH_4 production rate (mg CH_4-COD/(gVSS·d)) was calculated by dividing the CH_4 yields with the time period between the two sampling points.

Substrate consumption. Acetate concentration was measured by Gas chromatograph (HP5890 series Ⅱ GC, Germany) same as in the literature (Van Eerten-Jansen et al. 2013c). Acetate removal efficiencies were calculated using equation:

$$R = \frac{C_t - C_{t-1}}{C_{t-1}} \times 100 \quad (2)$$

Where C_t and C_{t-1} are the acetate concentration (mg/L) on sample time *t* and previous sample time *t-1*.

The CH_4 production efficiency was determined by the produced CH_4 over removed acetate.

Coulombic and cathodic CH_4 recovery efficiency. Current of the reactors was recorded each minute by the potentiostat. The average current per hour was used to calculate volumetric current density (I/V, where V is the working volume of the BES-AD-10 reactor, 20 mL).

Performance of the BES-AD reactor was evaluated by two kinds of efficiencies: namely coulombic efficiency and cathodic CH_4 recovery efficiency. Coulombic efficiency(η_{CE}) represents the ratio of electrons measured as electric current over the electrons available from the removed substrate (Feng et al. 2015), as shown in the following equation:

$$\eta_{CE} = \frac{\int_0^t I\,dt}{(C_1 - C_0) * \frac{V/1000}{M_{Ac}} * F * n} \times 100\% \quad (3)$$

Cathodic CH_4 recovery efficiency is the efficiency of capturing electrons from the electric current in CH_4, via following equation:

$$\eta_{CH_4} = \frac{n_{CH_4} * F * n}{\int_0^t I dt} \times 100\% \quad (4)$$

Where M_{Ac} is the molar weight of acetate (60 g/mole),n_{CH4} is CH_4 production (mole), *F* is the Faraday constant (96485 C/mole e^-), *n* is the moles of electrons per mole of CH_4 (8moles e^-/ mole CH_4), *I* is current (A), and *t* is time (s).

Polarization curves. Bioelectrochemical activity of the cathode in the BES-AD-10 reactor was investigated by polarization curves. These measurements were performed at the end of each batch and were also done for a control cathode, in (the same BES-AD-10 reactor with

fresh medium but without inoculum). The cathode potential was decreased from -0.80 V to-1.1 V with steps of 0.050 V, each cathode potential lasting for 15min. Current was recorded each minute and the last point at each potential was plotted in the polarization curve (Deeke et al. 2012).

RESUTLTS AND DISCUSSION

CH_4 production under different operational modes. The effect of combining BES and AD at low temperature was first investigated in three different reactors (BES-AD-10, BES-ADC-10, ADC-10) at the same operational temperature 10 ℃ As shown in Figure 3(a), CH_4 yields increased with time in all the reactors during all three batches. CH_4 yield was higher in the BES-AD-10 reactor compared to the other reactors, and varied between 20 and 30 mg CH_4-COD/gVSS during one batch period of 14 days. The maximum cumulative CH_4 yield was 31 mg CH_4-COD/g VSS in BES-AD-10 reactor during the second batch, which was 5.3-6.6 times higher than in the BES-ADC-10 reactor and 5.0-15 times higher than in the ADC-10 reactor. These results showed that BES enhanced CH_4 formation at 10 ℃. This is in line with other studies, that showed that at mesophilic conditions (30 ℃), BES enhanced the CH_4 yield (Feng et al. 2015, Tartakovsky et al. 2011).

The lower CH_4 yield of the BES-ADC-10, which contained electrodes but was operated at open circuit, compared with the BES-AD-10 reactor, in which electrical energy was supplied, showed that the enhanced CH_4 yield was the result of applied electrical energy, rather than of biomass retention on the electrodes, as has been found previously at 30 ℃ (De Vrieze et al., 2014). CH_4 yield of the BES-ADC-10 reactor was higher than that of ADC-10 (anaerobic digestion alone) in the first batch, and was lower in the second and third batch. The decrease of CH_4 yield in BES-ADC-10 reactor during three batches might be the result of differences in pH: the pH in the BES-ADC-10 had increased to 8.3 at the end of Batch 1, while the pH in the other two reactors was quite stable (<7.8) during three batches (see Figure. S2). This higher pH could have decreased the activity of methanogens (Chen et al. 2008). The pH in BES-AD-10 was 7.5±0.3, higher than ADC-10 (7.1±0.20), possibly the result of consumption of protons at the cathode, a phenomenon also found by previous studies working at mesosphilic conditions (Bo et al. 2014).

To compare the potential of CH_4 yield in the BES-AD system at low temperature to CH_4 yields at higher temperatures, we operated two additional AD reactors without electrodes and without electrical energy input, ADC-15 at 15 ℃and ADC-30 at 30 ℃. As shown in Figure 3(b), the cumulative CH_4 yields increased with the increasing temperature during the three batches. BES-AD-10 reactor had higher CH_4 yield than both control reactors at 10 ℃ and 15 ℃, and reached a CH_4 yield close to the ADC reactor at 30 ℃. Table 2. gives an overview of the CH_4 production rates of all the reactors at different temperatures during three consecutive batches. In each reactor, the maximum CH_4 production rate obtained from the first-time period (0-5 days) was 2-3 times higher than the average CH_4 production rate in the whole batch period.

Table 2. Comparison of average[a] and maximum[b] methane production rate for the reactors during each batch

No.	Batch 1		Batch 2		Batch 3	
(mgCOD/gVSS/d)	Average	Max	Average	Max	Average	Max
BES-AD-10	1.55	2.22	2.37	3.19	2.13	3.32
BES-ADC-10	0.41	0.68	0.16	0.54	0.25	0.48
ADC-10	0.36	0.45	0.40	0.49	0.44	0.51
ADC-15	1.13	2.29	1.35	2.35	1.50	2.41
ADC-30	2.29	5.55	2.62	5.91	2.98	7.62

[a] The average CH_4 production rate was calculated from the whole batch period (2 weeks).

[b] The maximum CH_4 production was calculated from the first period (0-5 days).

(a)

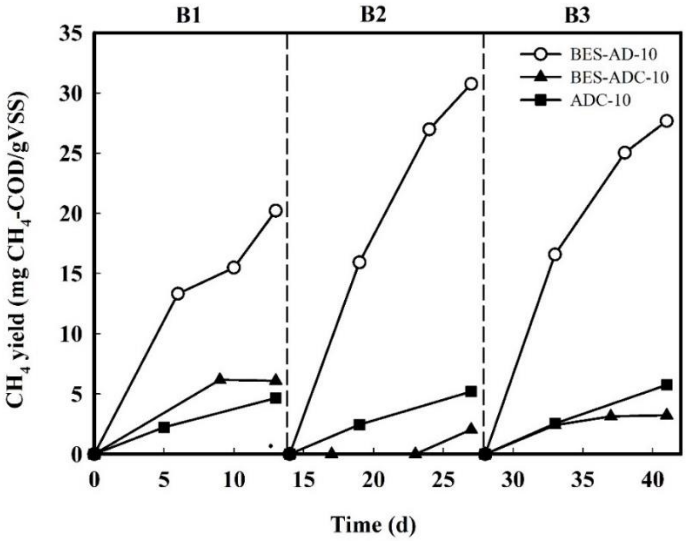

(b)

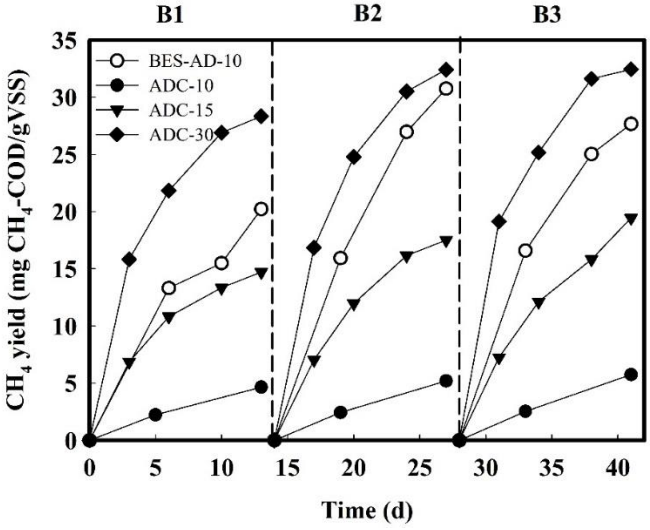

Figure 3. CH_4 yield of the different reactors and conditions during three consecutive batches (a) CH_4 yield of three reactors at 10℃. (b) CH_4 yield of four reactors at different temperature, 10℃, 15℃ and 30℃. The dashed line indicates medium replacement.

Acetate removal in AD with and without BES. Acetate removal efficiency for all reactors operated at 10 ℃ was analyzed to evaluate the overall process (Figure 4). For all the reactors, acetate was removed throughout each full batch, showing that acetate was not limiting CH_4 production. Acetate removal efficiency in BES-AD-10 was 45%, while acetate removal efficiency in ADC-10 was 8%. The difference in acetate removal efficiency between BES-AD-10 and ADC-10 could be the result of anodic oxidation by electroactive microorganisms (Zhao et al. 2014). However, BES-ADC-10 also had high acetate removal efficiency of 40%, which was comparable to that of BES-AD-10, even though there was no electric circuit and CH_4 production was much lower. Apparently, the presence of electrodes in the form of granular activated carbon, influences acetate removal. It is well known that granular activated carbon possesses excellent adsorption capability for organic matter (Gur-Reznik et al. 2008, Orshansky and Narkis 1997), although adsorption of acetate to granular activated carbon bioanodes has not been reported or discussed so far. Adsorption tests in batch bottles with acetate and granular activated carbon indeed showed that up to 25% of the acetate was adsorbed after around 2 days (data not shown). The acetate removal efficiency of BES-ADC-10 decreased from 40% to 28% during three batches, while CH_4 production rates increased, which is another indication of saturation of granular activated carbon with acetate. Not only acetate removal, but also CH_4 production efficiency was influenced by adsorption, because adsorption of part of the removed acetate would result in lower CH_4 production efficiency. Indeed, CH_4 production efficiency in the reactors with granular activated carbon as electrode material (both BES-ADC-10 and BES-AD-10), were 8 times lower than that without electrode materials (ADC), see Table S1.

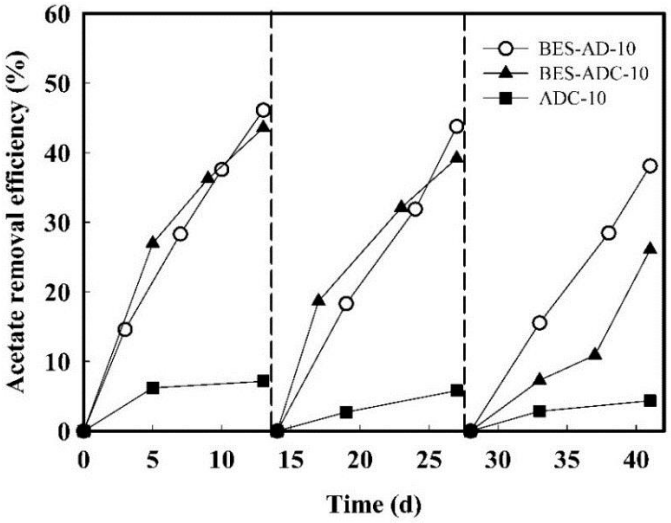

Figure 4. Acetate removal efficiency of reactors at 10℃ during three consecutive batches. The dashed line indicates medium replacement.

Bioelectrochemical analysis of anode and cathode. At low temperature, acetoclastic methanogenesis is more rate limiting than hydrogenotrophic methanogenesis (Enright et al. 2009). A potential mechanism for CH_4 generation in the BES-AD-10 reactor is that introducing a bioanode opens a new route for CH_4 formation, in which acetate is converted into electrons (Figure 1. R_4), and the applied voltage is used to generate either H_2 (R_5) or CH_4 (R_6) at the cathode. To further analyze the role of the (bio)electrodes in the BES-AD-10 reactor, volumetric current density, coulombic efficiency and cathodic CH_4 recovery efficiency were analysed (Figure 5.). Coulombic efficiency can be used to distinguish the contribution of anodic oxidation and acetoclastic methanogenesis in acetate removal (Zhao et al. 2014). Under a constant cathode potential -0.9 V, an average volumetric current density of -10 A/m^3 was observed (reported negative because it was measured as a cathodic current) (Figure 5.). The current density was quite stable during three batches. Anode potential was regularly measured and was always <-350 mV, indicating that the bioanode was active throughout the experiment. Coulombic efficiency increased from 44% to 60%, while the acetate removal efficiency in BES-AD-10 ranged between 37% and 43% (Figure 6). This increase in coulombic efficiency at stable acetate removal efficiencies showed that the contribution of the bioanode to acetate oxidation increased with time, which was likely

caused by the growth of electroactive microorganisms in the anode. Because CH_4 production rate in BES-AD-10 was several times higher than those of BES-ADC-10 and AD-10 throughout the experiment, we can conclude that BES became an alternative route to degrade acetate and produce CH_4. Cathodic CH_4 recovery efficiency shows which part of the electrical current is converted into CH_4 (either direct of via hydrogen) at the cathode. The highest cathodic CH_4 recovery efficiency was achieved around 20% in the first batch, and gradually increased to 25% in the third batch, which was relatively low compared to those in previous methane-producing BES study at higher temperature of 30 ℃ (Siegert et al. 2015). The causes for the low cathodic CH_4 recovery have not been further examined in our study, but could be the result of H_2 diffusion to the anode side and re-oxidation by the anode electroactive bacteria (Lee and Rittmann 2009). In our study, hydrogen concentration was analyzed regularly and was below the detection limit during all batches. Even though not detected, hydrogen could be an intermediate product and used in-situ by hydrogenotrophic methanogens (van Eerten-Jansen et al. 2015, Lohner et al. 2014). Other possible causes for the low CH_4 recovery may be biomass growth, or oxygen leakage during medium replacement. The combination of anodic and cathodic efficiency shows which part of the acetate is converted into CH_4 in the BES. This overall efficiency was around 9.5 %, indicating there is still much room for improvement in conversion efficiency.

Polarization curves of the biocathode in BES-AD-10 were measured at the end of each batch (Figure 6), and also for a control cathode (without inoculum). The biocathode in BES-AD-10 in all of the three batches had similar current densities, which were higher than that of the control cathode. At a cathode potential of -0.90 V, the biocathode in BES-AD-10 had a current density of -23 A/m^3, whereas the control cathode had a current density around -0.50 A/m^3. This indicated the formation of a cathodic biofilm, however, it cannot be concluded if this biofilm was catalytic for the production of H_2 and/or CH_4.

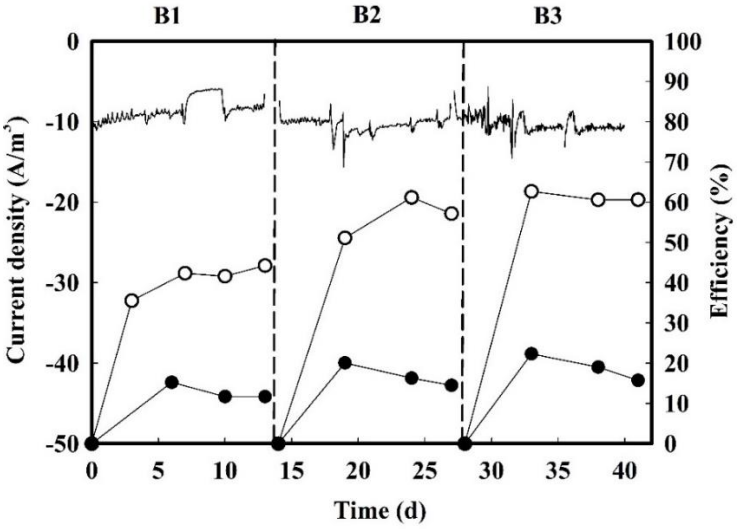

Figure 5. Trend of current density (line), coulombic efficiency (empty circle) and cathodic CH_4 recovery efficiency (filled circle) during the three consecutive batches in BES-AD-10 reactor. The dashed line indicates medium replacement.

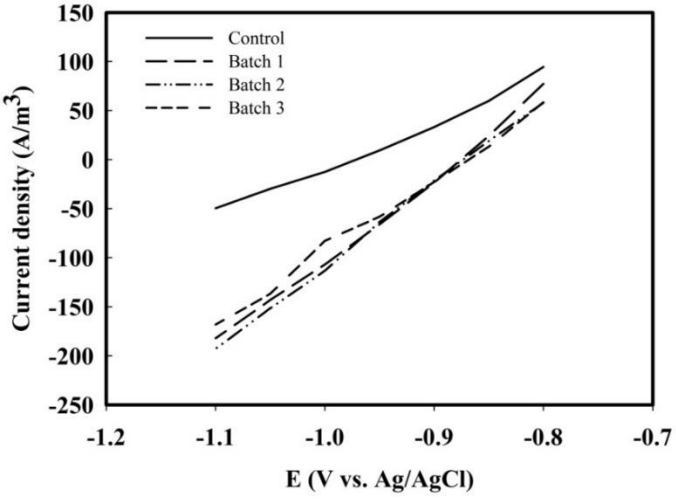

Figure 6. Polarization curve for BES-AD-10 reactor at the end of each batch. The control cathode was measured for the same BES-AD reactor with fresh medium and without sludge.

Evaluation of the enhancement of BES on AD at low temperature. The maximum specific methanogenic activity (SMA) of the BES-AD-10 reactor was 3.3 mg CH_4-COD/(gVSS·d). SMA of anaerobic sludge treating domestic sewage was about 300 mg CH_4-COD/ (gVSS·d) at 30 ℃ and 30-40 mg CH_4-COD/ (gVSS·d) at 15 ℃ (Zhang et al. 2013a). Maximum CH_4 production rate of the ADC-10 reactor in this study was lower than related results above, and was probably due to the differences in reactor design, substrate, and lower temperature of 10 ℃. Strategies to achieve higher SMA could be to use a longer cultivation time for the sludge in the reactor (De Vrieze et al. 2014), or to inoculate with sludge from low-temperature anaerobic digester(Zeeman et al. 1988), aspects that need further research.

CH_4 production rates of the previous studies on BES-AD systems under mesophilic conditions and the present study are summarized in Table 3. CH_4 production rate was different in different BES-AD systems, as it was affected by many factors, such as inoculum, reactor configuration, applied voltage and medium. However, the increased CH_4 production rate in our study outperformed most BES-AD systems operated at mesophilic conditions, except studies that operated with higher external voltage than this study (Zamalloa et al. 2013, Guo et al. 2013). The energy input of the BES-AD system was calculated in terms of electrical energy invested per volume (m^3) of produced CH_4 during one batch. In this experiment, the energy input for BES-AD-10 reactor was 39 kWh/m^3 CH_4 ($\frac{U \times I \times V \times T}{\mathrm{P}}$, U is the cell voltage 0.55 V; I is the volumetric current density 10 A/m^3; V is the reactor volume 20 mL ; T is the total three batches time 41 days; P is the total CH_4 yield during three batches 78.6 mg CH_4-COD/ (gVSS)). If this same amount of electrical energy would be used to heat up the reactor, which would also lead to higher conversion rates, the temperature of the reactor would only increase by 1.6 ℃ ($\Delta T = \frac{\mathrm{Q}}{m \cdot C}$, Q is the electrical energy during one batch; m is the mass of the medium 20 g; C is the heat capacity 4.179 J/℃/g). The energy input that would be required for heating up the digester from 10 ℃ to 30 ℃ in our experiment, would be, with the same calculation, 407.4 kWh/m^3 CH_4, which was almost 10 times higher than electrical energy invested in the BES-AD-10 reactor. If the cathodic CH_4 recovery efficiency could be increased from 25% to 80% this would lead to a further decrease in electricity input to 12 kWh/m^3 CH_4. Therefore, in addition to other processes aiming at enhancing CH_4 production during low-temperature

anaerobic digestion, e.g. co-digestion (Zhang et al. 2013a) and combing a solar energy heating-up system (Ren et al. 2012), BESs may serve as a cost-efficient alternative to enhance CH_4 production at low temperature.

Table 3. Comparison between BES-AD and AD in terms of CH_4 production rate

Temperature	Applied voltage (V)	Production Rate in AD alone (mgCOD/gVSS/d)	Improvement of BES-AD compared to control without electrodes	Reference
35℃	0.3~0.6	18	1.22 [a] times	*(Feng et al. 2015)*
25±2℃	0.7~0.8	557	1.25[b] times	*(Zhao et al. 2014)*
34℃	0.5~1	32	1.5[a] times	*(De Vrieze et al. 2014)*
37±1℃	1.4~1.8	0.47	11.4~13.6[a] times	*(Guo et al. 2013)*
30±2℃	2±0.1	0.17	5[a] times	*(Zamalloa et al. 2013)*
35℃	2.8~3.5	143	1.1~1.25[a] times	*(Tartakovsky et al. 2011)*
10℃	0.55	0.44	5~6 [a] times	*This study*

a. CH_4 yields

b. CH_4 production rate

CONCLUSIONS

At 10 ℃, CH_4 yield in the integrated BES-AD system was 5.3~6.6 times higher than those of the control (no external voltage and no electrodes). The comparison between reactors operated at different temperatures suggested that CH_4 production from a low-temperature anaerobic digestion assisted by BES might result in a similar performance as mesophilic anaerobic digestion. Energy input by the form of electricity in BES-AD system was lower than the energy for heating up the digester to mesophilic temperature. This study demonstrated that BES has potential to be an alternative strategy to enhance CH_4 production in low-temperature anaerobic digestion.

ASSOCIATED CONTENT

The Supporting Information is available at the end of this chapter.

ACKNOWLEDGEMENTS

This study was financially supported by Alliander (Netherlands) and DMT Environmental Technology together with the Chinese Scholarship Council.

REFERENCE

Álvarez, J.A., Armstrong, E., Presas, J., Gómez, M. and Soto (2004) Performance of a UASB-Digester System Treating Domestic Wastewater. Environmental Technology 25(10), 1189-1199.

Bo, T., Zhu, X., Zhang, L., Tao, Y., He, X., Li, D. and Yan, Z. (2014) A new upgraded biogas production process: Coupling microbial electrolysis cell and anaerobic digestion in single-chamber, barrel-shape stainless steel reactor. Electrochemistry Communications 45, 67-70.

Chen, Y., Cheng, J.J. and Creamer, K.S. (2008) Inhibition of anaerobic digestion process: A review. Bioresource Technology 99(10), 4044-4064.

Cheng, S.A., Xing, D.F., Call, D.F. and Logan, B.E. (2009) Direct Biological Conversion of Electrical Current into Methane by Electromethanogenesis. Environmental Science & Technology 43(10), 3953-3958.

Clauwaert, P. and Verstraete, W. (2009) Methanogenesis in membraneless microbial electrolysis cells. Applied Microbiology and Biotechnology 82(5), 829-836.

De Vrieze, J., Gildemyn, S., Arends, J.B.A., Vanwonterghem, I., Verbeken, K., Boon, N., Verstraete, W., Tyson, G.W., Hennebel, T. and Rabaey, K. (2014a) Biomass retention on electrodes rather than electrical current enhances stability in anaerobic digestion. Water Research 54(0), 211-221.

De Vrieze, J., Gildemyn, S., Arends, J.B.A., Vanwonterghem, I., Verbeken, K., Boon, N., Verstraete, W., Tyson, G.W., Hennebel, T. and Rabaey, K. (2014b) Biomass retention on electrodes rather than electrical current enhances stability in anaerobic digestion. Water Research 54, 211-221.

Deeke, A., Sleutels, T.H.J.A., Hamelers, H.V.M. and Buisman, C.J.N. (2012) Capacitive Bioanodes Enable Renewable Energy Storage in Microbial Fuel Cells. Environmental Science & Technology 46(6), 3554-3560.

Enright, A.-M., McGrath, V., Gill, D., Collins, G. and O'Flaherty, V. (2009) Effect of seed sludge and operation conditions on performance and archaeal community structure of low-

temperature anaerobic solvent-degrading bioreactors. Systematic and Applied Microbiology 32(1), 65-79.

Feng, Y., Zhang, Y., Chen, S. and Quan, X. (2015) Enhanced production of methane from waste activated sludge by the combination of high-solid anaerobic digestion and microbial electrolysis cell with iron-graphite electrode. Chemical Engineering Journal 259, 787-794.

Guo, X., Liu, J. and Xiao, B. (2013) Bioelectrochemical enhancement of hydrogen and methane production from the anaerobic digestion of sewage sludge in single-chamber membrane-free microbial electrolysis cells. International Journal Of Hydrogen Energy 38(3), 1342-1347.

Gur-Reznik, S., Katz, I. and Dosoretz, C.G. (2008) Removal of dissolved organic matter by granular-activated carbon adsorption as a pretreatment to reverse osmosis of membrane bioreactor effluents. Water Research 42(6–7), 1595-1605.

Hussain, A. and Dubey, S.K. (2015) Specific methanogenic activity test for anaerobic degradation of influents. Applied Water Science, 1-8.

Lee, H.-S. and Rittmann, B.E. (2009) Significance of biological hydrogen oxidation in a continuous single-chamber microbial electrolysis cell. Environmental Science & Technology 44(3), 948-954.

Lettinga, G., Rebac, S. and Zeeman, G. (2001) Challenge of psychrophilic anaerobic wastewater treatment. Trends In Biotechnology 19(9), 363-370.

Liu, W., Cai, W., Guo, Z., Wang, L., Yang, C., Varrone, C. and Wang, A. (2016) Microbial electrolysis contribution to anaerobic digestion of waste activated sludge, leading to accelerated methane production. Renewable Energy 91, 334-339.

Lohner, S.T., Deutzmann, J.S., Logan, B.E., Leigh, J. and Spormann, A.M. (2014) Hydrogenase-independent uptake and metabolism of electrons by the archaeon Methanococcus maripaludis.

Lu, L., Ren, N., Zhao, X., Wang, H., Wu, D. and Xing, D. (2011) Hydrogen production, methanogen inhibition and microbial community structures in psychrophilic single-chamber microbial electrolysis cells. Energy & Environmental Science 4(4), 1329-1336.

Mahmoud, N., Zeeman, G., Gijzen, H. and Lettinga, G. (2004) Anaerobic sewage treatment in a one-stage UASB reactor and a combined UASB-Digester system. Water Research 38(9), 2348-2358.

Orshansky, F. and Narkis, N. (1997) Characteristics of organics removal by PACT simultaneous adsorption and biodegradation. Water Research 31(3), 391-398.

Ren, Z., Chen, Z., Hou, L.-a., Wang, W., Xiong, K., Xiao, X. and Zhang, W. (2012) Design investigation of a solar energy heating system for anaerobic sewage treatment. Energy Procedia 14, 255-259.

Siegert, M., Li, X.-f., Yates, M.D. and Logan, B.E. (2015) The presence of hydrogenotrophic methanogens in the inoculum improves methane gas production in microbial electrolysis cells. Frontiers in Microbiology 5.

Speece, R.E. (2008) Anaerobic Biotechnology and Odor/corrosion Control for Municipalities and Industries, Fields Publishing, Incorporated.

Tartakovsky, B., Mehta, P., Bourque, J.S. and Guiot, S.R. (2011) Electrolysis-enhanced anaerobic digestion of wastewater. Bioresource Technology 102(10), 5685-5691.

Van Eerten-Jansen, M.C.A.A., Heijne, A.T., Buisman, C.J.N. and Hamelers, H.V.M. (2012) Microbial electrolysis cells for production of methane from CO_2: long-term performance and perspectives. International Journal Of Energy Research 36(6), 809-819.

van Eerten-Jansen, M.C.A.A., Jansen, N.C., Plugge, C.M., de Wilde, V., Buisman, C.J.N. and ter Heijne, A. (2015) Analysis of the mechanisms of bioelectrochemical methane production by mixed cultures. Journal of Chemical Technology & Biotechnology 90(5), 963-970.

Van Eerten-Jansen, M.C.A.A., Ter Heijne, A., Grootscholten, T.I.M., Steinbusch, K.J.J., Sleutels, T.H.J.A., Hamelers, H.V.M. and Buisman, C.J.N. (2013) Bioelectrochemical

Production of Caproate and Caprylate from Acetate by Mixed Cultures. ACS Sustainable Chemistry & Engineering 1(5), 513-518.

Villano, M., Aulenta, F., Ciucci, C., Ferri, T., Giuliano, A. and Majone, M. (2010) Bioelectrochemical reduction of CO2 to CH4 via direct and indirect extracellular electron transfer by a hydrogenophilic methanogenic culture. Bioresource Technology 101(9), 3085-3090.

Wang, X., Feng, Y., Ren, N., Wang, H., Lee, H., Li, N. and Zhao, Q. (2009) Accelerated start-up of two-chambered microbial fuel cells: Effect of anodic positive poised potential. Electrochimica Acta 54(3), 1109-1114.

Witarsa, F. and Lansing, S. (2015) Quantifying methane production from psychrophilic anaerobic digestion of separated and unseparated dairy manure. Ecological Engineering 78, 95-100.

Yang, Y., Guo, J. and Hu, Z. (2013) Impact of nano zero valent iron (NZVI) on methanogenic activity and population dynamics in anaerobic digestion. Water Research 47(17), 6790-6800.

Zamalloa, C., Arends, J.B.A., Boon, N. and Verstraete, W. (2013) Performance of a lab-scale bio-electrochemical assisted septic tank for the anaerobic treatment of black water. New Biotechnology 30(5), 573-580.

Zeeman, G., Sutter, K., Vens, T., Koster, M. and Wellinger, A. (1988) Psychrophilic digestion of dairy cattle and pig manure: Start-up procedures of batch, fed-batch and CSTR-type digesters. Biological Wastes 26(1), 15-31.

Zhang, L., Hendrickx, T.L.G., Kampman, C., Temmink, H. and Zeeman, G. (2013a) Co-digestion to support low temperature anaerobic pretreatment of municipal sewage in a UASB-digester. Bioresource Technology 148, 560-566.

Zhang, L., Hendrickx, T.L.G., Kampman, C., Temmink, H. and Zeeman, G. (2013b) Co-digestion to support low temperature anaerobic pretreatment of municipal sewage in a UASB–digester. Bioresource Technology 148(0), 560-566.

Zhao, Z., Zhang, Y., Chen, S., Quan, X. and Yu, Q. (2014) Bioelectrochemical enhancement of anaerobic methanogenesis for high organic load rate wastewater treatment in a up-flow anaerobic sludge blanket (UASB) reactor. Sci. Rep. 4.

SUPPORTING INFORMATION

Bioelectrochemical enhancement of methane production in low temperature anaerobic digestion at 10 °C

2 Figures, 1 Tables

Figure S1. BES-AD reactor.

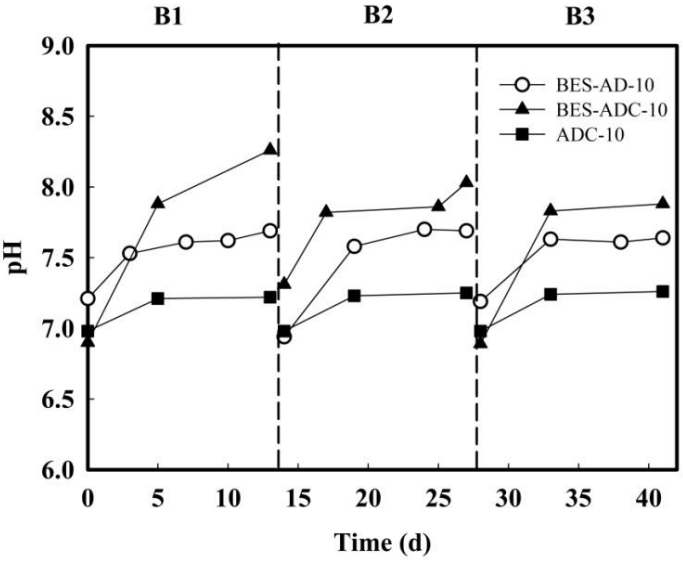

Figure S2. pH of three reactors at 10℃.

Table. S1 CH_4 production efficiency in different reactors for three batches operated at10℃

No. (%)	Batch 1	Batch 2	Batch 3
BES-AD-10	5.17	8.24	9.53
BES-ADC-10	3.58	1.99	4.01
ADC-10	70.74	73.58	85.33

Chapter 6. General Discussion

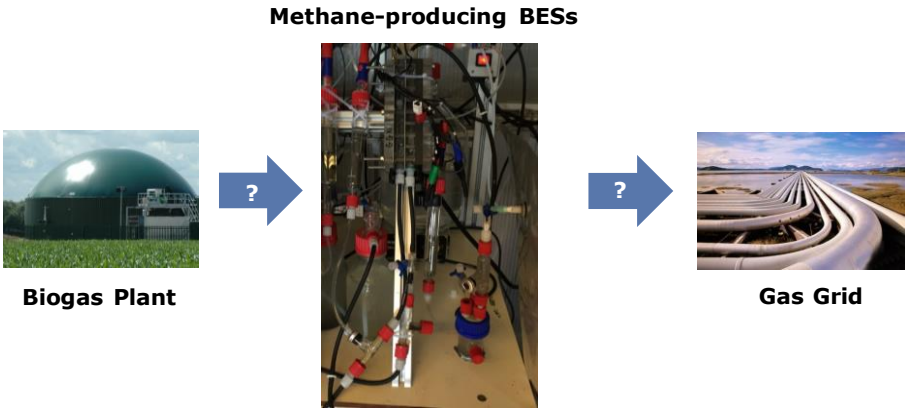

Concluding Remarks and Outlook

This chapter will provide a state-of-the-art survey about methane-producing BESs and address the main limitations and opportunities of the methane-producing BESs from an industrial scale-up perspective. This is done by summarizing the insights of this thesis, by assessing the critical components influencing the performance, by performing a techno-economic analysis of full-scale methane-producing BESs for biogas upgrading, and by evaluating competing power-to-gas technologies. This chapter will identify potential niche markets for methane-producing BESs to contribute to renewable electrical energy conversion and storage.

6.1 Summary of the research outcomes

This thesis describes the improvement of methane production in methane-producing bioelectrochemical systems. As the basis of the discussion, the most important outcomes and insights from each research chapter in this thesis are summarised as follows:

Chapter 2- Heat-treated stainless steel felt as a new cathode material in a methane-producing bioelectrochemical system

- Heat-treated stainless steel felt (HSSF) was used as a new cathode material.
- Heat-treated stainless steel felt (HSSF) produced more methane than stainless steel felt at cathode potentials of -1.1 and -1.3 V vs. Ag/AgCl.
- HSSF achieved a faster biocathode start-up than other materials tested, likely due to its good property for hydrogen evolution.
- Overall biocathode performance of HSSF was comparable to graphite felt.

Chapter 3- Granular activated carbon as cathode material for high-rate methane production at low overpotential

- Under galvanostatic control, methane-producing biocathodes achieved methane production rates of around 65 L $CH_4/m^2cat_{proj}/d$ at 35 A/m^2cat_{proj}, which is so far the highest methane production rate obtained with similar carbon-based electrodes in other studies.
- The granular activated carbon (GAC) biocathodes had a lower overpotential than the graphite granular (GG) biocathodes, with methane generation occurring at -0.52 V vs. Ag/AgCl for GAC and at -0.92 V for GG at a current density of 10 A/m^2cat_{proj}, and -0.58 V for GAC at 35 A/m^2cat_{proj}.
- *Methanobacterium* was the dominant methanogen in all biocathodes. The GAC biocathodes experienced a higher abundance of proteobacteria than the GG biocathodes, which is possibly related to the low overpotentials for methane production observed with GAC but not with GG.

Chapter 4- Effect of intermittent current supply on the performance of a methane-producing bioelectrochemical system (Chapter 4)

- The effect of intermittent electricity supply on the performance of methane-producing BESs was investigated.
- Current-to-methane efficiencies of all biocathodes during the tests of 6 min on/off cycle time, were stable and similar to those in the control tests (constant current supply), with around 50-60 % at 10 A/m^2 cat_{proj} and 80-90 % at 35 A/m^2 cat_{proj}.
- The effect of intermittent current supply became more evident, when operated at a higher current density (35 A/m^2 cat_{proj}) with 30 min on/off cycle time. Current-to-methane efficiency dropped to 70% under 20 min ON and 10 min OFF, 30% under 15 min ON and 15 min OFF, 50% under 10 min ON and 20 min OFF.
- The results show an unexpected and unexplained sensitivity of methane-producing BESs microorganisms for intermittent current.

Chapter 5- Bioelectrochemical enhancement of methane production in low temperature anaerobic digestion at 10 °C

- Integration of bioelectrochemical system (BES) with anaerobic digestion (AD) can be an attractive alternative strategy to enhance the performance of AD at low temperature e.g. in cold areas.
- The highest CH_4 yield of 31 mg CH_4-COD/g VSS was achieved in the combined BES-AD system at a cathode potential of -0.90 V (Ag/AgCl), which was 5.3 to 6.6 times higher than in the comparable AD reactor at 10 ℃.
- CH_4 production rate achieved in the combined BES-AD system at 10 ℃ was only slightly lower than in the AD reactor at 30 ℃.
- BES uses 10 times less energy to assist AD at 10℃than heating up AD to mesophilic condition

6.2 High-rate methane production

In this section, we compared the methane production rate achieved in this thesis (Chapter 3) with other studies working on methane-producing BESs (Figure 1). The methane production rate is normalized by cathode project area and by cathode electrode volume. Methane-producing BESs using carbon-based granular electrodes (i.e. activated carbon granular, graphite granular) as cathode electrode, show the highest methane production rate, which are 2-3000 times higher than those achieved in other studies. The granular electrode, as a typical three-dimensional (3D) porous electrode material, has a high specific surface area which may enhance biofilm attachment, and thus result in high methane production rate. Besides the advantages of 3D porous electrode materials, activated carbon granular (GAC) has another feature, namely that it seems beneficial to hydrogenotrophic methanogens, which is the most dominate microorganim within a methane-producing biocathode. A previous study (Liu et al. 2012) reported an improved methane production rate in anaerobic digestion by adding GAC into the digester, as the conductive GAC might faciliate direct interspecies electron transfer between bacteria (e.g. *Geobacter* species) and methanogens (e.g. *Methanosarcina*). In another study, although GAC was not used as cathode electrode, effective inoculation with methanogenic communities pre-enriched by GAC could improve methane production rates and decrease start-up times in methane-producing BESs (LaBarge et al. 2017).

The effect of the electrode bed thickness on the performance of methane-producing BESs is still unclear. On the one hand, an increase in the methane producion rate could occur when the thickness of granluar electrode bed increases, since the thicker granluar electrode provides higher surface area for biofilm growth, leading to higher the cathodic reaction rate (hydrogen and/or methane production). On the other hand, visible inspection of our granular electrode beds used in chapter 3 (both GAC and GG) showed that the biofilm growth mainly occurred at the anolyte side of the electrode bed. This phenomenon was also found by a previous study using graphite felt as bioanode in Microbial Electrolysis Cells for hydrogen production (Sleutels et al. 2009a). Possible reasons could be: substrate limitation inside the electrode bed due to non-ideal mixing, and local pH increase inside the electrode bed because of slow diffusion of protons from the membrane to the inside electrode bed. Further study into the thickness of the electrode bed and its effect on the methane production rate is required.

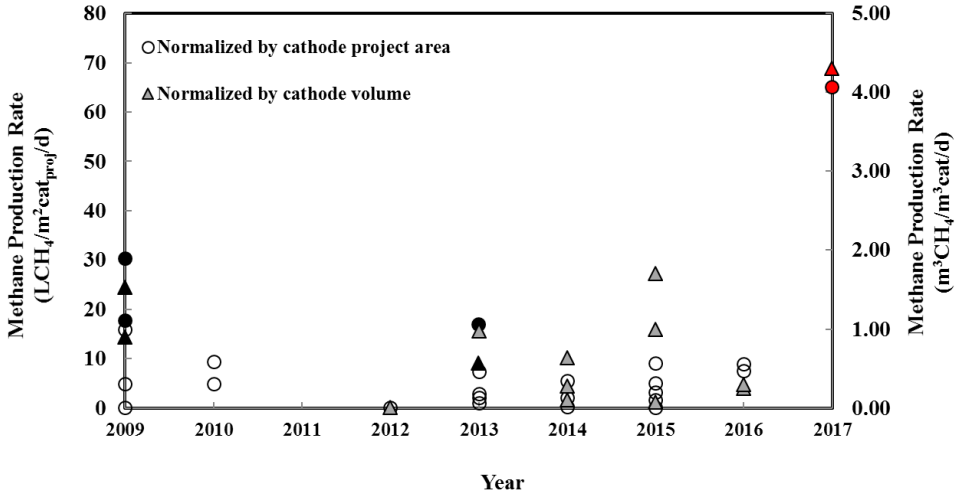

Figure 1. Development of methane production rate in methane-producing BESs (based on Geppert et al. 2016). Methane production rates are expressed in unites of L CH_4/m^2 cat_{proj}/d (circles) and m^3 CH_4/m^3 cat/d (triangles). The open circles and grey triangles represent the flat cathode electrodes, whereas the filled black circles and triangles indicate the 3D cathode electrodes. In addition, the circle filled with red color represent the resutlts obtained in this thesis in Chapter 3.

6.3 Anode rather than biocathode limits energy efficiency of methane-producing BESs

According to the experimental results in chapter 3, we analyzed the potential loss within the methane-producing BESs consisting of two types of cathode materials: activated carbon granules (GAC) and graphite granules (GG). The detailed calculations were shown in supporting information. Based on the potential loss analysis, we further quantified the contribution of each component of the total applied voltage (Figure 2). In fact, the distribution of potential losses is the same as the distribution of energy losses, because the current density is equal for both cathode materials. Our results reveal that the biocathode overpotential accounted for only 3% of the total applied voltage for GAC biocathodes, and for 12% for GG biocathodes. The largest potential loss occurred at the anode, accounting for about 40% of the total applied voltage in both cases, GAC and GG reactors. Transport losses were the second dominant potential loss, accounting for 20% of the applied voltage

for GAC reactors and 14% for GG reactors. The processes underlying transport losses are not yet understood and need further study, however, reducing the anode overpotentials would be the priority for improving the overall energy efficiency of methane producing BESs. The high energy loss at the anode may be the result of the low surface area of the flat plate anode electrode, that was in these experiments covered with a layer of glass beads in order to keep the cathode granule bed well-connected to the cathode current collector. An anode with a higher specific surface area could be an option to reduce the overpotential for water oxidation (Shi and Zhao 2014).

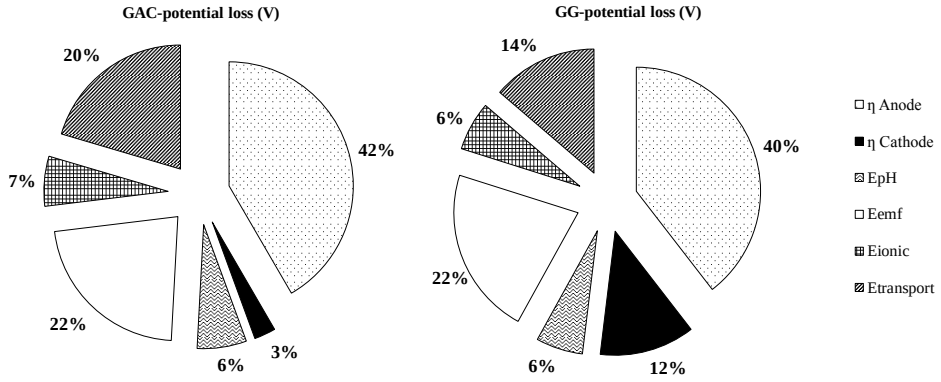

Figure 2. The distribution of potential loss in GAC and GG at current density of 35A/m^{2}cat$_{proj}$. The average applied voltage for GAC biocathodes and GG biocathodes are 4.77 V and 4.85 V, respectively. The share of each component is calculated by averaging 4 samples (2 samples for each reactor × 2 reactors for each biocathode material) during the stable performance phase.

6.4 Outlook: Scale-up Issues

Since the discovery of methane-producing biocathodes (Cheng et al. 2009), methane-producing BESs have attracted interest in various aspects, including the possible electron transfer mechanisms, key microbial species involved in the process and system optimization regarding cathode material, membrane, operational conditions, etc.(Geppert et al. 2016). However, the methane-producing BESs is still in its infancy, and many issues related to scalability and economic feasibility should be addressed.

Herein, we do a techno-economic analysis based on a case study for methane-producing BES application, which is to upgrade biogas from anaerobic digestion of food waste (Figure 3). Food waste from households is abundant in the urban area and requires sustainable treatment under the concept of urban circular economy. Anaerobic digestion, a mature technology applied worldwide, has proven to be a desirable treatment process for food wastes as it can treat organic waste streams by less capital investment, meanwhile recovering energy from these waste streams. The biogas from anaerobic digestion is a mixture of CH_4 and CO_2. Upgrading biogas using electricity and methane-producing BESs is an attractive and sustainable way for CO_2 emission reduction. The upgraded biogas (90~99% CH_4) is injected into the gas grid and this can be compared to renewable electricity storage. For a thorough evaluation, a techno-economic analysis was performed with the software SuperPro Designer® (SPD). This software is used widely in both industry and scientific field for simulation many integrated processes, such as wastewater treatment (Vergili et al. 2012), production of pharmaceuticals (Nandi et al. 2016) and biofuels (Sebastião et al. 2016).

All equipment required for this case study is shown in the SPD flowsheet (Supporting information Figure S2). The flowsheet consists three different sections: feedstock preparation, product synthesis and biogas upgrading. In the feedstock section, the fresh catholyte and anolyte are fed into the blending tank at a certain flow rate to have sufficient nutrients for biocathode growth, and water in the anodic chamber. In addition, the raw biogas is fed into the catholyte blending tank to serve as CO_2 supply. In product synthesis section, a generic box is used to mimic the methane-producing BES reactor, where electrochemical and biological reactions take place. The gas products (O_2 and CH_4) are isolated from each outflow stream in the gas-liquid separation tank. The final effluent is

partially recycled back to the corresponding blending tank to decrease the material costs, whereas the rest of the effluent was discharged to keep the mass balance. The cathodic gas produced is a mixture of CH_4 and unconsumed CO_2. A biogas upgrading section was necessary and essential to meet the requirement of gas grid standard (CO_2 concentration< 2 vol. %) in several European countries(Persson et al. 2006). In our case study, the water scrubber technique, as a cost-effective and widespread upgrading technique (Teghammar et al. 2014), was used to ensure 99% CH_4 content in the upgraded biogas. The upgraded biogas is injected into the gas grid. The unconsumed CO_2 is recycled back into the catholyte blending tank of the feedstock section to increase carbon utilization of the process.

The overview economic evaluation report and itemized cost report were generated in SPD. The detailed settings and parameters used for all equipment in SPD can be found in the Supporting Information Table S2 and Table S3. Different current densities and internal resistances were investigated to explore the relationship between the performance of methane-producing BES and the production cost. According to the breakdown of production costs regarding different cost items within different sections, primary factors influencing the production cost were identified. Finally, the revenue of the case study was also examined in the sensitivity analysis according to the price of O_2 and CH_4.

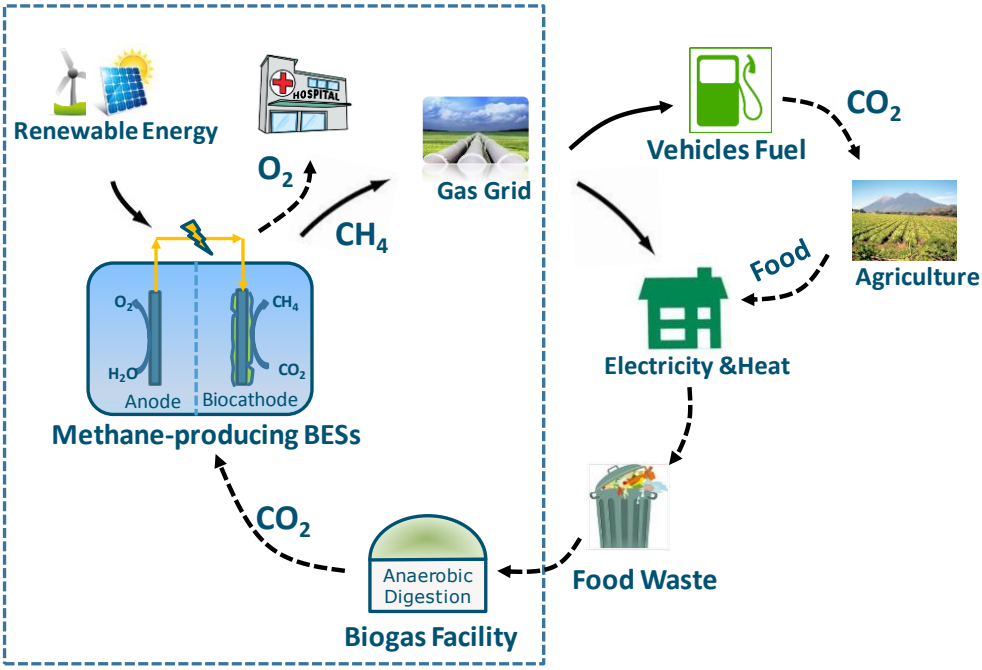

Figure 3. A schematic diagram for the case study on biogas upgrading by methane-producing BESs. Driven by renewable energy, methane-producing BES upgrades raw biogas from biogas plant to 99% methane, together with O_2 as a by-product. The O_2 can be used in the hospital, whereas 99% methane is injected into the gas grid for energy storage. The energy is consumed by a variety of different end uses, e.g. vehicle fuel, electricity and heat for households. In addition, vehicles combustion produces CO_2, which can be fixed by crops. Crops are supplied to households, and parts of them become food waste. Food waste is then fed into anaerobic digestion for raw biogas production. The techno-economic analysis focuses on the processes inside in the dotted square (system boundary).

6.4.1 Current density and internal resistance determine practical applicability

In our case study, different current densities of 35, 140, 1400, 2800 A/m^2 (based on projected cathode surface area) were studied. 35 A/m^2 is so far the highest current density reported in this thesis (Chapter 3). 140 A/m^2 is also a realistic value for CH_4 production, although not demonstrated yet, as acetate production at current density around 200 A/m^2 has been achieved with 99% of electron recovery efficiency (Jourdin et al. 2016). It is likely that this performance for acetate producing biocathode can be translated to methane production, as in all acetate producing biocathodes, the methanogenic inhibitor 2-BES was added to the catholyte to prevent methanogenesis (Bajracharya et al. 2017, Jourdin et al. 2015). 1400 and 2800 A/m^2 are exceptionally high current density compared to reported current densities for all kinds of biocathodes. Even though such high range of current densities could seem unrealistic, they are studied for a thorough understanding of the influence of current density on the costs of a methane-producing BESs plant. Theoretically, high current densities can be reached in the methane-producing BESs if enough external electricity energy is supplied to the systems and as long as methanogenic activity is high enough to consume this electricity (or its equivalent in hydrogen). For the anode, a platinum-iridium electrode for the water splitting reaction can reach current densities up to 10000 A/m^2 (Millet and Grigoriev 2013).

(a)

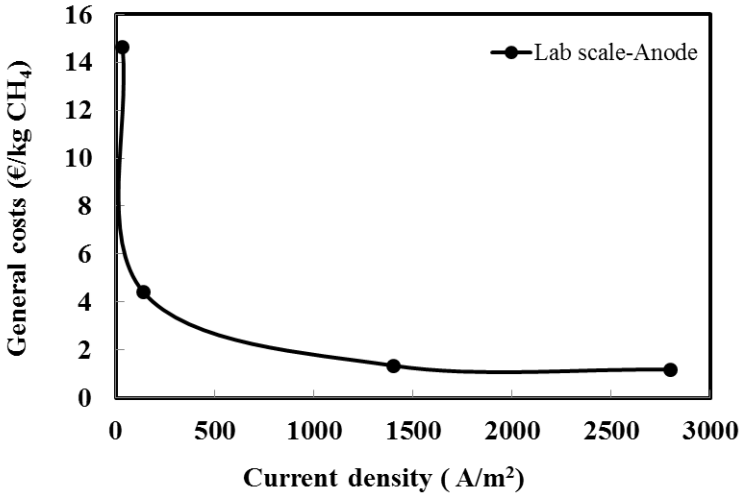

(b)

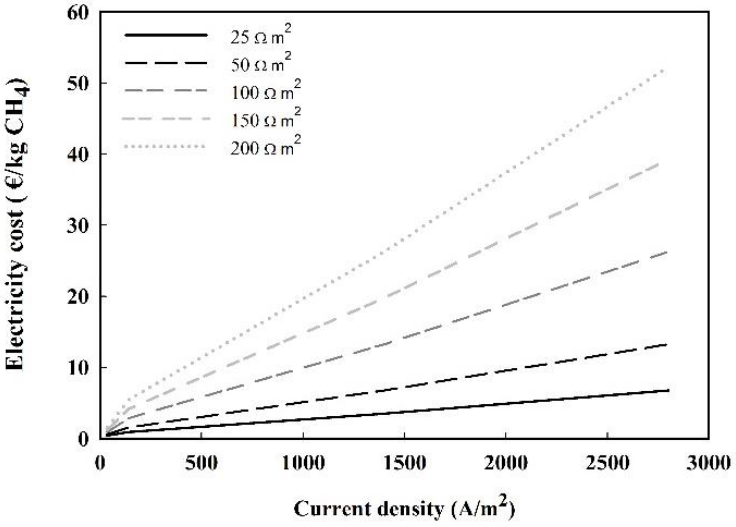

Figure 4. Production costs of the case study at different current densities. (a) The general costs decrease significantly with increasing current density and keep constant after reaching current density of 1500 A/m^2; (b) The electricity cost for the methane-producing BES reactor increase linearly along with the current density, and its decrease with decreasing internal resistance.

The general costs, shown in Figure 4(a), include the capital and operational costs, such as the purchase of the equipment, materials, and consumables (electrode, membrane, reactor housing for the methane-producing BESs reactor). In the range of 0-1400 A/m^2, general costs decrease along with the increase in current densities. This declining trend is clear especially at current densities lower than 140 A/m^2. However, general costs stabilize at current density higher than 1500 A/m^2. As the raw biogas input is constant at each current density, the higher the current density (rate of product formation), the smaller the methane-producing BES reactor will be, which means that costs of electrodes, membrane, and reactor housing of the BES reactor are lower. Therefore, the general costs reduction is mainly related to the methane-producing BES reactor, i.e. product synthesis section. Because the raw biogas input was constant, the operational costs for supplying fresh electrolyte and upgrading biogas (feedstock and biogas upgrading section) are independent of current density (Figure 8b). At current densities higher than 1500 A/m^2, the majority of the costs (about 80%) are related to feedstock and biogas upgrading section, resulting in stable general costs.

In addition to the general costs, the cost of electricity energy input of the methane-producing BESs reactor under different internal resistances as a function of current density is demonstrated in Figure 4(b). The internal resistance consists of several aspects, including pH gradient, anode, membrane, and cathode. Moreover, the internal resistance is expressed as $m\Omega\ m^2$ with systematic independence, therefore, can be easily used for comparison among different methane-producing BESs (Sleutels et al. 2009b). For a certain internal resistance, the electrical energy cost increases linearly with the increasing current density because higher electricity energy input is needed to drive a higher current density. At the same current density, the electricity cost increased with the increasing internal resistance, as a higher internal resistance at a certain fixed current results in a higher voltage to be applied. In Chapter 3 of this thesis, the largest internal resistance loss was found in the anode (55 $m\Omega\ m^2$), accounting for about 40% of the total internal resistance, whereas the biocathode resistance (4 $m\Omega\ m^2$ for GAC) has been reduced considerably to 3 % of total internal resistance (about 140 $m\Omega\ m^2$). Therefore, it is of vital importance to reduce the anode resistance to decrease the costs for electrical energy input for methane-producing BESs.

As all costs are expressed in euro per kg of CH_4 produced (€/kg CH_4), different costs can be summed up as total costs (Figure 5). For low current densities, the general costs are dominant; for high current densities, the electricity cost is the key factor that determines the total costs. A minimum total cost was observed at a certain current density and decreased with decreasing internal resistance. Reducing internal resistance in combination with operating at a certain current density can thus improve the cost-effectiveness of the methane-producing BESs reactor. Assuming that the methane-producing BES reactor in this case study has the same internal resistance as our lab-scale reactor in Chapter 3 (around 140 mΩ m^2), the minimum total cost was about 8.5 €/kg CH_4 at a current density of ≈120 A/m^2. The trends of the total costs influenced by the internal resistance and current density are in line with the techno-economic study for hydrogen-producing BESs, which is overall a comparable process (Sleutels et al. 2012).

(a)

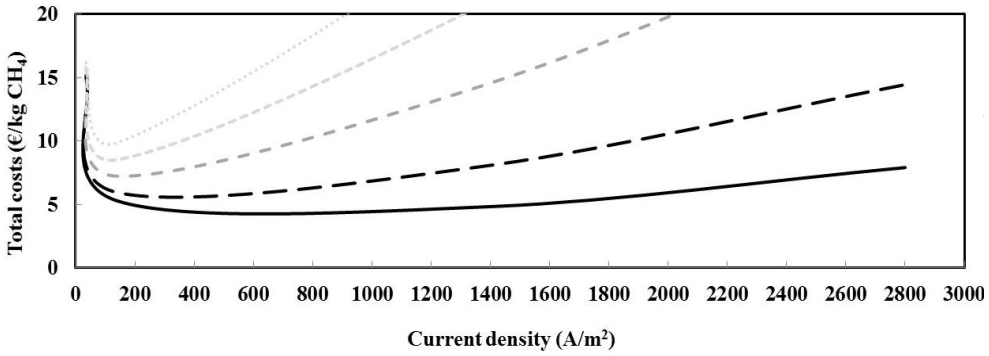

(b)

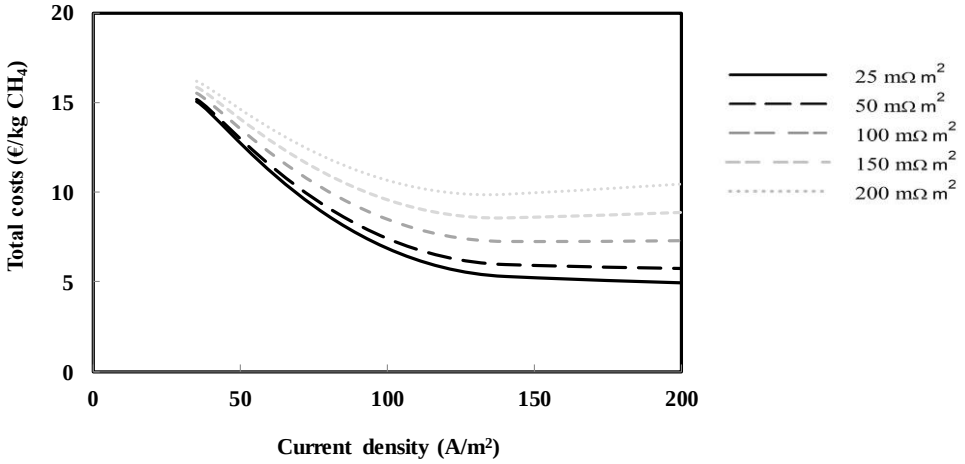

Figure 5. Total costs of the whole plant with the lab-scale anode for 5 different internal resistance levels, i.e. 25, 50, 100, 150, 200 mΩ m^2, as a function of current density: (a) within a current density range of 0-3000 A/m^2; (b) enlarged within a current density range of 0-500 A/m^2. The total cost is the sum of general costs and the electricity energy costs of the methane-producing BES reactor. For internal resistance level higher than 100 mΩ m^2, the minimum total costs can be obtained at a current density of about 120 A/m^2.

6.4.2 Platinum anode is the key element to general costs reduction at low current densities

So far, the current densities of state-of-the-art the methane-producing BESs are in a range of 0.1- 35 A/m^2 (Geppert et al. 2016, Chapter 3 in this thesis). For such current densities, a cost-effective full-scale methane-producing BESs seems not feasible, due to the high general costs explained in previous subchapter 6.3.1. Identifying the key element affecting the general costs is necessery for improving the process or system design of the methane-producing BESs in practice. In our study, the platinum-iridium anode is found to be the key element to the general cost reduction.

Firstly, breaking down the general costs associated with three different sections at each current density is shown in Figure 8 (b). At a current density of 35 A/m^2, the general cost in product synthesis section was 13.6 €/kg CH_4, accounting for more than 90% of the total general cost. Within the production synthesis section, costs for purchasing consumables had the highest share of around 90%, followed by the facility-dependent costs, including maintenance of the methane-producing BESs reactor (Figure 6).

Secondly, we further investigeated the consumables of the whole plant, which included the platinum-iridium anode, membrane, graphite current collector and the concrete of the methane-producing BESs reactor (Figure 7). A cost breakdown indicated that platinum-iridium anode was the main cost driver with a share of 60% of the total consumable costs.

Considering the decisive factor of the platinum-iridium anode in the general cost, reducing the amount of platinum-iridium anode used in the methane-producing BESs reactor can effectively contribute to the general costs reduction of the whole plant. In the base of our case study, lab scale anode had the surface area of 1:1 ratio of platinum-iridium anode area and cathode electrode area according to the lab experiment (Chapter 3). Such design of anode electrode suggested that the anodic current density is equal to the cathodic current density. However, it is not necessary for the anode electrode having the same current density as the cathode, especially at low cathodic current densities, because platinum-iridium anode can even achieve a high current density up to10000 A/m^2 for the water splitting reaction (Millet and Grigoriev 2013).Therefore, a full-scale anode with 15 m^2 of platinum-iridium anode surface area was proposed in combination with a cathode of 3520 m^2 (the raio of the platinum-iridium anode area to the cathode project area is 0.004). By

comparison with the lab scale anode, a significant decrease of general costs for lower current densities was obtained in Figure 8(a). This general costs reduction is mainly attributed to the cost reduction in the product synthesis section shown in Figure 8(b).

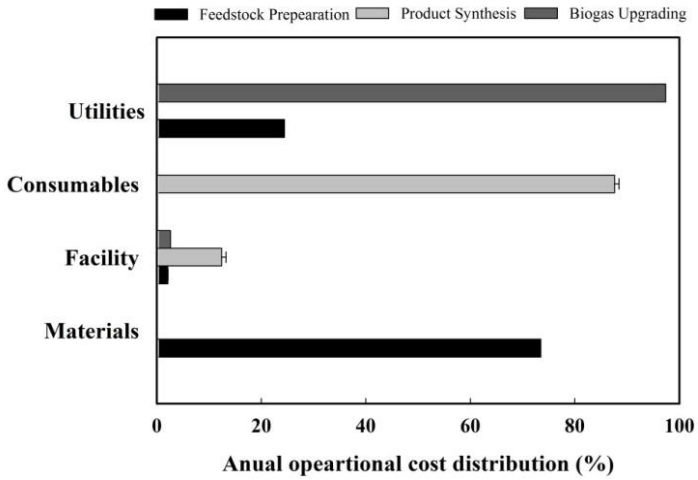

Figure 6. The share of different cost items among annual general coats of each section based on case study operating at a current density of 35 A/m^2. The highest share of the general costs in each section is: materials costs for feedstock section, consumables costs for production synthesis section and utilities costs for biogas upgrading section.

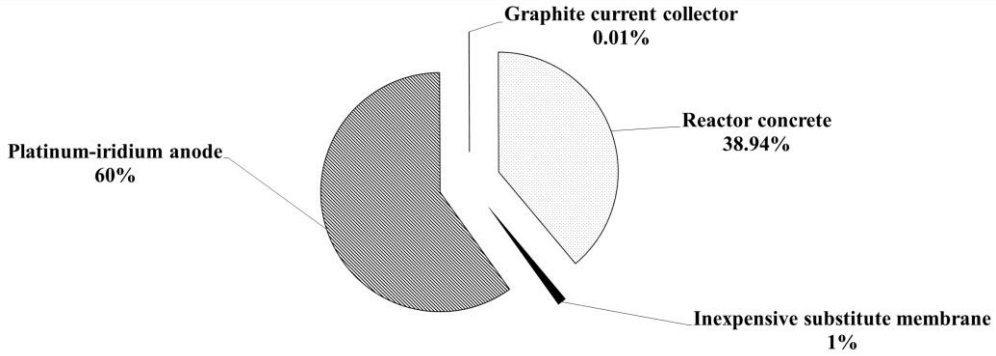

Figure 7. The costs distribution of various materials among consumables costs of the product synthesis section. Platinum-iridium anode accounted for 60% of the total consumable costs, followed by the reactor housing of the methane-producing BES about

39%, whereas the contributions of both inexpensive substitute membrane (1%) and graphite current collector (0.01%) were negligible.

(a)

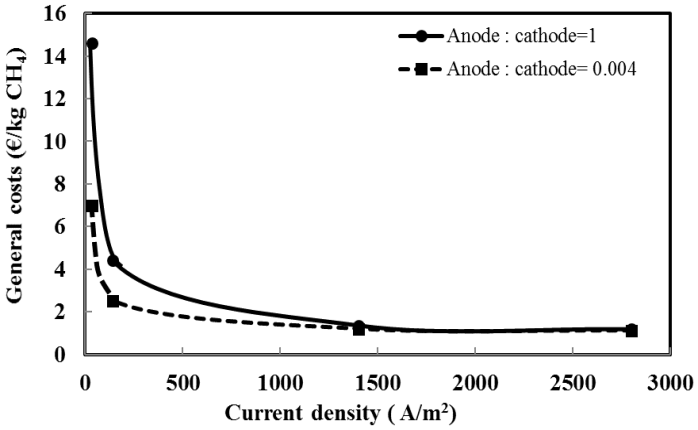

(b)

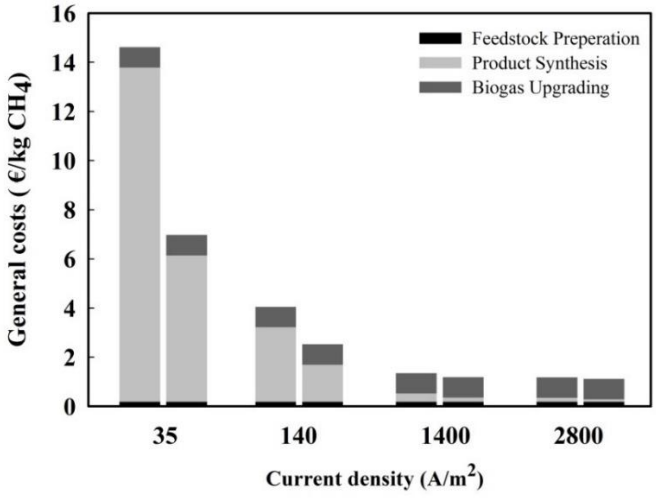

Figure 8. A comparison of general costs between two different ratios of electrode areas for anode and cathode. The ratio of platinum-iridium anode area to GAC cathode project area is 1 for lab-scale anode and 0.004 for full-scale anode. (a) the general costs of the full-scale anode decreased significantly at current densities < 200 A/m^2, compared to that in the lab-scale anode. (b) Breakdown of the general costs for lab-scale anode (Left) and full-scale anode (Right) into three sections.

6.4.3 Oxygen is the main revenue product

For better comparison of the cost and the revenue, the revenue is represented in the same unit as the cost (€/kg CH_4). According to this unit, a constant revenue of 8.92 €/kg CH_4 was found for each current density/internal resistance. The reason for this constant revenue is that the revenue was calculated based on the price of CH_4 and O_2, and the ratio in which they are produced. As long as the quality of input raw biogas does not change (as assumed in the model), the composition of the overall products should be constant, and thus the revenue per kg of CH_4 is stable.

It is worth mentioning that the revenues for O_2 are much higher than for CH_4. On the one hand, the selling price of O_2 (4.4 €/kg) is almost 2.5 times higher than the CH_4 (1.90 €/kg); on the other hand, in terms of weight, the O_2 yield is 1.6 times higher than the total amount of CH_4 in the final upgraded biogas. The raw biogas contains 60 vol. % of CH_4 and 40 vol. % of CO_2, and only CO_2 is reduced in the methane-producing BESs reactor, where 4 kg of O_2 are generated for per kg of CH_4 produced based on chemical reaction ($CO_2 + 2H_2O \rightarrow CH_4 + 2O_2$). In this case study, the overall products ratio of O_2 and CH_4 (in kg) turned out to be 1.6:1. The revenue from O_2 is, therefore, around 4 times higher than that for CH_4. This factor can also be found in the Economic Evaluation Report (EER) of SPD.

For practical application of the methane-producing BESs, the revenues over the costs are crucial. The methane-producing BES in this case study is only profitable if the production cost per kg of CH_4 is lower than the revenue. As discussed in the 6.3.2, the general costs of the whole plant working at low current density can be considerably decreased if anode electrode are reduced. We recalculated the total cost based on a lower anode area (full-scale anode) and compared that with the total revenue (CH_4 and O_2) and the sub-revenue (CH_4) (Figure 9). When and the total revenue of CH_4 and O_2 are taken into account, the application of the methane-producing BESs is almost within reach based on the lab operating performance (current density of 35 A/m^2 and internal resistance of 150 Ω m^2), when current-to-methane efficiency is 100%. However, without considering the sub-revenue of O_2, it is so far not possible to have a profitable full-scale plant of the methane-producing BESs. Selling O_2 is essential to make the full-scale application of the methane-producing BESs economically feasible or unless storage of electricity becomes valuable. Unlike the methane production in biocathodes, the O_2 production performance of the anodic

process in the methane-producing BESs has not yet been studied. We advise that in the future more attention should be paid on the optimization of the anodic process, e.g. using high-surface area platinum electrode or choosing another anodic reaction, which improves the cost-effectiveness of the methane-producing BESs considerably.

(a)

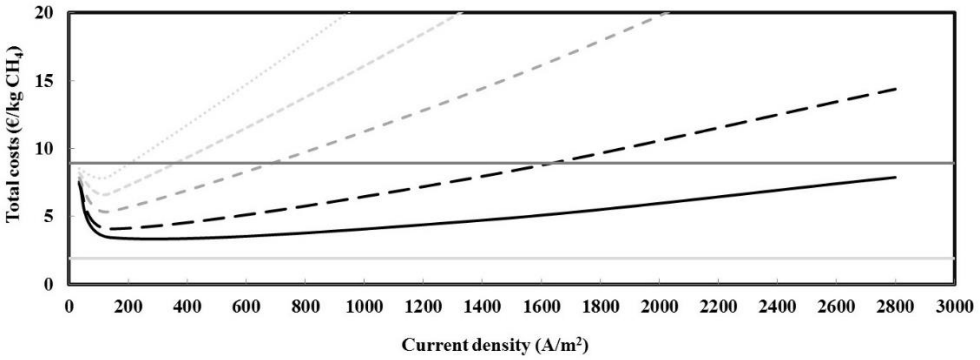

(b)

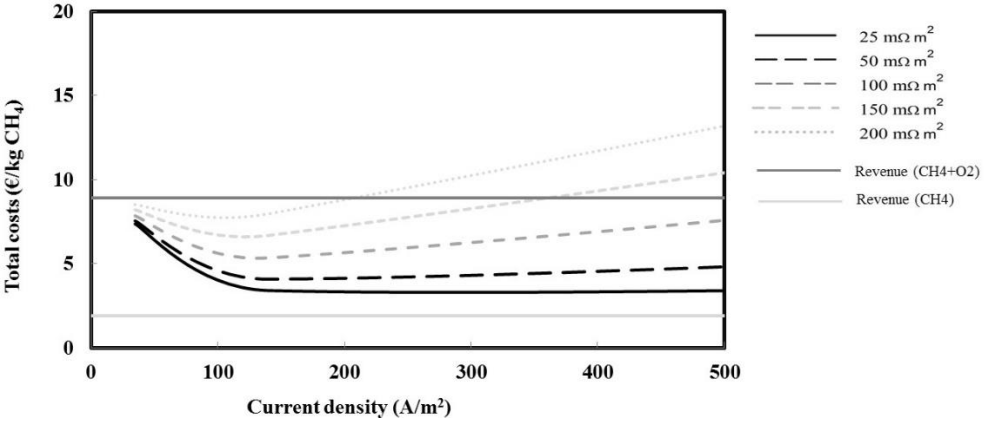

Figure 9. Total costs and revenue of the whole plant as a function of current density, under the assumption that the whole plant is carried out by the full-scale anode with 5 different internal resistance levels, i.e. 25, 50, 100, 150 and 200 mΩ m^2. (a) within a current density range of 0-3000 A/m^2; (b) enlarged within a current density range of 0-500 A/m^2. The cost-effective area is the area below the dark gray solid line.

6.5 Power-to-gas by methane-producing BESs: perspectives

Based on the simulation results of the previous section, we calculated the total costs of methane-producing BESs plant in terms of storage per kWh electrical energy (€/kWh) (Figure 10.). The total cost of 1 kWh electricity storage, is variable and determined by the internal resistance and the applied current density. According to the lab performance of methane-producing BESs in chapter 3 of this thesis (current density of 35 A/m^2 and internal resistance of 150 Ω m^2), the total cost is about 0.60 €/kWh. Although it is much more expensive than the natural gas (0.02-0.03 €/kWh) and biomethane (0.07 €/ kWh) (Götz et al. 2016), it is still within the range for substitute natural gas generation costs (0.04-0.90 €/kWh) summarized in the literature (Götz et al. 2016). These costs do not include the effect of oxygen utilization; however, a foreseen cost reduction will be achieved if these oxygen produced can be sold.

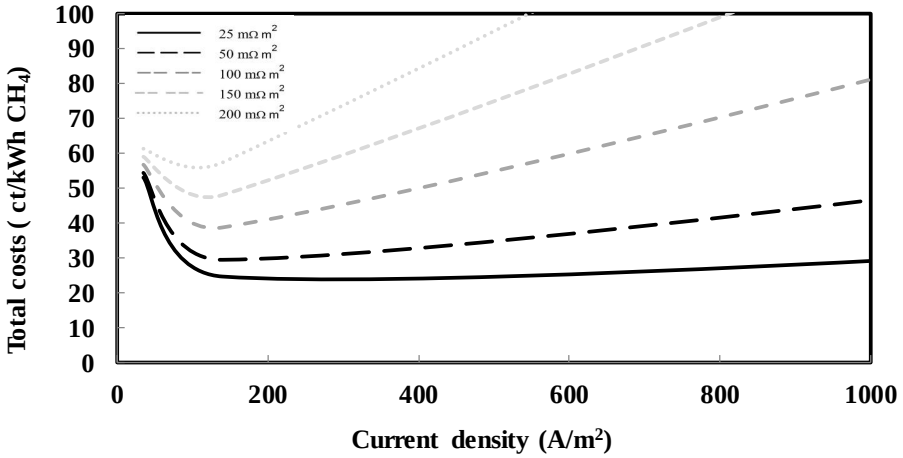

Figure 10. Total costs of the whole plant regarding per kWh of renewable energy storage. The results are shown as a function of current density, under the assumption that the whole plant is carried out by the full-scale anode with 5 different internal resistance levels, i.e. 25, 50, 100, 150 and 200 mΩ m^2.

Among methanation technologies, methane-producing BES is a relatively new concept and is still under research. The energy efficiency of methane-producing BES is still low, about 20%. As the anode electrode used in the reactor in Chapter 3 is not efficient for water splitting, better anode electrode and system optimization will definitely improve the energy

efficiency. Reducing anode losses, for instance, will result in an estimated maximum energy efficiency (suppose an anode overpotential of 0.3 V at the electrode modified with $NiCoO_4$ Nano platelets and it can achieve a current density up to1000 A/m^2) could reach 45% for GAC reactor and 40% for GG reactor. The feasibility of methane-producing BESs is not only limited by the energy efficiency, but also rely on the operational conditions and capital costs, since these practical issues play important roles in determining the application niche. In Table 1, specifics of the three types of methanation processes are summarized. The nature for methane-producing BES indicates that it is better adapted to small-scale applications, for example street-level household solar panel energy storage. On the one hand, it is much safer to operate methane-producing BESs under mild conditions (room temperature and 1 bar), compared with thermochemical methanation (300~400℃, 50-200 bar). On the other hand, methane-producing BESs may be easier to apply and less expensive, compared with biological methanogenesis, which requires hydrogen storage.

6.6 Concluding remarks

In this last chapter, an overview was given regarding the development of methane production rate in methane-producing BESs since 2009, indicating that in this PhD thesis, so far, the highest methane production rate of 65 L CH_4/m^2 cat_{proj}/d has been achieved. We have investigated the potential loss within the whole system (reactor operated in Chapter 3), revealing that the anode overpotential for water splitting had the biggest share of the total applied voltage. The anode was therefore the main limiting factor to the energy efficiency, which requires further study. Techno-economic analysis of a case study upgrading biogas by methane producing BESs indicates that reduction of size of the platinum anode plays an important role in capital costs reduction, especially at low current densities. Based on this techno-economic analysis, the application of methane-producing BESs can be cost-efficient when the bioelectrochemical system is optimized with low internal resistance and operated under high current densities. Oxygen is overall the most significant product influencing the profit due to its high market price. Finally, methane-producing BESs shows great promise in application to store renewable energy at small scale.

Table 1. Comparative perspectives on methanation process.

	Thermochemical methanation (electrolysis +Sabatier)	**Biological methanogensis** (electrolysis + methanogenesis)	**Methane-producing BESs**
Temperature	300~400℃	50-70℃	20-30 ℃
Pressure	50-200 bar	1 bar	1 bar
CO_2 sources	Biogas (biomass-to-methane), CO_2 capture plants from industry		
Tolerance to contaminants	H_2S: low O_2: low	H_2S: high O_2: limited	H_2S: high O_2: limited
Power-to-methane energy efficiency (excluding heat recovery)	60%	55%	20%
Operational advantages	Low maintenance	High flexibility	High flexibility, low costs (without hydrogen storage)
Technical maturity	Demonstration phase	Early demonstration phase	Research phase
Scale	Large/centralized	Small/decentralized	Small/decentralized

SUPPORTING INFORMATION

Chapter 6. General Discussion

2 Figures, 3 Tables

A. Calculations of Potential Losses at Current Density of 35 A/m^{2}cat$_{proj}$

The applied cell voltage (E_{cell}) is divided into the reversible energy loss and irreversible energy losses(Sleutels et al. 2009b). The reversible energy loss is the energy used for conversion of CO_2 and H_2O into CH_4 and O_2, respectively (equilibrium voltage, E_{eq}). The irreversible energy losses belong to anode (η_{an}) and cathode (η_{cat}) overpotentials, pH gradient between anode and cathode chambers ($E_{\Delta pH}$), ionic loss (E_{ionic}) and transport loss through the membrane ($E_{transport}$). These potential losses were calculated using the following equations (1-8) according to literature(Sleutels et al. 2009b), where R is ideal gas law constant (8.314 J/kmol); T is the absolute temperature (303.15 K); F is the Faraday's constant (96485 C/mol); P_{CH4} is the CH_4 partial pressure (1bar); P_{O2} is the O_2 partial pressure (1 bar); pH_{anode} is the anolyte pH (2); $pH_{cathode}$ is the catholyte pH (7); d_{an} is the distance between the anode electrode and the membrane (0.01m); d_{cat} is the distance between the cathode electrode and the membrane (0 m); σ_{an} is the anolyte conductivity (0.50 ± 0.06 S/m); and σ_{cat} is the catholyte conductivity. In addition, Table S1 summarizes all cell voltages, anode potentials and cathode potentials measured at current density of 35 A/m^{2}cat$_{proj}$.

$$E_{cell} = E_{eq} - \eta_{an} - \eta_{cat} - E_{\Delta pH} - E_{ionic} - E_{transport} \quad (1)$$

$$E_{cat} = E^0_{cat} - \frac{RT}{2F}\ln\left(\frac{p_{CH4}}{[H^+]^9[HCO_3^-]^9}\right) = -\frac{-175.46\times1000}{8\times96485} - \frac{8.314\times303.15}{8\times96485}\times ln\left[\frac{1}{(10^{-7})^9\times1}\right] = -0.25\,V\ vs.\ SHE \quad (2)$$

$$E_{an} = E^0_{an} - \frac{RT}{4F}\ln\left(\frac{1}{[H^{+4}[p_{O2}]}\right) = -\frac{-474.38\times1000}{4\times96485} - \frac{8.314\times303.15}{4\times96485}\times ln\left[\frac{1}{(10^{-7})^4\times1}\right] = 0.81\,V\ vs.SHE \quad (3)$$

$$E_{eq} = E_{cat} - E_{an} = -0.25\,V - 0.81\,V = -1.06\,V \quad (4)$$

$$\eta_{an} = E_{an,measured} - E_{an} \quad (5)$$

$$\eta_{cat} = E_{cat} - E_{cat,measured} \quad (6)$$

$$E_{\Delta pH} = \frac{RT}{F}\ln\left(10^{(pH_{cathode}-pH_{anode})}\right) = \frac{8.314\times303.15}{96485}\ln(10^{(7-2)}) = 0.30\,V \quad (7)$$

$$E_{ionic} = I_{inos}\left(\frac{1}{2}R_{an} + \frac{1}{2}R_{cat}\right) = I_{inos}\left(\frac{d_{an}}{2A\sigma_{an}} + \frac{d_{cat}}{2A\sigma_{cat}}\right) = 0.07\times\left(\frac{0.01}{2\times0.0022\times0.5}\right) = 0.31\,V \quad (8)$$

Table S1. Measured cell voltages, anode and cathode potentials for all four reactors at a current density of 35 A/m^{2}cat$_{proj.}$ Data represent the average ± standard deviation of 4 separate samples for each reactor.

Reactor	E_{cell} (V)	$E_{an,measured}$ (V vs. Ag/AgCl)	$E_{cat,measured}$ (V vs. Ag/AgCl)
GG$_1$	-4.67 ± 0.07	2.44 ± 0.10	-1.03 ± 0.06
GG$_2$	-5.02 ± 0.04	2.61 ± 0.04	-1.07 ± 0.01
GAC$_1$	-4.76 ± 0.13	2.64 ± 0.08	-0.58 ± 0.01
GAC$_2$	-4.78 ± 0.13	2.55 ± 0.05	-0.59 ± 0.02

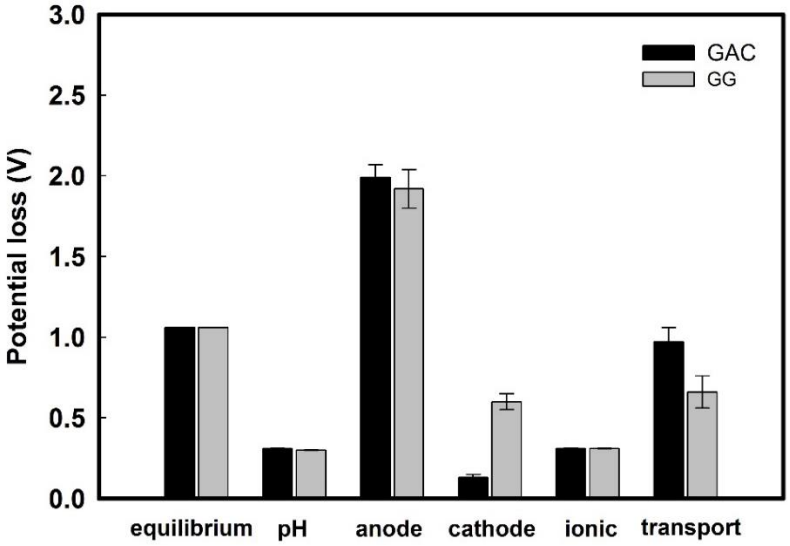

Figure S1. The breakdown of potential losses in GAC and GG at current density of $35 A/m^2 cat_{proj}$. The average and standard deviation of each electrode material are calculated based on 4 data points, each of which is duplicated, within 2 weeks of stable performance.

B. Methodology: Process Simulation and Economic Analysis

After determining inflow streams and initial settings for each unit in our case study, the *SuperPro Designer*® 9.0 firstly solves material and energy balances, and then generate several economic reports. Some initial settings of our case study are listed in Table S3. In general, the costs of the system is consisted of general costs (capital and operational costs) and electricity energy cost for the methane-producing BESs reactor.

In the capital cost, the purchase price for the equipment is estimated based the website of Alibaba.com, whereas the costs for installation, instrumentation, buildings, yard improvements, auxiliary facilities, contractor's fee and contingency are estimated according to software default settings (sum up to 5.2 times of the equipment purchase price). The project lifetime is set to 20 years. The assumed construction period is 24 months and the biocathode start-up period of 2 months is used according to experimental results from lab scale (our capacitive paper).

In the annual operational costs, the purchase price for raw materials (biogas, nutrients, buffer solution, and water) and consumables (membrane, electrodes, BEP2G reactor housing) are listed according to the literature (Rozendal et al. 2008). The costs of both labour and waste management are not included in this case study due to many uncertainties. The estimated lifetime of the BEP2G reactor is 20 years, whereas the lifetime of the rest of the consumables is set to 5 years. The maintenance cost is assumed 0.01% of the purchase cost for each facility, excluding gear pump (which is 0.1% of the purchase cost). The costs for utilities refers to the expense of heating or cooling agent (mention value), and electricity energy used by the whole system but excluding BEP2G reactor.

The electrical energy input for BEP2G reactor is calculated separately based on different internal resistances (between 25 to 200 mΩ m^2) and variable current densities (between 35 A/m^2 to 2800 A/m^2) and assumed to have 100% of current-to-methane efficiency. The cost for this electricity is calculated based on 0.035 €/kWh for industry usage. In this case study, we investigated both scenarios to identify the key process or significant components in such key process that determines the practicability of the whole system.

Each model methane-producing BES reactor in this discussion chapter was proportional to (20x bigger than) the rector used in Chapter 3 and Chapter 4 of this thesis (Table S2) . As

the inflow of the biogas was fixed, the amount of methane-producing BES model reactor is dependent on the maximum operating current density. These reactors are constructed in parallel.

Table S2. Footprint of our methane-producing BESs reactor under different current density modelled in the SuperPro designer.

Methane-producing BES	**Length (m)**	**Height (m)**	**Width (m)**	
Size of each reactor	0.28	3.2	1.4	
Current density (A/m^2)	35	140	1400	2800
Number of reactors in parallel	1410	353	36	18

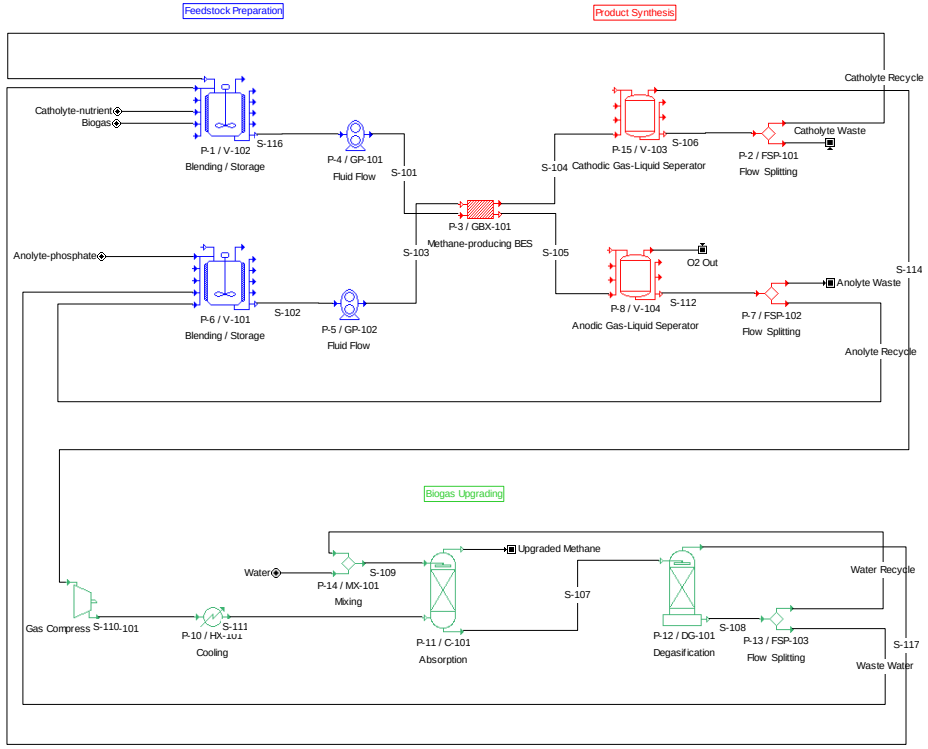

Figure S2. Process flow diagram in *SuperPro Designer*®. The whole system was divided into three different sections: Feedstock Preparation (blue), which also included the recirculation of water and CO_2 from the degasification; Product Synthesis (red), which mainly referred to methane-producing BESs; Biogas Upgrading (green), which consisted of a gas compressor, an adsorption tower for CO_2 adsorption in water and a degasification tower for CO_2 and water separation.

Table S3. Cost estimates for materials, products and utilities.

Item		Cost		Reference
Medium	Catholyte (mineral & Vitamin)	1.69	€/L	Calculated based on (Chapter 3 in this thesis)
	Anolyte (phosphate buffer)	1.45	€/L	Calculated based on (Chapter 3 in this thesis)
	Fresh water	0.000067	€/kg	(Teghammar et al. 2014)
	Raw biogas [a]	10	€/tonne	(Skovsgaard and Jacobsen 2017)
Products	Methane [b]	1.895	€/kg	(Teghammar et al. 2014)
	Oxygen	4000	€/ton	Market price [c]
Membrane	Inexpensive substitute membrane	10	€/m^2	(Rozendal et al. 2008)
Electrodes	Single sided platinum-iridium coated titanium plate	500	€/m^2	(Rozendal et al. 2008)
	Activated carbon granules	1000	€/m^2	Market price [c]
Utilities	Blending/storage tank	8000	€	Market price [c]
	Gear pump	50	€	
	Gas-liquid separator	2000	€	
	Gas compressor (60 bar)	30000	€	
	Cooling machine	54280	€	
	Absorption tower	5000	€	
	Degasification tower	5500	€	
	Concrete for methane-producing BESs reactor	99.28	€/m^2	Market price [d]
	Electricity	0.0346	€/kW h	(Teghammar et al. 2014)

a. Raw biogas contains approximately 60% CH_4 and 40% CO_2 at production rate of 2 m^3 of biogas per m^3 of the digester volume per day. (Kondusamy and Kalamdhad 2014). In this case study, the digester volume is assumed 100 m^3, leading to the biogas input of 200 m^3 per day.

b. The final price of methane after subtraction the cost for tank stations and injection into the gas grid.

c. www.alibaba.com

d. http://www.livios.be/nl/bouwinformatie/ruwbouw/beton/fundering/richtprijzen-fundering-en-beton/

Reference

Bajracharya, S., Yuliasni, R., Vanbroekhoven, K., Buisman, C.J.N., Strik, D.P.B.T.B. and Pant, D. (2017) Long-term operation of microbial electrosynthesis cell reducing CO_2 to multi-carbon chemicals with a mixed culture avoiding methanogenesis. Bioelectrochemistry 113, 26-34.

Cheng, S.A., Xing, D.F., Call, D.F. and Logan, B.E. (2009) Direct Biological Conversion of Electrical Current into Methane by Electromethanogenesis. Environmental Science & Technology 43(10), 3953-3958.

Götz, M., Lefebvre, J., Mörs, F., McDaniel Koch, A., Graf, F., Bajohr, S., Reimert, R. and Kolb, T. (2016) Renewable Power-to-Gas: A technological and economic review. Renewable Energy 85, 1371-1390.

Geppert, F., Liu, D., van Eerten-Jansen, M., Weidner, E., Buisman, C. and Ter Heijne, A. (2016) Bioelectrochemical Power-to-Gas: State of the Art and Future Perspectives. Trends In Biotechnology.

Jourdin, L., Freguia, S., Flexer, V. and Keller, J. (2016) Bringing high-rate, CO_2-based microbial electrosynthesis closer to practical implementation through improved electrode design and operating conditions. Environmental Science & Technology 50(4), 1982-1989.

Jourdin, L., Grieger, T., Monetti, J., Flexer, V., Freguia, S., Lu, Y., Chen, J., Romano, M., Wallace, G.G. and Keller, J. (2015) High Acetic Acid Production Rate Obtained by Microbial Electrosynthesis from Carbon Dioxide. Environmental Science & Technology 49(22), 13566-13574.

Kondusamy, D. and Kalamdhad, A.S. (2014) Pre-treatment and anaerobic digestion of food waste for high rate methane production – A review. Journal of Environmental Chemical Engineering 2(3), 1821-1830.

LaBarge, N., Yilmazel, Y.D., Hong, P.-Y. and Logan, B.E. (2017) Effect of pre-acclimation of granular activated carbon on microbial electrolysis cell startup and performance. Bioelectrochemistry 113, 20-25.

Liu, F., Rotaru, A.-E., Shrestha, P.M., Malvankar, N.S., Nevin, K.P. and Lovley, D.R. (2012) Promoting direct interspecies electron transfer with activated carbon. Energy & Environmental Science 5(10), 8982-8989.

Millet, P. and Grigoriev, S. (2013) Renewable Hydrogen Technologies. Arzamendi, G. and Diéguez, P.M. (eds), pp. 19-41, Elsevier, Amsterdam.

Nandi, S., Kwong, A.T., Holtz, B.R., Erwin, R.L., Marcel, S. and McDonald, K.A. (2016) Techno-economic analysis of a transient plant-based platform for monoclonal antibody production, pp. 1456-1466, Taylor & Francis.

Persson, M., Jönsson, O. and Wellinger, A. (2006) Biogas upgrading to vehicle fuel standards and grid injection, Brochure of IEA Task 37 "Energy from Biogas and Landfill Gas".

Rozendal, R.A., Hamelers, H.V.M., Rabaey, K., Keller, J. and Buisman, C.J.N. (2008) Towards practical implementation of bioelectrochemical wastewater treatment. Trends in Biotechnology 26(8), 450-459.

Sebastião, D., Gonçalves, M.S., Marques, S., Fonseca, C., Gírio, F., Oliveira, A.C. and Matos, C.T. (2016) Life cycle assessment of advanced bioethanol production from pulp and paper sludge. Bioresource Technology 208, 100-109.

Shi, H. and Zhao, G. (2014) Water Oxidation on Spinel $NiCo_2O_4$ Nanoneedles Anode: Microstructures, Specific Surface Character, and the Enhanced Electrocatalytic Performance. The Journal of Physical Chemistry C 118(45), 25939-25946.

Skovsgaard, L. and Jacobsen, H.K. (2017) Economies of scale in biogas production and the significance of flexible regulation. Energy Policy 101, 77-89.

Sleutels, T.H., Lodder, R., Hamelers, H.V. and Buisman, C.J. (2009a) Improved performance of porous bio-anodes in microbial electrolysis cells by enhancing mass and charge transport. International Journal of Hydrogen Energy 34(24), 9655-9661.

Sleutels, T.H., Ter Heijne, A., Buisman, C.J. and Hamelers, H.V. (2012) Bioelectrochemical systems: an outlook for practical applications. ChemSusChem 5(6), 1012-1019.

Sleutels, T.H.J.A., Hamelers, H.V.M., Rozendal, R.A. and Buisman, C.J.N. (2009b) Ion transport resistance in Microbial Electrolysis Cells with anion and cation exchange membranes. International Journal Of Hydrogen Energy 34(9), 3612-3620.

Teghammar, A., Forgács, G., Sárvári Horváth, I. and Taherzadeh, M.J. (2014) Techno-economic study of NMMO pretreatment and biogas production from forest residues. Applied Energy 116, 125-133.

Vergili, I., Kaya, Y., Sen, U., Gönder, Z.B. and Aydiner, C. (2012) Techno-economic analysis of textile dye bath wastewater treatment by integrated membrane processes under the zero liquid discharge approach. Resources, Conservation and Recycling 58, 25-35.

Summary

Summary

Methane-producing BESs are a promising technology for renewable electricity storage

There is a rapidly increasing demand for energy due to the population growth and economic boost in the world. We have strived to meet such energy demand without compromising the environmental quality by implementing renewable energy technologies. As described in **chapter 1**, renewable energy is abundant and are utilised in three forms: electricity, heat and biofuels. Among these renewable energy forms, electricity has the largest share, accounting for 78% of the total renewable energy capacity supplied in 2015. It is well known that renewable electricity supply is intermittent and fluctuating. Developing flexible electricity storage systems is thus essential to stimulate a larger share of renewable energy market.

Methane-producing BESs are an emerging technology for converting renewable electricity into methane. They utilize CO_2 from waste-streams to produce methane in one-step conversion; in addition, they operate at room temperature (20-30℃) and atmospheric pressure with open-culture microorganisms, an inexpensive, self-regenerating biocatalyst. This thesis aims at achieving efficient methane production in methane-producing BESs by improving the CO_2 reduction reaction at the biocathode, as the biocathode is by far the rate limiting process in the whole methane-producing BESs.

Searching for cathode materials to improve biocathode performance

Methane-producing BES consists of two electrodes (anode and cathode), which are typically separately by a cation exchange membrane. At the anode, water is oxidized into O_2, protons and electrons. The produced electrons flow through the external circuit to the cathode electrode, at where methane production takes place by means of microbial reaction with these electrons. The cathode with the attached microorganisms is called the biocathode. The biocathode is the most crucial part of the methane-producing BES; the bioactivity of the microorganisms and its interaction with electrodes, which occur in the biocathode, determine the methane production rate. Therefore, there is a need for searching cathode electrode materials that provide a high biocompatibility and a large electrode surface area. Electrode materials can be categorised into two types: metal-based and

carbon-based electrode. Firstly, a metal-based electrode, i.e. heat-treated stainless steel felt (HSSF), was investigated for methane-producing biocathode in **chapter 2**. The HSSF had superior electrocatalytic properties for hydrogen evolution compared to untreated stainless steel felt (SSF) and graphite felt (GF), leading to a faster start-up of the biocathodes. HSSF improved methane production rates of SSF when operated at -1.1 V and -1.3 V vs. Ag/AgCl, with a performance approximating to GF. HSSF is shown to be an alternative cathode material with a comparable performance to GF, making it suitable for application in methane-producing BESs.

Secondly, use of granulated activated carbon (GACs), a carbon-based material, as a methane-producing biocathodes was investigated in **chapter 3** and **4.** GACs are selected due to that it has a higher specific surface area compared with that of graphite granules (GGs). Under galvanostatic control, the reactors in our study achieved a methane production rate of around 65 L $CH_4/m^2cat_{proj}/d$ at 35 A/m^2cat_{proj}. The GAC biocathodes had a lower overpotential than the GG biocathodes, with methane generation occurring at -0.52 V vs. Ag/AgCl for GAC and at -0.92 V for GG at a current density of 10 A/m^2cat_{proj}, and still at only -0.58 V for GAC at 35 A/m^2cat_{proj}. 16S rRNA gene analysis showed that *Methanobacterium* was the dominant methanogen at both GAC and GG biocathodes. To further study the mechanism of methane production in GAC biocathodes, we replaced CO_2 supply by flushing with pure N_2 in the catholyte. In absence of CO_2 supply, the cathode potential decreased to a more negative value of -0.9 V vs. Ag/AgCl. Overall, this suggests the possibility that methane is produced via direct electron transfer at GAC biocathodes. Based on this experimental set-up, we investigated the effect of intermittent current on both GAC and GG biocathodes of methane-producing BESs, by operating them under three different current supply modes (time-ON/time-OFF: 4'- 2', 3'- 3', 2'- 4'), at two current densities (10 and 35 A/m^2 cat_{proj}). Methane production rates increased with longer time-ON modes for both GAC and GG biocathodes. The current-to-methane efficiencies of all biocathodes at intermittent current were similar to those under constant current, with 50-60 % at 10 A/m^2 cat_{proj} and 80-90 % at 35 A/m^2 cat_{proj}. After switching to continuous current supply, all biocathodes recovered their original performance directly. Our results reveal that methane-producing biocathodes can be robust when operating under intermittent current.

Exploring a new application for Methane-producing BESs

Many studies were done to explore new application opportunities for Methane-producing BESs, focusing on the locations where CO_2 and electricity is abundant and relatively cheap. Biogas production sites are one of these locations, because raw biogas contains about 40% CO_2, which needs to be upgraded before use. In addition to upgrading biogas, methane-producing BESs was also shown to enhance methane production of anaerobic digesters. In **chapter 5**, we integrated the methane-producing BES with anaerobic digestion (AD) to investigate if methane-producing BESs can enhance methane production from organic matter in low-temperature anaerobic digestion. At 10 ℃, methane yield in the integrated BES-AD system was 5.3~6.6 times higher than those of the control (no external voltage and no electrodes). Methane production rate achieved in the combined BES-AD system at 10 ℃ was slightly lower than that in the AD system operating at 30 ℃. Energy input by the form of electricity in BES-AD system was only 10 % of the energy for heating up the digester to mesophilic temperature.

Scaling-up issues for methane-producing BESs

So far, all methane-producing BESs studies are performed with small-scale setups in the laboratory. It is, however, of importance to up-scale the experimental setups and prepare it for implementation. In **chapter 6**, a techno-economic analysis of a methane producing BESs used for upgrading biogas showed that use of platinum as the anode material plays a key role in capital cost due to the expensive purchase costs, especially when the current densities is far lower than35 A/m^2. The application of methane-producing BESs can be cost-efficient when the bioelectrochemical system is optimized with a lower internal resistance and operated under high current densities. Moreover, oxygen is identified as the most crucial product due to its high market price; the production and selling of oxygen produced in this case has a great influence on the overall profit. Overall, this outcome of this thesis contributes to the improvement of methane-producing BESs at small-scale setups, extends the application of methane-producing BESs and evaluates the techno-economic feasibility of such in an up-scaled condition. This may furnish methane-producing BESs with more application potentials as a renewable energy storage and saving technology.

Acknowledgement

Acknowledgement

Finally come to the end of the thesis. Time is short, four years fly. As a Chinese girl from a small city in northeast China, I would never imagine that I can be in The Netherlands and finally accomplish my PhD thesis here. I would like to use this chapter to thank all of the people who gave me help and support along this journey. Without them, I could not successfully complete this PhD thesis.

First of all, I would give my greatest gratitude to my family. My parents and my relatives give me endless support and care. Mom and Dad, even though you have missed me very much and been worried about my life in The Netherlands, you have been always there to support me and encourage me to go for my dream and live a happy life. 感谢我的父母，你们给我一个温暖又善良的家庭，教会我做事勤劳努力，待人真诚友善。我知道你们一直都很担忧我人在异乡面对攻读博士的压力，害怕我不能够好好的照顾自己。每次视频，我都能感受到你们对我的浓浓思念和关怀。感谢我的亲戚们，每次我回到家乡，你们都会热情的欢迎我，给我很多问候和祝福。在我不在家的日子里，帮助我照顾我的父母。感谢我的两个温暖的大家庭！Of course, I want to thank my boyfriend, Wei-Shan (Momo). You are the sunshine in my life and you help me break many self-imposed limits. I am an emotional girl with ups and downs. You said that your life is more colourful because of me, on the other side, my life is more stable and cheerful because of you. You take the best care of me and also my families. Also, thank you for sharing such a lovely family of yours with me. I am so glad to be part of it.

Secondly, I would like to say many thanks to my daily supervisor Annemiek. You are so intelligent and efficient at work. Your feedback is very instant and useful. I always enjoyed our conversations about science and many other things in life. I admire your excellent skill and wisdom to keep a balance between the research work and the personal life. Your guidance over the past 4 years is a great treasure for me. You have been always supportive and encouraging along this journey. You gave me lots of flexibility in my PhD. I could explore my interest in so many different research fields, and therefore, I had the opportunities to cooperate with so many research fellows- Lei Zhang, Wenbo, Florian, Liere, Ludo, Rieks, Margo, Jan Klok (to whom I also would like to say thank you, too!). I

really appreciate that you broaden my research domain as well as my vision. Luckily, I got a chance to continue work with you after my PhD. I look forward to all the excitement and challenges laying ahead.

I would also like to give my gratitude to my promoter, Cees. Thank you for giving me the chance to pursue my PhD in WUR-ETE. I really appreciate your inspiring inputs in my research. You always fire lots of creative ideas during our Aio meetings, and to be honest, I often get a bit of frustration after our meetings as it was quite hard for me to follow your fast thinking. However, later on, I tend to enjoy our meetings and like to discuss with you and look forward to your critical feedback about my research results. By the way, I also enjoy every biorecovery gathering in your place, but for this I have to give half of the gratitude to your wife for being a super nice host and a good tea-mate!

Special thanks go to my students that helped me a lot and did many hard works in the lab and data analysis. MSc students: Casper, Si, Tianye, Imko, Marta, Gerwin, Bonny, Siqi, Pieter (part time) and Vincent (part time). BSc students: Marijke and Christine. I enjoyed working with you guys. Besides research, you guys are also my supervisors. You helped me, intentionally or not, to become a good project manager. The diverse cultures and perspectives from you makes my research life very colourful.

I would like to thank the chair group of ETE and ALL the ETErs. Lots of gratitude to the supporting team, Vinnie, Bert, Katja, Jean, Hans, Ilse, Livio, Jan Kubiak and Piter. You gave me the instant support and helped me solve many technical problems and troubles. I learned from you that the most important thing for Lab work is “safety” and following that is the “trustable results”. I am also grateful for all the help from our secretary team: Liesbeth, Gea, Hewin and Caroline. You helped me work smooth and enjoyable.

I want to thank my office mates in TT.1.091. First with Lei, Bruna, Shokouh, Justine and Sophie, and later on with Azie, Emilius, Leire, Laura, Rosanne. You guys are lovely and have accompanied me throughout my study at ETE. The office is always joyful because of you. Rosanne, thank you for decorating our office with lots of green plants. Azie, thank you for giving me lots of mental support, you said lots of “Jia You” to me during my PhD life. Emilius and Laura, thank you for being my squash partners. Leire, thank you for giving us so much fun and joyful in the office. Also, I like our office dinner programme very much.

I would like to thank these Chinese colleagues and MSc students during these 4 years in ETE. I did have a great time and delicious Chinese food with you and you make me feel less homesick. Lei Zhang you help me adapt to the new environment and give lots of advice and help especially at the beginning of my PhD life. Yujie and Wenbo, thank you for the support and accompany. As the same batch of CSC students in ETE, we shared our feelings and knowledge about the PhD life. We had laughs and tears together. I feel like we are the Three Musketeers in ETE. Right now, both of you are in China and start to work as independent researchers, I wish you all the best. Also, I would like to thank Zhuobiao, Celia, Yingdi, Lei Yu, Bao Park, Jinye, Zhimo, Chunjing, Yifan, Shengle, Shiyang, Xuan, Ruizhe, Yujia, Yin, Lei Yang, Yina, Rui Gao. I did enjoy the wonderful times we spent together during our lunch and coffee breaks. I like to hear from you about the news and stories, which gave me lots of fun. Therefore, let's keep in touch with each other.

I want to thank my best friends, Meiyue. I am so lucky to have you in my life since my bachelor study. I appreciate that you share your wisdom with me. Our conversation is always pleasant and comfortable. Every time we meet and catch up, I feel that there is so much to talk and share with you, but time passes so fast. Luckily, the distance between The Netherlands and Germany is not so far. I wish you all the best in Germany and let's keep meeting each other more often.

Many thanks to two experts from the companies that had sponsored my PhD project, Marcel Geers (Alliander AG) and Jort Langerak (DMT), who contributed their expertise in my research. Special thanks to Jort Langerak for the suggestions he made in Chapter 6 of this thesis.

I want to thank my paranymphs, Lucia and Leire for standing next to me and giving me their supports during my defence. Lucia and Leire, you are both very kind, sweet and innocent girls, just like me. Thank you for all the fun time we had during many gathering moments. I am very happy to meet you and will miss your shining smiles.

Last but not least, I would like to give my most grateful regards to my previous supervisor Aijie. I have learnt so much from you and the Aijie Team. I still remember the first time I koncked on your door and asked for the possiblity to do my BSc thesis with you. At that moment, I would like to do something completely new. You said to me that there is almost

not a completely new research field in the world, but there must be something new need to be discovered in any research field. You give me the great opportunites to develop my intrest by working with different PhD students from different projects for several weeks. Thereafter, I entered the most interesting and my favorite reserach field "Bioelectrochemical Systems". During my bechlor and master thesis, I have laied a solid foundation in bioelectrochemical system by learning from so many the Aijie team including: Haoyi Cheng, Wenzong, Dan Cui, Aijuan, Bin Liang, Dan Sun, Weiwei, Zechong, Chunxue, Xu Zhang. I had a great time working with you, and I learnt so much valuable experience that still guides me along my research jorney. Dear Aijie, even though I went abroad to pursue my PhD, we still have constant contact with each other and you still give me lots of advice and support, from co-applying grant, PhD trip, writing books together to being an opponent and witnessing my defense. I really appreacite having you as my supervisor and guide, withing and beyond my time in Aijie team. Many, many thanks to you that are beyond words.

Dandan (丹丹)

List of publications

Publication list

Scientific journals

D Liu, M R Puigros, F Geppert, L Caizán-Juanarena, S P Na Ayudthaya, CJN Buisman, A ter Heijne. (2018) Granular electrode as cathodes in Methane-Producing Bioelectrochemical Systems. Frontiers in Energy Research. Submitted.

A Ter Heijne, **D Liu**, M Sulonenb, THJA Sleutels, F Fabregat-Santiago. (2018) Biofilm Capacitance: a measure of bio-anode activity in bioelectrochemical systems. Journal of Power Source. Submitted.

D Liu, T Zheng, CJN Buisman, A Ter Heijne. (2017) Heat-Treated Stainless Steel Felt as a New Cathode Material in a Methane-Producing Bioelectrochemical System. ACS sustainable chemistry & engineering 5 (12), 11346-11353.

F Geppert, **D Liu**, M van Eerten-Jansen, E Weidner, CJN Buisman, A Ter Heijne. (2016) Bioelectrochemical power-to-gas: State of the art and future perspectives. Trends in Biotechnology 34 (11), 879-894.

C Borsje, **D Liu**, THJA Sleutels, CJN Buisman, A ter Heijne. (2016) Performance of single carbon granules as perspective for larger scale capacitive bioanodes. Journal of Power Sources 325, 690-696.

D Liu*, L Zhang*, S Chen, CJN Buisman, A ter Heijne. (2016) Bioelectrochemical enhancement of methane production in low temperature anaerobic digestion at 10 °C. Water research 99, 281-287

A Zhou, C Yang, F Kong, **D Liu**, Z Chen, N Ren, A Wang. (2013) Improving the short-chain fatty acids production of waste activated sludge stimulated by a bi-frequency ultrasonic pretreatment. Journal of environmental biology 34 (2 suppl), 381-9.

Book Chapter

D Liu, M Zeppilli, M Villano, CJN Buisman, A Ter Heijne. (2018) Methane production at biocathodes: principles and applications. WILEY Publishing. Submitted.

A ter Heijne, F Geppert, THJA Sleutels, P Batlle-Vilanova, **D Liu**, S Puig. (2017) Mixed Culture Biocathodes for Production of Hydrogen, Methane, and Carboxylates. Adv Biochem Eng Biotechnol. Springer, Berlin, Heidelberg.

About the Author

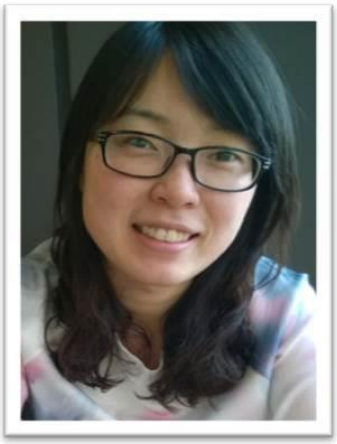

Dandan Liu was born on the 1st of January 1988 in Jilin Province, China. She studied Environmental Science at Harbin Institute of Technology from 2007 and received her bachelor degree in 2011. The bachelor thesis was about the bioelectrochemical systems for azo dye wastewater treatment. Based on the performance during the 4 years bachelor programme, she was admitted to the postgraduate programme in Harbin Institute of Technology without examination. Finally, she got her Master degree in 2013. Her Master thesis was about the electrode modification using bio-based nanomaterials for nitrobenzene reduction.

In May of 2013, she got the personal grant from Chinese Scholarship Council to study aboard for doctorate degree. In October of 2013, she started her PhD research at the sub-department of Environmental Technology, Wageningen University. The main topic is about conversion CO_2 into CH_4 via bioelectrochemical systems (BESs).